Interactive effects of nutrients and physical factors on phytoplankton growth

Dissertation

zur Erlangung des akademischen Grades
doctor rerum naturalium
(Dr. rer. nat.)
im Fach Biologie
eingereicht an der

Mathematisch-Naturwissenschaftlichen Fakultät I
der Humboldt-Universität zu Berlin
von

Tom Shatwell BE(Hons1), MSc

Präsident der Humboldt-Universität zu Berlin
Prof. Dr. Jan-Hendrik Olbertz

Dekan der Mathematisch-Naturwissenschaftlichen Fakultät I
Prof. Stefan Hecht PhD

Gutachter/innen: 1. Dr. sc. nat. Andreas Nicklisch
2. PD Dr. Elly Spijkerman
3. Prof. Dr. Christian Steinberg

Tag der mündlichen Prüfung: 12. Dezember 2013

Summary

Phytoplankton species have different resource requirements and different sensitivities to important growth factors. Interactions between nutrients and physical factors, such as temperature and light should therefore influence the species composition. Understanding these interactions will provide insights into the consequences of climate and trophic change, which shift the relationship between nutrients, temperature and light. Because these interactions are poorly understood, this study investigated the interactive effects of temperature and photoperiod on phytoplankton growth controlled by fluctuating light, phosphorus (P) and silicon (Si). Growth and competition experiments were performed in the laboratory on *Stephanodiscus minutulus*, *Nitzschia acicularis* (both diatoms) and *Limnothrix redekei* (cyanobacterium). A model of factor interactions was developed and long-term field data from Lake Müggelsee (Berlin) were statistically analysed. The fluctuating light regime used in experiments on all three species was designed to simulate the natural variation of light intensity that algae experience when they are transported through the mixed layer due to mixing.

Temperature and photoperiod had the same influence on growth under constant light as they did under fluctuating light induced by mixing in lakes. The photoperiod and short term light fluctuations had additive effects on growth, indicating that they are inherently related as different aspects of temporal variation of the light supply. Their combined effects were accounted for with a simple, yet accurate empirical equation, which avoids many of the inaccuracies of deriving growth rates from photosynthesis.

The photoperiod did not influence the degree of limitation by P or Si (multiplicative interaction), nor did it influence relative P-uptake rates. In contrast, the temperature interactions were more complex and species-specific. Regardless of whether growth was controlled by P, Si or fluctuating light, *S. minutulus* (an early spring centric species) became more competitive under lower temperatures and short photoperiods, whereas *N. acicularis* (a late spring pennate species) became more competitive under higher temperatures and longer photoperiods. The field data analysis confirmed the predictions of the culture experiments, showing that Si, P, temperature and photoperiod were the most important predictors of centric diatom biomass. Pennate diatoms depended on temperature and light, but starting population size and zooplankton abundance also played an important role.

Contrary to established views, the minimum P-quota (internal P-content, Q_0) may be independent of temperature, reflecting instead a temperature dependent half-saturation coefficient (k_Q), which fixed-form quota curves without a k_Q like the Droop model cannot account for. In contrast to the assumptions of the Droop model, the results here and a review of 50 published experiments suggested that k_Q is higher than Q_0 for most phytoplankton species. A cell-cycle model was developed in which Si-uptake is uncoupled from growth. This model described diatom competition substantially better than the equivalent Monod model, indicating that non-steady state dynamics influence Si competition in diatoms and the degree of Si-limitation in lakes derived from Monod parameters may be strongly underestimated. Current standard models of nutrient limited growth (Droop for P, Monod for Si) should be revised.

The results demonstrate that increases in temperature or photoperiod can partially compensate for a decrease in P-quota under moderately limiting conditions, like during spring in temperate lakes. Thus warming may counteract reoligotrophication to some degree and co-limitation by temperature and P or Si can influence the phytoplankton species composition. Altogether, the types of factor interactions are generally species-specific, reflect adaptation and enhance niche differentiation. Understanding them should improve our knowledge of phytoplankton diversity and increase our ability to predict phytoplankton response to climate and trophic change.

Keywords: spring phytoplankton, temperature, photoperiod, light, phosphorus, silicon, mixing, Droop model, Monod model, Si:P ratio, diatoms, cyanobacteria, *Nitzschia acicularis*, *Stephanodiscus minutulus, Limnothrix redekei*

Zusammenfassung

Phytoplanktonarten unterscheiden sich in ihren Ansprüchen hinsichtlich Ressourcen wie Nährstoffe, Licht und andere physikalische Faktoren. Wechselwirkungen zwischen Nährstoffen und physikalischen Faktoren beeinflussen daher die Artenzusammensetzung einer Phytoplanktongemeinschaft. Kenntnisse dieser Wechselwirkungen tragen zum besseren Verständnis der Auswirkungen von Klimawandel und Veränderungen der Trophie bei, die mit einer Verschiebung der Verhältnisse zwischen Nährstoffen, Temperatur und Licht einhergehen. In der vorliegenden Arbeit wurde der Einfluss von Temperatur und Photoperiode auf das Phytoplanktonwachstum in Abhängigkeit vom Lichtregime und dem Angebot an Phosphor (P) und Silizium (Si) untersucht. Hierfür wurden Wachstums- und Konkurrenzexperimente unter Laborverhältnissen mit *Stephanodiscus minutulus*, *Nitzschia acicularis* (beides Bacillariophyceae) und *Limnothrix redekei* (Cyanophyceae) durchgeführt, ein Modell der Faktorinteraktionen entwickelt sowie ökologische Langzeitdaten des Müggelsees (Berlin) statistisch ausgewertet. Das sich *in-situ* durch Vertikaltransport in der Durchmischungsschicht veränderte Lichtangebot wurde in Experimenten mit allen drei Arten durch ein fluktuierendes Lichtregime simuliert.

Die Effekte von Temperatur und Photoperiode auf die Wachstumsraten unterschieden sich nicht zwischen konstantem und fluktuierendem Licht. Die Auswirkungen der Photoperiode und der Lichtfluktuationen auf die Wachstumsraten waren hierbei additiv. Das deutet darauf hin, dass beide Faktoren verschiedene Aspekte einer zeitlichen Variation der Lichtversorgung bei prinzipiell gleichen Wirkungsmechanismen darstellen. Die gemeinsamen Effekte konnten durch eine einfache, präzise empirische Gleichung beschrieben werden, die viele Ungenauigkeiten, die mit der Ableitung von Wachstumsraten aus der photosynthetischen Kohlenstoffassimilierung einhergehen, vermeidet.

Der Grad der Limitation der Wachstumsraten durch P oder Si und die P-Aufnahmeraten wurden durch die Photoperiode (multiplikative Interaktionen) nicht signifikant beeinflusst. Wechselwirkungen zwischen Temperatur und P oder Si waren hingegen komplex und artspezifisch. Unabhängig davon, ob die Wachstumsraten durch P, Si oder fluktuierendes Licht gesteuert wurden, war *S. minutulus* (eine zentrischen Diatomee, die zeitig im Frühjahr vorkommt) konkurrenzstärker bei niedrigeren Temperaturen und *N. acicularis* (eine spät im Frühjahr vorkommende, pennate Form) bei höheren Temperaturen. Diese Ergebnisse wurden durch die Auswertung der Langzeitdaten bestätigt. Für die Biomasse der zentrischen

Diatomeen waren Temperatur, Photoperiode und die Nährstoffe Si, und P die wichtigsten Einflussgrößen. Für die pennaten Diatomeen hingegen waren die wichtigsten Einflussgrößen Temperatur, Licht, die Größe der Ausgangspopulation sowie die Zooplanktonabundanz.

Konträr zu etablierten Ansichten konnte in dieser Arbeit gezeigt werden, dass die minimale zellinterne P-Quote (Q_0) unabhängig von der Temperatur ist. Die gemessene Wachstumsraten konnten hierbei durch eine Temperaturabhängigkeit der Halbsättigungskonstante (Modellparameter, k_Q) erklärt werden, die nicht mit dem Droop-Modell beschrieben werden kann. Im Gegensatz zu der Annahme des Droop-Modells ist für die meisten der aus der Literatur ausgewerteten Arten k_Q höher als Q_0. Für die Si-Limitation wurde ein Zell-Zyklus-Modell entwickelt, in dem die Si-Aufnahme von der Biomassezunahme entkoppelt wurde. Die Dynamik der Si-Konkurrenz wurde durch das Zell-Zyklus-Modell deutlich besser beschrieben als durch das entsprechend parametrisierte Monod-Modell. Dies bedeutet, dass eine wechselnde Si-Zufuhr das Konkurrenzverhalten von Diatomeen beeinflusst und der von Monod-Parametern abgeleitete Grad der Si-Limitation in Seen deutlich unterschätzt werden kann. Hieraus ergibt sich die Notwendigkeit der Weiterentwicklung von Standardmodellen für nährstofflimitiertes Wachstum (Droop für P, Monod für Si).

Zusammenfassend zeigen die Ergebnisse, dass bei P-Limitation eine Abnahme der P-Quote teilweise durch eine Zunahme der Temperatur oder Photoperiode kompensiert werden kann. Folglich wirkt die Klimaerwärmung beispielsweise einer Reoligotrophierung von Seen entgegen. Eine gleichzeitige Limitation der Wachstumsraten durch Temperatur sowie P oder Si kann außerdem die Artenzusammensetzung des Phytoplanktons beeinflussen. Die Faktorinteraktionstypen sind artspezifisch, spiegeln die Adaptation der Arten wider und tragen so zur Nischen-Differenzierung bei. Kenntnisse dieser Wechselwirkungen fördern deshalb unser Verständnis der Komplexität von Phytoplanktongemeinschaften und ermöglichen es, Reaktionen des Phytoplanktons auf Klimaerwärmung und Trophieveränderung besser vorherzusagen.

Schlagwörter: Phytoplankton, Frühjahr, Temperatur, Photoperiode, Licht, Phosphor, Silizium, Durchmischung, Droop-Modell, Monod-Modell, Si:P-Verhältnis, Diatomeen, Cyanobakterien, *Nitzschia acicularis*, *Stephanodiscus minutulus, Limnothrix redekei*

Preface

The thesis presents the results of experimental and statistical investigations into the interactive effects of physical factors and nutrients on phytoplankton growth. It is structured around three groups of experiments, which examine the effect of temperature and photoperiod on 1) growth under **fluctuating light**, 2) growth under **phosphorus limitation**, and 3) growth under **silicon limitation**. The results of these experiments are published in the following articles:

- **Shatwell, T.**, Nicklisch, A. & Köhler, J. (2012). Temperature and photoperiod effects on phytoplankton growing under simulated mixed layer light fluctuations. *Limnology and Oceanography* 57:541-53.
- **Shatwell, T.**, Köhler, J. and Nicklisch, A. (in review) Temperature and photoperiod interactions with phosphorus limited growth and competition of two diatoms.
- **Shatwell, T.**, Köhler, J. and Nicklisch, A. (2013). Temperature and photoperiod interactions with silicon limited growth and competition of two diatoms. *Journal of Plankton Research,* 35, 957-971.

In addition, the thesis builds on and extends a base model of factor interactions, and a statistical analysis of spring phytoplankton in Lake Müggelsee which investigates the role of interactions in situ. These results are presented in the following articles:

- Nicklisch, A., **Shatwell, T.** & Köhler, J. 2008. Analysis and modelling of the interactive effects of temperature and light on phytoplankton growth and relevance for the spring bloom. *Journal of Plankton Research* 30:75-91.
- **Shatwell, T.**, Köhler, J. & Nicklisch, A. 2008. Warming promotes cold-adapted phytoplankton in temperate lakes and opens a loophole for Oscillatoriales in spring. *Global Change Biology* 14:2194-200.

Contents

Summary ..... **i**

Zusammenfassung ..... **iii**

Preface ..... **v**

Abbreviations ..... **ix**

1. Introduction **1**

1.1 Role of limiting factors and their interactions for phytoplankton growth 1

1.2 Overview of factor interactions 4

1.2.1 Constant light interactions with temperature and photoperiod 5

1.2.2 Fluctuating light interactions with temperature and photoperiod 6

1.2.3 Phosphorus interactions with temperature and photoperiod 7

1.2.4 Silicon interactions with temperature and photoperiod 8

1.3 Aims and approach 9

2. Methods **12**

2.1 Algae strains 12

2.2 Nutrient solution 12

2.3 Algae cultivation 13

2.3.1 Semi-continuous and batch cultures 14

2.3.2 Continuous chemostat cultures 15

2.4 Biomass measurements 16

2.5 Specific growth rate determinations 17

2.6 Fluctuating light experiments 18

2.7 Phosphorus limitation experiments 21

2.7.1 Growth rate experiments 21

2.7.2 Competition experiments 22

2.8 Silicon limitation experiments 23

2.8.1 Growth rate experiments in continuous culture 23

2.8.2 Growth rate experiments in batch culture 24

2.8.3 Competition experiments 24

2.9 Measurement of pigment content 25

2.10 Electron transport rates 26

2.11 Silicate determination 27

2.12 Lake data 27

2.13 Statistical models and analyses 28

2.13.1 The base model of nutrient replete growth 28

2.13.2 Fluctuating light experiments 30

2.13.3 Phosphorus limitation experiments....31
2.13.4 The Droop relation....32
2.13.5 Silicon limitation experiments....34
2.13.6 Statistical analysis of lake data....34
2.14 Dynamic models and simulations....35
2.14.1 P-limited competition and relative P uptake rates....35
2.14.2 Silicon-limited competition....37

3. Results....43

3.1 Fluctuating light and the effects of temperature and photoperiod....43
3.1.1 Effect of fluctuating light on growth....43
3.1.2 Effect of temperature....45
3.1.3 Effect of photoperiod....46
3.1.4 Effect of z_{eu}:z_{mix}....47
3.1.5 Pigments....49
3.1.6 Photosynthetic parameters....52
3.2 Phosphorus and its interactions with temperature and photoperiod....53
3.2.1 Phosphorus-replete growth....53
3.2.2 Temperature and photoperiod effects on P-limited growth....57
3.2.3 Model of factor interactions under P-limitation....58
3.2.4 Competition experiments under P-limitation....60
3.2.5 Relative P uptake rates....62
3.3 Silicon and its interactions with temperature and photoperiod....63
3.3.1 Chemostat experiments under silicon limitation....63
3.3.2 Batch experiments under silicon limitation....66
3.3.3 Model of factor interactions under silicon limitation....68
3.3.4 Competition experiments in semi-continuous culture....70
3.4 Nutrient interactions in situ....72

4. Discussion....75

4.1 Hypotheses....75
4.2 Fluctuating light interactions....77
4.2.1 Effect of fluctuating light....77
4.2.2 Temperature....78
4.2.3 Photoperiod and z_{eu}:z_{mix}....80
4.2.4 Photosynthesis and growth....82
4.2.5 Light limitation and ecological considerations....84
4.3 Phosphorus interactions....86
4.3.1 The Droop relation and model comparison....86
4.3.2 Temperature....88

4.3.3 Photoperiod....90
4.3.4 Competition and P-uptake....91
4.4 Silicon interactions....93
4.4.1 Temperature and photoperiod effects....94
4.4.2 Competition and Monod vs. cell-cycle model....95
4.5 Other factor interactions....97
4.5.1 Interactions between nutrients....97
4.5.2 Interactions between light and nutrients....98
4.6 Ecological implications of factor interactions....99
4.6.1 Niche differentiation....99
4.6.2 Spring phytoplankton composition....100
5. Conclusions....103
6. References....104
Acknowledgements....118
Appendix 1: Literature data to assess the "Droop relation"....120
Appendix 2: Final equations for model of factor interactions....126
Selbständigkeitserklärung (declaration)....131
Publications....132
Presentations....134

Abbreviations

Table 1: Symbols and abbreviations

Abbrev.	Description	Units
α_{LE}	Initial slope of growth-light (μ vs. LE) curve	m^2 mol^{-1} quanta
α_{LP}	Initial slope of maximum growth-photoperiod (μ_m vs. LP) curve	h^{-1}
α_I*	Initial slope of ETR vs. I curve	relative units
α_Q	Initial slope of the quota (μ vs. Q) curve	mm^3 μg^{-1} P d^{-1}
α_{Qm}	Initial slope of the quota (μ vs. Q) curve at optimum temperature	mm^3 μg^{-1} P d^{-1}
α_S	Initial slope of Monod (μ vs. S) curve ($=\mu_m/k_s$)	L μmol^{-1} d^{-1}
κ_Q	Normalised half saturation coefficient for P-limitation ($=Q_0/k_Q$)	dimensionless
τ_0	Si-uptake duration (G2) as proportion of the cell cycle at μ_{NR}	dimensionless
μ	Specific growth rate	d^{-1}
μ_m	Light saturated specific growth rate at suboptimal T & LP	d^{-1}
μ_{mc}	Light saturated specific growth rate under constant light	d^{-1}
μ_{mf}	Light saturated specific growth rate under fluctuating light	d^{-1}
μ_{mLP}	Light saturated specific growth rate at 24 h d^{-1} photoperiod	d^{-1}
μ_{NR}	Nutrient replete specific growth rate, suboptimal T, LP, LE	d^{-1}
μ'_{NR}	Theoretical nutrient replete specific growth rate at infinite Q	d^{-1}
μ_{max}	Absolute maximum specific growth rate, all conditions optimal	d^{-1}
AIC	Akaike's An Information Criterion	-
ANOVA	Analysis of variance	-
ANCOVA	Analysis of covariance	-
B; B_0	Cell size; minimum cell size	μm^3 $cell^{-1}$
c_i	Biovolume-specific proportion of P absorbed by species *i*	dimensionless
CA	Competitive ability	dimensionless
Chl*a*, *c*	Chlorophyll *a* or *c*	see text
CL_6	Constant light, short photoperiod = 6 h d^{-1}	-
CL_{12}	Constant light, long photoperiod = 12 h d^{-1}	-
D	Dilution rate	d^{-1}
df	Degrees of freedom	-
DSi	Dissolved silicate concentration	μmol L^{-1}
E_k	Light saturation intensity for growth	μmol quanta m^{-2} s^{-1}
ETR	Electron transport rate	relative units
ETR_{max}	Maximum electron transport rate	relative units
FL_6	Fluctuating light, short photoperiod = 6 h d^{-1}	-
FL_{12}	Fluctuating light, long photoperiod = 12 h d^{-1}	-
$FL_{12}D$	Fluctuating light, long photoperiod = 12 h d^{-1}, deep mixing	-
f	Dilution factor (proportion of culture retained at dilution)	dimensionless
F_o	Minimum fluorescence of dark-adapted cultures	relative units

F_v	Variable fluorescence of dark-adapted cultures (Kautsky effect)	relative units
i, j (subs.)	Species *i* and *j* (in competition experiments)	-
I	Irradiance	μmol quanta m^{-2} s^{-1}
I_o	Irradiance at the water surface	μmol quanta m^{-2} s^{-1}
I_{max}	Maximum irradiance in the middle of the photoperiod	μmol quanta m^{-2} s^{-1}
I_{mean}	Mean irradiance over the photoperiod	μmol quanta m^{-2} s^{-1}
I_k	Light saturation intensity for electron transport rates	μmol quanta m^{-2} s^{-1}
k_Q	Half-saturation coefficient of the quota curve (P-limitation)	μg mm^{-3}
k_S	Half-saturation coefficient of the Monod curve (Si-limitation)	μmol L^{-1}
k_m	Half-saturation coefficient of nutrient uptake (Michaelis-Menten)	μmol L^{-1}
LP	Photoperiod	h d^{-1}
LP_{eff}	Effective photoperiod when $z_{eu}:z_{mix} < 1$ (see Eq. 4)	h d^{-1}
LP_{min}	Minimum photoperiod	h d^{-1}
LE	Daily light exposure	mol quanta m^{-2} d^{-1}
LE_{min}	Light compensation point for growth	mol quanta m^{-2} d^{-1}
LF	Light fluctuation factor	dimensionless
LF_α	Factor to decrease α_{LE} under fluctuating light	dimensionless
N	Cell concentration (or “nitrogen”, as is obvious from context)	10^9 cells L^{-1}
P	Phosphorus	-
PAR	Photosynthetically active radiation (400-700 nm)	quanta
PAM	Pulse amplitude modulated	-
PSI/II	Photosystem I or II	-
Q	Nutrient quota	μg mm^{-3}
Q_0	Minimum nutrient quota for growth	μg mm^{-3}
R*	Minimum equilibrium resource concentration for zero net growth	μmol L^{-1}
RSE	Residual standard error	same as resp. variable
S	Nutrient (Si) concentration	μmol L^{-1}
S_0	Minimum nutrient (Si) concentration for growth or uptake	μmol L^{-1}
S_m	Nutrient (Si, P) concentration in fresh medium	μmol L^{-1}
SD, SE	Standard deviation, standard error	same as resp. variable
Si	Silicon	-
t; Δt	Time; time until next dilution	d
T	Temperature	°C
T_{opt}	Optimum temperature	°C
T_{min}, T_{minQ}	Minimum temperature (for dependency of μ_m and α_Q, respectively)	°C
V	Nutrient uptake rate (Michaelis-Menten)	μmol mm^{-3} d^{-1}
V_m	Maximum nutrient uptake rate (Michaelis-Menten)	μmol mm^{-3} d^{-1}
X	Biovolume	mm^3 L^{-1}
$z_{eu}:z_{mix}$	Ratio of euphotic to mixed depth	dimensionless

1. Introduction

1.1 Role of limiting factors and their interactions for phytoplankton growth

The main resources that typically limit phytoplankton growth in freshwater are light and macronutrients such as phosphorus, nitrogen, and also silicon in the case of siliceous algae such as diatoms. In addition, the temperature plays an important role because it influences how phytoplankton use these resources. These abiotic growth factors are continually changing relative to each other, which, together with biotic interactions, causes the seasonal succession of phytoplankton. The PEG model (Sommer et al., 1986, Sommer et al., 2012) is a good starting point to illustrate the seasonal variation in the main growth factors for phytoplankton (Figure 1). During winter, physical factors like temperature and light limit phytoplankton growth. Increasing light and temperature during spring, combined with abundant nutrients made available by mixing, lead to the spring phytoplankton bloom. The bloom, which typically consists of diatoms, is terminated by the onset of nutrient limitation and zooplankton grazing, which initiates the clear water phase. During summer, nutrients are controlled by import and recycling, and generally limit phytoplankton growth before growth control reverts to physical factors in winter. Light may also be limiting during summer in turbid systems.

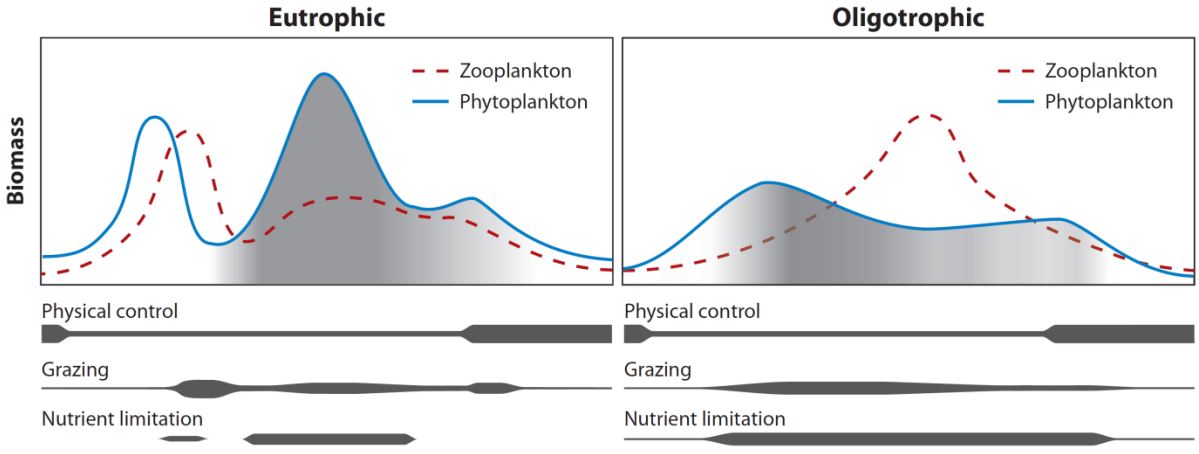

Figure 1: The PEG model of seasonal succession. This is a reproduction of the upper portion of Figure 1 from the PEG review paper (Sommer et al., 2012), with kind permission of Annual Reviews Inc. publishers.

Since different phytoplankton species have different sensitivities to the growth factors, interactions between these factors should alter the species composition. The situation is quite complex. Nutrients and light are interdependent in surface waters because low nutrient levels restrict the phytoplankton biomass, and therefore typically occur in clearer water (Jeppesen et al., 2005). In turn, clearer water leads to higher underwater irradiances and a longer effective photoperiod due to a deeper euphotic depth (Shatwell et al., 2008). On the other hand turbidity, for example due to high phytoplankton biomass, increases absorbed radiation and therefore influences the thermal structure and water temperature (Rinke et al., 2010, Kirillin, 2010), which affects nutrient cycling processes (Jeppesen et al., 2010). Therefore, in addition to seasonal cycles, the relationships between nutrients and physical factors can shift, for example due to global warming or eutrophication (Köhler et al., 2005, Jeppesen et al., 2010). These effects can be particularly pronounced in spring, when the rapid increase in temperature, day-length and light following winter, and the subsequent transition to nutrient control, mean that factor interactions are especially relevant.

The interactive effects of temperature and nutrients on phytoplankton communities, which for example result from eutrophication, climate warming, or simply the seasonality of the climate, can be difficult to predict. For example, the dominance of filamentous cyanobacteria during spring in a shallow lake depended on the combined effects of winter temperature and the Si:P ratio (Shatwell et al., 2008), and the timing of the phytoplankton bloom was synergistically affected by water temperature and phosphorus supply (Köhler et al., 2005). Another study showed that filamentous cyanobacteria dominance depended on both light and nutrients (Nixdorf et al., 2003). Furthermore, several studies indicate that low initial silicon concentrations in lakes, combined with warming, advance the spring diatom peak, whereas low initial phosphorus concentrations delay it, and that different species are affected in different ways (Huber et al., 2008, Thackeray et al., 2008, Meis et al., 2009, Feuchtmayr et al., 2012).

The interactions with light are no less complex than those with nutrients because light has a temporal component as well as a quantitative one (the amount of energy). Phytoplankton experience a continually changing light supply due to the variation of sunlight throughout the day, as well as fluctuations caused by cloud cover, wave reflection and the exponential increase and decrease in light intensity as cells are transported vertically in the water column due to mixing (Figure 2).

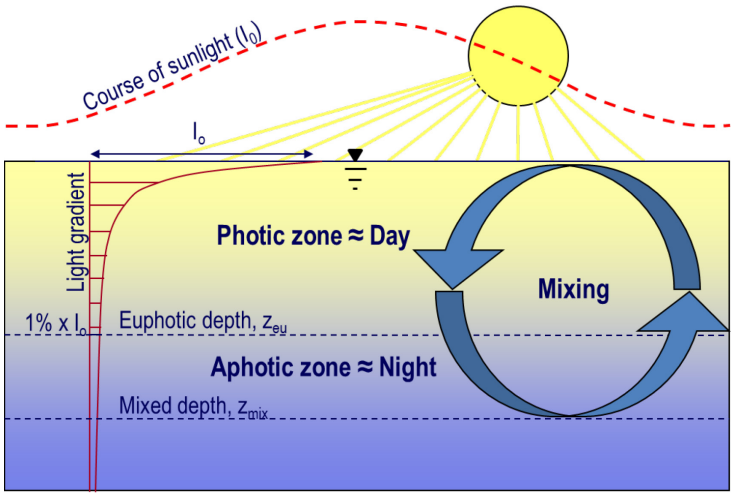

Figure 2: The effect of the vertical light gradient and mixing on the photoperiod. The effective photoperiod is the length of the solar day times the ratio z_{eu} : z_{mix}. The euphotic depth is defined as the depth where irradiance reaches 1% of surface irradiance (I_0).

In terms of phytoplankton growth, 'light limitation' generally refers to limitation by the amount of light energy; however there are other complicating factors. During spring, there is evidence that it is not the daily amount of light energy (as mol quanta m^{-2} d^{-1}), but the photoperiod that combines with temperature to co-limit algal growth, at least in shallow lakes (Nicklisch et al., 2008). In the study of Nicklisch *et al.*, calculations based on laboratory measurements of interactions between daily irradiance, photoperiod and temperature demonstrated that, under spring conditions in a temperate lake (Müggelsee), the amount of light energy was only growth limiting for the species tested on certain overcast days, whereas temperature and photoperiod were always important. Preliminary calculations in this study indicated that mixing-induced light fluctuations should also limit growth. If the temporal components of the daily light supply, such as photoperiod and light fluctuations, limit growth, then phytoplankton would be able to achieve higher growth rates if the light energy were distributed more evenly over the day. On the other hand, increasing the amount of light energy delivered would have little effect on growth rates if the photoperiod and amplitude of light fluctuations remained the same.

The photoperiod is determined by the length of the solar day, and if the euphotic depth (z_{eu}) is smaller than the mixed depth (z_{mix}), then algae spend a certain amount of additional time in the aphotic zone in relative darkness, and the effective photoperiod decreases by the ratio z_{eu}:z_{mix} (Figure 2). Since algae respond in a species-specific and non-linear way to the photoperiod (Castenholz, 1964, Paasche, 1968, Foy et al., 1976, Gibson and Foy, 1983, Nicklisch and Kohl, 1989, Nicklisch, 1998, Thompson, 1999, Nicklisch et al., 2008), light

fluctuations (Nicklisch, 1998, Litchman, 2000, Mitrovic et al., 2003), and of course temperature, a shift in the relationship between co-limiting factors should have an effect on the species composition. Understanding these effects may depend on how well we understand the physiological response of individual species, including the species-specific interactions between phytoplankton growth factors.

1.2 Overview of factor interactions

Several different types of interactions between resources or growth factors are possible (Tilman, 1980, Tilman, 1982). The most relevant types for nutrients and physical factors range between Liebig's Minimum Law and a multiplicative interaction type (Figure 3).

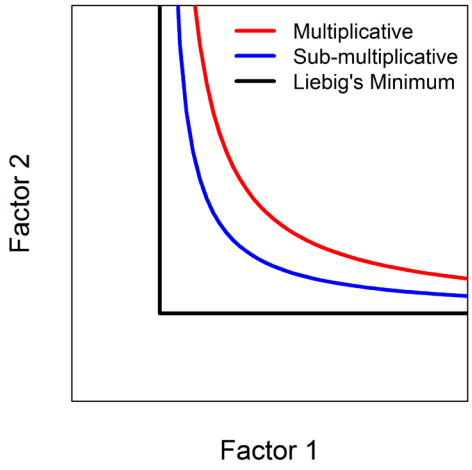

Figure 3: Some different types of interaction between two factors. The lines represent isoclines of equal growth rate after Tilman (1982). The models used to generate the lines were the same for each factor, but linked by different interaction types. Liebig's Minimum Law is depicted as two lines that intersect at the optimum resource ratio.

Liebig's Minimum Law applies essentially when there is no interaction between two factors; that is, only the most limiting factor determines the growth rate, whereas other factor(s) have no effect (growth rate = min[f(factor1); f(factor2)]). A multiplicative interaction applies when two factors co-limit growth (independent co-limitation: growth rate = f(factor1) × f(factor2)). In this case, the degree of limitation of one factor is independent of the degree of limitation of the other factor (Spijkerman et al., 2011), and the interaction is strong (Figure 4). Weaker interactions are also possible: for instance, a sub-multiplicative type applies when co-limitation of two factors is restricted to certain ranges, or in other words, when the degree of limitation of one factor depends on the magnitude of the other factor (dependent co-limitation, e.g. growth rate = f(factor1, factor2) × f(factor2)). For example, if one factor is either particularly low or particularly high, then the other factor may have no influence (Figure 4).

With respect to growth kinetics, the type of interaction generally determines the degree to which an increase in one factor can compensate for a shortage of another factor.

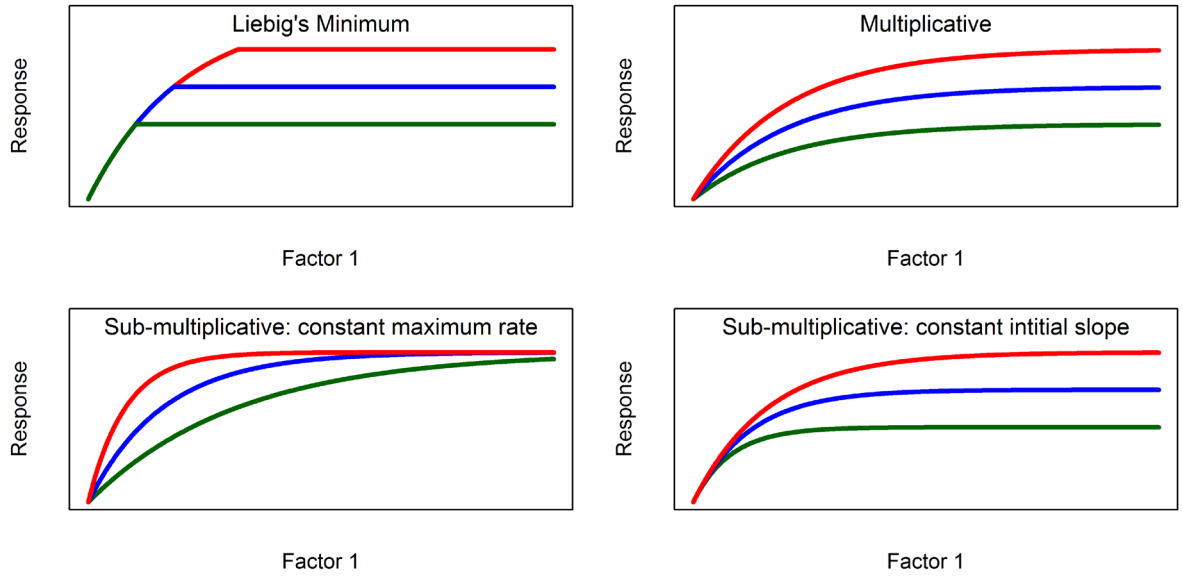

Figure 4: Some different interaction types, shown in terms of the response variable (generally growth rate). Lines represent different levels of Factor 2, increasing in the order green, blue red.

The following subsections present an overview of the published literature on the interactions between physical factors and nutrients. This study addresses the special role that interactions play during spring. In spring, the limiting nutrients are typically phosphorus and silicon (Reynolds, 2006), and the most influential physical factors are temperature and photoperiod (Nicklisch et al., 2008, Shatwell et al., 2008), at least in shallow lakes. Of course, light is also considered, and particularly the effect of intensified mixing on the light supply (Sommer et al., 1986, Sommer et al., 2012).

1.2.1 Constant light interactions with temperature and photoperiod

The interactions between temperature, photoperiod and light exposure (daily light dose) have been characterised under constant light for a number of phytoplankton species. Temperature only affects light saturated growth, when enzymatic processes determine the growth rate, but has little influence on strongly light-limited growth, when the photochemistry of light absorption determines the growth rate (Yoder, 1979, Foy, 1983, Gibson and Foy, 1983, Kohl and Nicklisch, 1988, Nicklisch, 1992, Foy and Gibson, 1993, Thompson, 1999), so that the

growth light curve has a constant initial slope (Figure 4). This type of interaction is sub-multiplicative because temperature and light only co-limit growth at intermediate light levels. The interaction between light exposure and the photoperiod is similar, where light-saturated but not light-limited growth depends on the photoperiod (Gibson, 1985, Thompson, 1999, Nicklisch et al., 2008, Shatwell et al., 2012). On the other hand, the interaction between temperature and the photoperiod under constant saturating light exposure is less well-known and appears to be species specific. In the marine diatom *Thalassiosira pseudonana*, this interaction was sub-multiplicative because temperature did not influence the light-saturated growth rate under short photoperiods (Thompson, 1999). This was not the case with the arctic cyanobacterium *Schizothrix calcicola* (Tang and Vincent, 2000) nor for the freshwater cyanobacteria *Aphanizomenon flos-aquae*, *Planktothrix agardhii* and *Limnothrix redekei* (Gibson, 1985) where the interaction was more multiplicative. Nicklisch et al. (2008) compiled a large set of new and published data on four freshwater species, and developed a model describing the three-way interactions between temperature, photoperiod and the daily light exposure. This factor interaction model forms the starting point of this thesis and is described in section 2.13.1 (p. 28). Nicklisch *et al*. found that the interaction between temperature and photoperiod was multiplicative for *Nitzschia acicularis* (diatom), as well as *Limnothrix redekei* and *Planktothrix agardhii*, but the interaction was sub-multiplicative for the centric diatom *Stephanodiscus minutulus*. It appears therefore that both interaction types are possible.

1.2.2 Fluctuating light interactions with temperature and photoperiod

Since most laboratory experiments on phytoplankton growth are performed under constant light, there is little information available on the interactions of light with temperature and photoperiod under fluctuating light. It is therefore only possible to summarise the general effects of mixing-induced fluctuating light on growth. Laboratory studies have produced varying results. In some cases growth rates under fluctuating light remained the same in comparison to constant light (Cosper, 1982, Litchman, 2000), but in the majority of cases growth rates tended to decrease (Marra, 1978, Nicklisch, 1998, Nicklisch and Fietz, 2001). These differences might be due to the type of fluctuating light regime and the light intensities used. For example, a decrease in growth rates may depend on whether peak irradiances are higher than the saturation intensity of photosynthesis, which in turn depends on how much an alga can acclimate its photosynthesis to the changing light supply (Fietz and Nicklisch, 2002). Some species showed a high degree of acclimation to dynamic light regimes, suggesting that

the daily amount of light rather than temporal components is important (Dimier et al., 2009). Several studies show that phytoplankton acclimate to fluctuating light in a complex way that has similarities with both low and high light acclimation (Fietz and Nicklisch, 2002, Dimier et al., 2009, Havelkova-Dousova et al., 2004). Frequency of light fluctuations and photoperiod should also affect phytoplankton community structure (Litchman and Klausmeier, 2001). Most published laboratory measurements of growth rates under fluctuating light were performed at 20°C (Nicklisch, 1998, Litchman, 2000, Dimier et al., 2009) or 17-18°C (Havelkova-Dousova et al., 2004, van de Poll et al., 2007). However, intensive or even deep mixing generally occurs at lower temperatures, such as those encountered during spring and autumn when days are shorter. The effect of fluctuating light on growth at these lower temperatures and photoperiods seems not to have been investigated and the interactive effects are thus unknown.

1.2.3 Phosphorus interactions with temperature and photoperiod

While Liebig's Law of the Minimum is assumed to apply to interactions between nutrients, this is not the case between nutrients and physical factors (Healey, 1985). The temperature and photoperiod have species-specific interactive effects on nutrient-replete growth as described above, but these interactions may be different under nutrient limitation, because temperature and light also affect N- and P-quotas (Rhee and Gotham, 1981a, Rhee and Gotham, 1981b, Ahlgren, 1988). At the same time, light and temperature influence nutrient uptake rates in a nutrient- and species-specific manner (Cembella et al., 1984a), whereby the temperature dependence of uptake is typically different to that of growth (Goldman, 1977).

The interaction of the photoperiod with phosphorus limitation is relatively unexplored. If phosphorus uptake rates differ in the dark and light (Riegman et al., 2000), then there may be an interaction between phosphorus and the photoperiod (Litchman et al., 2004), particularly given the influence of light on phytoplankton stoichiometry (Dickman et al., 2006). Litchman et al. (2003) showed that the combined effects of photoperiod and P-limitation were species-specific and greater than the sum of individual effects for several phytoplankton species, whereas Riegman and Mur (1985) found a more either/or (Liebig) type of limitation between photoperiod and phosphorus for *Planktothrix* (formerly *Oscillatoria*) *agardhii*. Overall, it seems difficult to form definite conclusions from these studies on photoperiod interactions with phosphorus, especially because comparison is difficult when the irradiance and not the daily light exposure is held constant in daylength treatments.

More recently research has stressed the importance of developing a mechanistic or biochemical basis for Droop's (1968) quota model (Flynn, 2008c, Klausmeier et al., 2008), and interactions between phosphorus and physical factors have become particularly relevant. Droop's model relates the growth rate to the nutrient quota in terms of the minimum quota Q_0 and the theoretical maximum growth rate at infinite quota. Q_0 is the quota at which growth is zero and represents the amount of nutrient required for cell structure and machinery (Klausmeier et al., 2008). Q_m is the maximum quota at the real maximum growth rate when the nutrient is not limiting, and provides information on the amount of nutrient a cell can store. The form of Droop's quota curve is fixed by the ratio Q_0:Q_m, in other words the curve is half-saturated when the quota is double Q_0. Q_0 seems to decrease with increasing temperature (Goldman, 1979, Rhee and Gotham, 1981b, Cembella et al., 1984b, Ahlgren, 1987), although there are exceptions (Wernicke and Nicklisch, 1986, van Donk and Kilham, 1990). Furthermore, not only the maximum growth rate and Q, but also Q_0:Q_m (Goldman, 1979) are all temperature dependent. Because the upper part of the quota curve is probably more important for competitive advantage between species than the lower part near Q_0 (Flynn, 2008a), the Droop model may not provide an adequate model of temperature or photoperiod interactions with P-limited growth. Of equal or greater importance than the growth-quota relationship are the nutrient uptake kinetics, and the feedback between uptake and quota (Flynn, 2008c). The growth-quota relationship thus needs to be considered in conjunction with uptake.

1.2.4 Silicon interactions with temperature and photoperiod

The effect of temperature on silicon limited growth kinetics has been investigated with somewhat varying results, with some studies suggesting that the Monod half-saturation constant of silicon limited growth (k_S) decreased with increasing temperature (Paasche, 1975), increased with increasing temperature (Mechling and Kilham, 1982) or was relatively independent of temperature (Tilman et al., 1981). The photoperiod has also been shown to interact with phytoplankton dynamics along a Si:P gradient (Shatwell et al., 2008) and influence nutrient competition among marine phytoplankton along a Si:N gradient (Sommer, 1994). The photoperiod may also influence silicon uptake, particularly when growth is synchronised through light/dark cycles (Chisholm et al., 1978) since silicon metabolism is closely coupled to the cell cycle (Brzezinski et al., 1990), although this effect appears to be variable and species specific (Martin-Jézéquel et al., 2000). One consequence of this is that silicate uptake is not continuous, but restricted to certain parts of the cell cycle (Claquin et al.,

2002, Thamatrakoln and Hildebrand, 2008). Uptake rates can therefore be substantially higher than estimated from the Monod model (Brzezinski, 1992, Leynaert et al., 2009), which assumes constant stoichiometry and steady growth and uptake (Flynn, 2003). Without the buffering capacity of any significant internal storage of silicate, non-steady uptake may influence the factor interactions or competition outcome. Whereas the studies on photoperiod effects mentioned above focused on silicon uptake in marine diatoms, there appear to be no studies that investigated the influence of the photoperiod on the kinetics of silicon limited growth. The overall picture on the interactions of temperature and photoperiod with silicon limited growth seems inconclusive.

1.3 Aims and approach

Taken together, there is substantial evidence that factor interactions play an important role in controlling species-specific growth of phytoplankton and thus shaping the phytoplankton community. Whereas the impact of individual factors alone is well known, the interactions between them are poorly understood. Therefore the main objective of this thesis is to investigate the interactions between the most important physical factors and nutrients with respect to phytoplankton growth in spring. Specifically, I aim to experimentally characterise the interactive effects of temperature and photoperiod on phytoplankton growth controlled by

- fluctuating light
- phosphorus, and
- silicon.

I further aim to combine the results into a model and make inferences about phytoplankton ecology and how factor interactions contribute to the species composition.

This thesis addresses the following hypotheses:

1) Temperature and photoperiod modify the effects of light fluctuations on growth
2) Temperature and photoperiod influence the form of the P-quota curve as well as relative P-uptake rates
3) Temperature and photoperiod influence the kinetics of silicon limited growth

4) The interactions of temperature and photoperiod with nutrient-limited growth are relevant in situ in spring for the spring species investigated
5) The types of interaction are species-specific and thus contribute towards niche differentiation, competitive ability and composition of the spring phytoplankton community

To examine these hypotheses, my approach is to use a series of laboratory culture experiments under phosphorus limitation, silicon limitation and limitation by fluctuating light, combined with statistical modelling of experimental and field data, and simple dynamic modelling of specific processes. The experiments were performed with the species *Stephanodiscus minutulus*, *Nitzschia acicularis* (diatoms) and *Limnothrix redekei* (cyanobacterium) because they are typical spring species and because extensive information on the growth kinetics of these species is available. To characterise the factor interactions, each growth experiment was performed at different temperatures and photoperiods under light saturation and the effects on the kinetic parameters of growth were examined. The aim of fluctuating light experiments was to determine whether the species-specific reduction in growth rates, which was found due to fluctuating light at 18-20°C, also applies at lower temperatures, which are associated with more intense mixing. I also aim to find out how the photoperiod and light fluctuations (as two aspects of temporal variability of the light supply) are related in terms of growth. The fluctuating light regime used simulates the exponential increase and decrease of irradiance due to intermittent vertical transport of algae in the mixed layer and the sinusoidal change of sunlight during the day.

The outcome of competition between species under nutrient limitation depends largely on the nutrient uptake affinity (Healey, 1980), but accurate uptake measurements can be difficult to obtain (Roloff and Nicklisch, 1993, Falkner et al., 1995). As an alternative, I used competition experiments between *S. minutulus* and *N. acicularis* under phosphorus and silicon limitation to provide some information on nutrient uptake characteristics. Using the measured growth kinetics and the rates of competitive exclusion, I deduced the relative P-uptake affinities and examined the consequences of discontinuous silicate uptake linked to the cell cycle. Furthermore, I investigated the applicability of the Droop and Monod models, which are the standard models for phosphorus- and silicon-limited growth, respectively (Martin-Jézéquel et al., 2000, Flynn, 2008c).

Light-saturated growth rates do not increase linearly with the photoperiod, but show saturation characteristics (Castenholz, 1964, Paasche, 1968, Foy et al., 1976, Gibson and Foy, 1983, Thompson, 1999, Nicklisch et al., 2008). Because of this nonlinear response, photoperiod treatments can only be compared if the daily light exposure (in mol m^{-2} d^{-1}) rather than the irradiance (in μmol m^{-2} s^{-1}) is kept constant (Kohl and Giersdorf, 1991, Nicklisch, 1998, Nicklisch et al., 2008). Therefore the irradiance was adjusted in experiments with different photoperiods to maintain approximately constant daily light exposure.

To examine the relative importance of the different growth factors and assess the relevance of factor interactions, long-term phytoplankton data from 1979-2004 during spring from a temperate, eutrophic lake (Müggelsee) were analysed. Since the timing and duration of the spring bloom can vary considerably depending on climatic and in situ conditions (Winder and Schindler, 2004, Berger et al., 2010, Berger et al., 2007), spring was defined not according to the calendar, but as the period between ice thaw and the clear water phase (Sommer et al., 1986, Sommer et al., 2012). Thus, the phytoplankton biomass and community structure could be statistically related to the actual conditions that prevailed during growth (Shatwell et al., 2008). Although this thesis focuses on spring, the results to some extent should be applicable to other seasons as well.

2. Methods

2.1 Algae strains

Growth experiments were performed with the phytoplankton species *Stephanodiscus minutulus* (Kütz.) Cleve and Möller (Bacillariophyceae), strain Mue0511A6, *Nitzschia acicularis* W. Smith (Bacillariophyceae), strain Mue070319C1, and *Limnothrix redekei* (Van Goor) Meffert (Cyanobacteria), strain HUB 010 (Figure 5). All strains were isolated from Lake Müggelsee (Berlin, 52.44°N 13.65°E). Cultures were unialgal except in competition experiments as described below. Cultures were axenic for phosphorus limitation experiments and also silicon limitation experiments. However, bacteria were usually detected in chemostats (Si-limitation) after about one to two weeks. Cultures for nutrient replete experiments under light fluctuations or light limitation were not bacteria free.

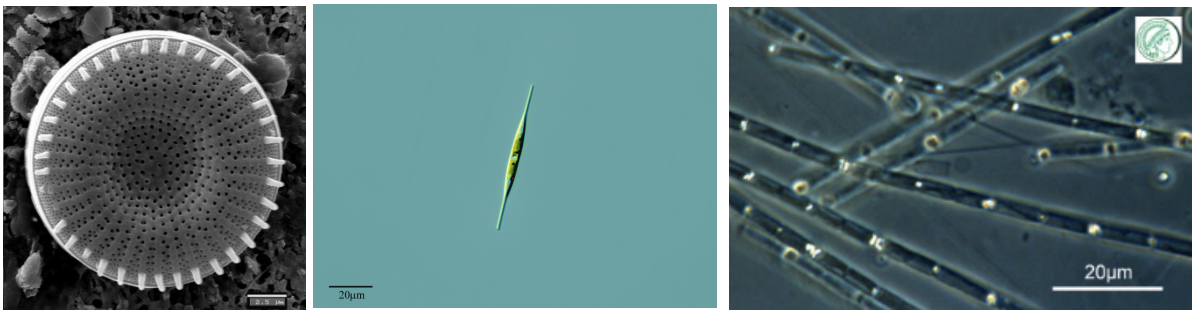

Figure 5: *Stephanodiscus minutulus* (left; scale bar 2.5 µm; photo author: Juan Alcober Bosch, http://eportal.magrama.gob.es/id_tax/ficha/buscador/1/30655), *Nitzschia acicularis* (centre; scale bar 20 µm; photo author Proyecto Agua **/** Water Project), *Limnothrix redekei* (right; scale bar 20 µm; photo author Barbara Meyer, Max Planck Institute of Limnology, planktonnet.awi.de)

2.2 Nutrient solution

S. minutulus and *N. acicularis* were grown in semi-continuous culture according to the chemostat principle (Nicklisch, 1999) under P limitation and according to the turbidostat principle under P-replete conditions. Algae were cultivated in a fully synthetic freshwater nutrient solution with an ionic-composition similar to the water of Lake Müggelsee (FW04, Nicklisch et al. 2008). The basis for this FW04-medium was the dissolution of calcium carbonate (0.9 mmol L^{-1}) in pure water with carbon dioxide under pressure. This basis solution was supplemented with 0.3 Na_2SiO_3, 0.1 Ca $(NO_3)_2$, 0.25 $MgSO_4$, 0.1 KCl, 0.01

KH_2PO_4, 0.20 HCl, all in mmol L^{-1}, a FeNaEDTA solution (final concentration 2 μmol L^{-1} Fe and 4 μmol L^{-1} EDTA), a trace element solution according to Nicklisch (1999) and a vitamin solution according to Guillard & Lorenzen (1972) slightly modified (final concentrations: 1 μg L^{-1} biotin, 1 μg L^{-1} cobalamin and 100 μg L^{-1} thiamine). The nutrients (300 μM Si, 200 μM N, 10 μM P, 2 μM Fe) were not limiting in the nutrient replete experiments at the low algal biomass densities used (< 300 μg Chl*a* L^{-1}) (Nicklisch and Steinberg, 2009). For P-limitation experiments, the P-concentration was decreased to 1.2 μM P. For Si-limitation experiments in chemostats and semi-continuous cultures, the Si and HCl concentrations were reduced to 1/5 of the nutrient-replete concentrations (60 μM Si and 40 μM HCl). For batch experiments under Si-limitation, flasks were prepared with different silicate concentrations ranging from 0.5 to 25 μmol Si L^{-1} by mixing different amounts of silicon-free medium and medium with 60 μmol Si L^{-1}. One flask in each Si-limited batch experiment was also maintained with complete FW04 solution at 300 μmol Si L^{-1}. Preliminary experiments showed that the Si concentration of 60 μM Si in chemostats was growth limiting for *S. minutulus,* because halving the concentration to 30 μM Si (keeping all other nutrients constant) decreased the steady-state biovolume by approximately half, while the residual Si concentration in the medium remained the same. Si was growth limiting in batch culture experiments with *N. acicularis* because biomass no longer increased after Si became depleted, as determined by monitoring concentrations and biomass until stationary phase. The solution was allowed to equilibrate with air by shaking to reach a pH of about 8.3 at 20°C and then sterilised by filtering it through a membrane of 0.2 μm pore diameter. In all cases except for chemostat experiments, the solution was subsequently heated by microwave to just below 100°C but not allowed to boil.

2.3 Algae cultivation

Stephanodiscus minutulus, *Nitzschia acicularis* and *Limnothrix redekei* were cultivated under a range of conditions to investigate the interactions with temperature and photoperiod (Table 2). All constant (light limited) and fluctuating light experiments were performed under nutrient-replete conditions and all nutrient limitation experiments were performed under constant saturating or near saturating light. All temperature treatments were performed under a 12 h d^{-1} photoperiod and all photoperiod treatments were performed at 15°C. Nutrient limited experiments were cultivated according to the chemostat principle (fixed dilution rate) (Nicklisch, 1999) and all nutrient replete experiments were cultivated according to the

turbidostat principle (fixed starting biovolume). In all experiments the light exposure in mol quanta m^{-2} d^{-1} was calculated as the sum of the irradiance over the photoperiod.

Table 2: Overview of algal culture experiments (T = temperature, LP = photoperiod)

Experiment	Culture type	Species	Light	Nutrients	T (°C)	LP (h d^{-1})
Growth under constant light	Semi-continuous (turbidostat)	*S. minutulus, N. acicularis, L. redekei*	Limiting-saturating, constant	Replete	10, 15, 20 15	12 6, 12
Growth under fluctuating light	Semi-continuous (turbidostat)	*S. minutulus, N. acicularis, L. redekei*	Limiting-saturating, fluctuating	Replete	10, 15, 20 15	12 6, 12
P-limited growth	Semi-continuous (chemostat)	*S. minutulus, N. acicularis*	Saturating, constant	1.2 μM P	10, 15, 20 15	12 6, 9, 12
P-limited competition	Semi-continuous (chemostat)	*S. minutulus, N. acicularis*	Saturating, constant	1.2 μM P	10, 15, 20 15	12 6, 12
Si-limited growth	Continuous (chemostat)	*S. minutulus,*	Saturating, constant	60 μM Si	5, 10, 15, 20 15	12 6, 9, 12
Si-limited growth	Batch	*N. acicularis*	Saturating, constant	0.5-25 μM Si	10, 15 15	12 9, 12
Si-limited competition	Semi-continuous (chemostat)	*S. minutulus, N. acicularis*	Saturating, constant	60 μM Si	10, 15, 20	12

2.3.1 Semi-continuous and batch cultures

Semi-continuous cultures were maintained in 300 mL Erlenmeyer flasks with 100 mL algal suspension. Batch cultures for growth experiments with *N. acicularis* under silicon limitation were grown in 1 L polycarbonate flasks with 300 mL suspension. All cultures were grown on an orbital shaker at 65-90 revolutions per minute in a climate chamber (± 0.5°C). Flasks were sealed with aluminium foil or, when light was supplied from above in fluctuating light experiments, with an inverted glass beaker. Nutrient replete cultures grown according to the turbidostat principle were diluted to a fixed biovolume of about 10 mm^3 L^{-1} every one to two

days (Table 2). Nutrient-limited cultures grown according to the chemostat principle were diluted every one or two days at a fixed dilution rate (0.2-0.9 d^{-1}). In experiments with constant light (see Table 2), irradiance was supplied by fluorescent tubes of light colour Biolux and Warm White (Osram, Munich, Germany) at a ratio of 1:1. In nutrient limitation experiments, cultures were positioned relative to the light source so that each culture received the same light intensity, whereas in light-limitation experiments, cultures were arranged asymmetrically to get different irradiances. The scalar photon flux density of the photosynthetically available radiation (PAR in μmol quanta m^{-2} s^{-1}) was measured using a spherical sensor (QSL-101, Biospherical Instruments, California, USA). The irradiances used in nutrient limitation experiments were saturating as determined from growth-irradiance curves previously measured for these species at the experimental temperatures and photoperiods (Kohl and Giersdorf, 1991, Nicklisch et al., 2008) and from the light limitation experiments performed in this study. The irradiances or light exposures are given in the tables and figures in the results section. The light conditions and measurement methods for fluctuating light experiments are described in section 2.6 (p. 18). Self-shading was minimised by the low biomass concentration (< 300 μg Chl *a* L^{-1}) and the shallow depth of the culture suspension in the flasks.

2.3.2 Continuous chemostat cultures

In Si-limited continuous culture experiments, 3 chemostats (boro-silicate glass) of volume 200, 400 and 600 mL were used (Figure 6). Fresh medium was added at a constant dilution rate using peristaltic pumps (Gilson Minipuls 3, Wisonsin, USA). It was assumed that leaching of silicate from the glass chemostats was negligible compared to the inflow of silicon in the medium (3 – 30 μmol Si d^{-1}). The dilution rate was monitored by collecting the overflow in a flask on a laboratory balance and automatically recording the weight every 30 minutes. The cultures were mixed and aerated by bubbling with air at approx. 2 L min^{-1}, which was previously passed through deionised water and two sterile inline air filters (Sartorius 0.2 μm pore size). Contamination of the stock nutrient solution by algae and bacteria was prevented by the positive air pressure gradient, a bacteria trap and the pump. Any wall-growth inside the chemostats, which was not visibly evident during the experiments, was minimised by scraping each day the inside walls using a magnet and magnetic rod inside the chemostat. Areas of low turbulence in the chemostat as well as tubing were covered with light-impermeable foil to further minimise wall growth. Chemostats were fitted with a water jacket and cooled to the desired temperature using a circulating refrigerated bath. The volume

of the chemostats at equilibrium with the air supply was previously measured both volumetrically and by weight. Cultures were illuminated with fluorescent tubes of light colour "warm white", "neutral white" and "daylight" in equal proportions and light intensity was measured with a spherical sensor (QSL-101, Biospherical Instruments, California, USA).

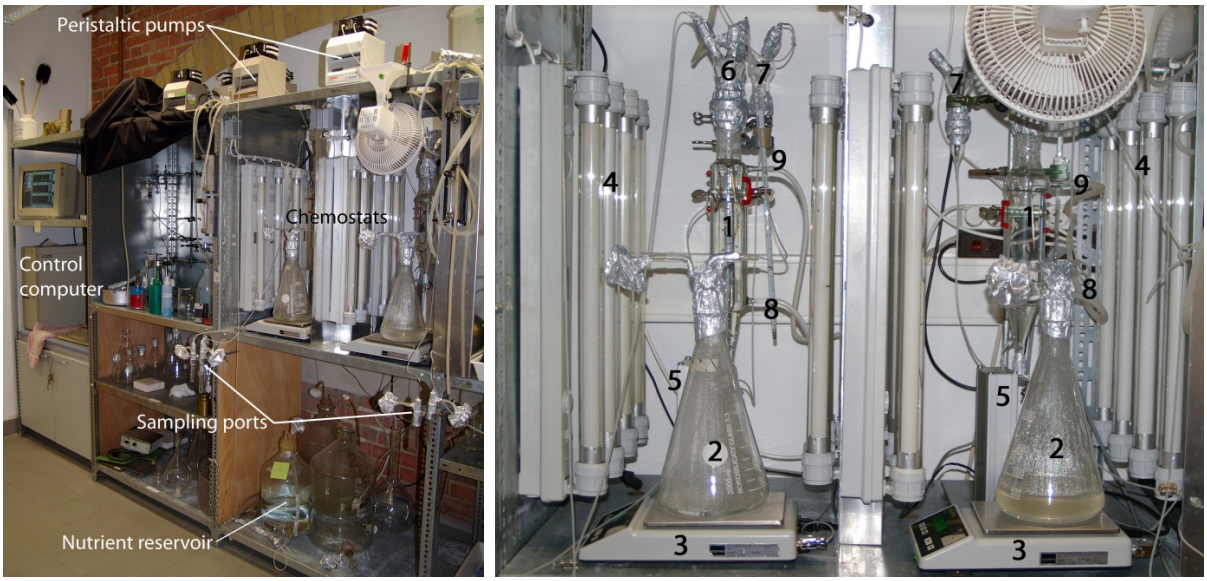

Figure 6: Continuous chemostat experimental setup. 1: culture chamber, 2: overflow reservoir, 3: lab balance, 4: light source, 5: automatic turbidity meter, 6: connections and tubing for overflow and sampling, 7: bacteria trap and vessel for mixing air and nutrient supply, 8: cooling water inflow, 9: cooling water outflow.

2.4 Biomass measurements

For steady-state growth rate experiments (i.e. all experiments excluding batch cultures and competition experiments, see Table 2) the biomass was determined by photometry at a wavelength of 436 nm (5 cm cuvette, Shimadzu photometer type UV-2401 PC). The focus of the light beam and the distance between cuvette and photomultiplier in this photometer excludes most of the scattered light, including forward scattered light, from detection. Therefore, the measured absorbance was due to scattering (about 80 %) and pigment absorption (about 20 %). In parallel, chlorophyll fluorescence (F_o) and variable fluorescence (F_v) were measured using a Xenon-PAM Fluorometer (Heinz Walz GmbH) after dark adaptation for 20 minutes. F_o is closely correlated to Chl *a* content and F_v (the increase in fluorescence above F_o after a light saturation pulse, known as the Kautsky effect) is closely related to the total photosystem II activity (PS II; Schreiber and Bilger, 1993). The chlorophyll and variable fluorescence were used to monitor the condition of the cultures and

also as surrogates for biomass. Since F_v reacts very sensitively to the onset of nutrient limitation (Nicklisch and Steinberg, 2009), I could ensure that nutrients did not become limiting in the nutrient-replete treatments. Photometric measurements of biomass were calibrated using cell counts and biovolume, which were measured regularly using a cell counter (Casy, Model TTC, Schärfe System) for the two unicellular diatoms. For *L. redekei* the biomass was determined using the following relationship, which provided accurate results as verified by microscopic measurements (Nicklisch unpublished):

$$X = -197.4\left(\ln\left(1 - \frac{\Delta E_{436}}{4.2032}\right)\right) \quad (1)$$

where X is the biovolume in $mm^3\ L^{-1}$ and ΔE_{436} is the absorbance at 436 nm. Samples were only taken from cultures when growth was balanced (where all biomass components grow at the same overall rate per day, but vary hour by hour under light : dark cycles). In this case, the biomass composition is similar at the same measuring time each day and the specific growth rates are not only biomass-specific but also carbon or Chl *a*-specific.

2.5 Specific growth rate determinations

Under balanced growth, the specific growth rates can be calculated using the change in absorbance at 436 nm, F_o and F_v, where the growth rates calculated separately with these three parameters are equal when the culture is in quasi-steady state. The three growth rates estimated from absorbance, F_0 and F_v were therefore averaged to obtain the most accurate estimate of the true rate. The different calculation methods produced nearly identical results (< 1% difference) and there was no systematic bias between methods ($p = 0.8$). In semi-continuous cultures, the specific growth rate (μ) is given by

$$\mu = \ln\left(\frac{X_1}{X_0}\right) \times \frac{1}{\Delta t} \quad (2)$$

where X_0 is the initial biomass and X_1 is the biomass after time Δt. Accordingly, the overall growth rate was calculated as the mean of the growth rates based on absorbance at 436 nm, F_o and F_v. For continuous chemostat cultures, the dilution rate (D) must also be considered:

$$\mu = \ln\left(\frac{X_1}{X_0}\right) \times \frac{1}{\Delta t} + D \quad (3)$$

In nutrient-replete cultures, means of the specific growth rates were determined over two to four weeks for high and low growth rates respectively. In nutrient-limited cultures grown at a fixed dilution rate (chemostat mode), the specific growth rate is equal to the dilution rate at (quasi) steady state. However, there were day to day fluctuations in growth rate, and the individual growth rates measured on each sampling day were related to the corresponding P-quota or DSi concentration measured on that sampling day rather than to long-term means for each culture.

In batch cultures under silicon limitation, cell counts and biovolume were measured daily directly with a cell counter (Casy, Model TTC, Schärfe System). The growth rates were calculated according to Eq. 2 as the slope of the linear regression line through the natural logarithms of cell counts and biovolumes plotted over time. A mean was taken of cell and biovolume-based growth rates.

2.6 Fluctuating light experiments

Fluctuating light experiments were performed with *S. minutulus*, *N. acicularis*, and *L. redekei* in semi-continuous culture. Light fluctuations were designed to simulate the natural light environment in the mixed layer of a lake, with two components: the exponential increase and decrease of intensity that algae experience as they are transported through the mixed layer due to vertical mixing, and the sinusoidal variation of intensity of sunlight over a cloudless day. When the mixing depth (z_{mix}) is greater than the euphotic depth (z_{eu}) the photoperiod is reduced according to the time spent outside the euphotic zone as follows:

$$LP_{eff} = LP \times \min\left\{\begin{matrix} z_{eu} : z_{mix} \\ 1 \end{matrix}\right\} \quad (4)$$

where LP_{eff} (for light period, h d^{-1}) is the effective photoperiod and LP (h d^{-1}) is the overall photoperiod (see Table 1 for abbreviations). Fluctuating light was provided by four 400 W halogen metal vapour lamps of colour Neutral White and Daylight (two each, Hydrargyrum Quartz Iodide, HQI) above the climate chamber (Figure 7). Mounted between the climate

chamber and the light source was a shutter with lamellae which open and close to generate the light fluctuations, and a glass water bath (distilled water, layer thickness 5-8 cm) to absorb heat and ultraviolet radiation from the lamps.

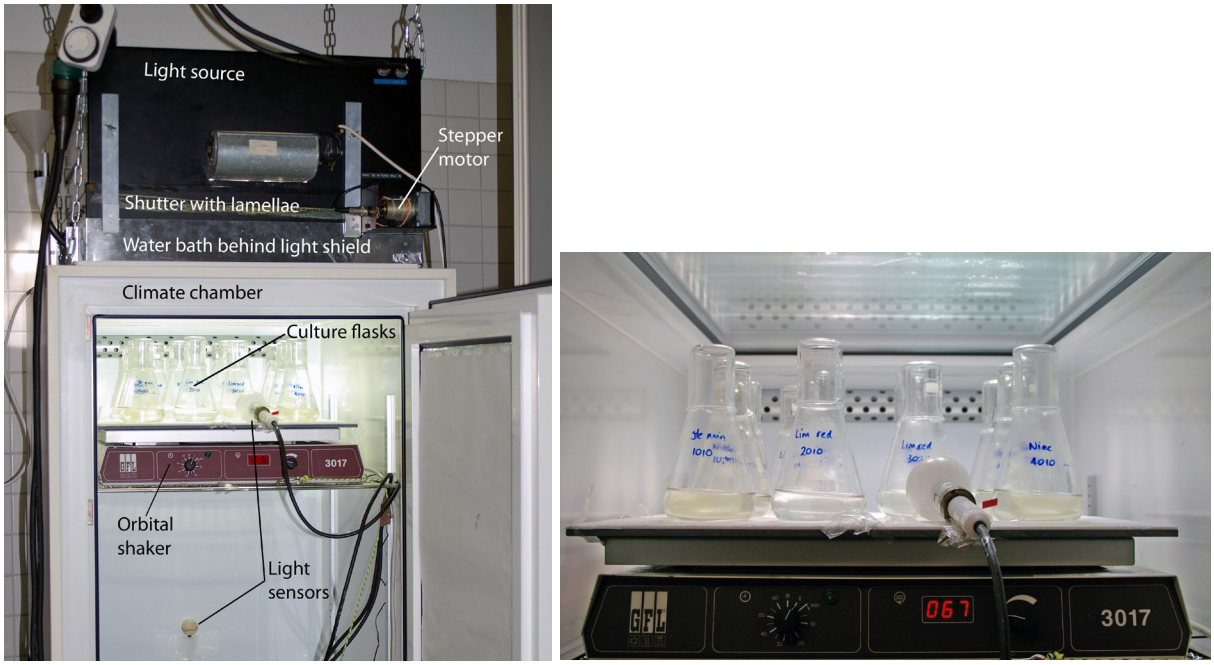

Figure 7: Experimental setup for fluctuating light experiments

The lamellae were driven by a stepper motor and programmed to generate an exponential increase of light intensity up to I_o (surface irradiance) and decrease down to I_{zmix} with a period of 30 minutes (used here to roughly describe intermittent vertical transport), where I_o follows a sine curve over the overall photoperiod (daily course of sunlight) with an overall maximum intensity of I_{max} (Figure 8). I_{zmix} was set to 1% and 0.01% of I_o to simulate fluctuations with z_{eu}:z_{mix} of 1 and 0.5, respectively, assuming that the euphotic depth occurs when the irradiance is 1% of the surface irradiance.

To investigate the temperature interactions, growth rates were measured at 10°C, 15°C, and 20°C under constant light and 12 h d^{-1} photoperiod (CL_{12}, Table 3) and under fluctuating light at 12 h d^{-1} photoperiod with z_{eu}:z_{mix} = 1 (FL_{12}). To investigate the photoperiod interactions, growth rates were also measured at 15°C under constant light at 6 h d^{-1} photoperiod (CL_6) and under fluctuating light at 6 h d^{-1} photoperiod with z_{eu}:z_{mix} = 1 (FL_6). Finally, growth rates were measured under fluctuating light at 12 h d^{-1} photoperiod simulating deep mixing with z_{eu}:z_{mix} = 0.5 ($FL_{12}D$).

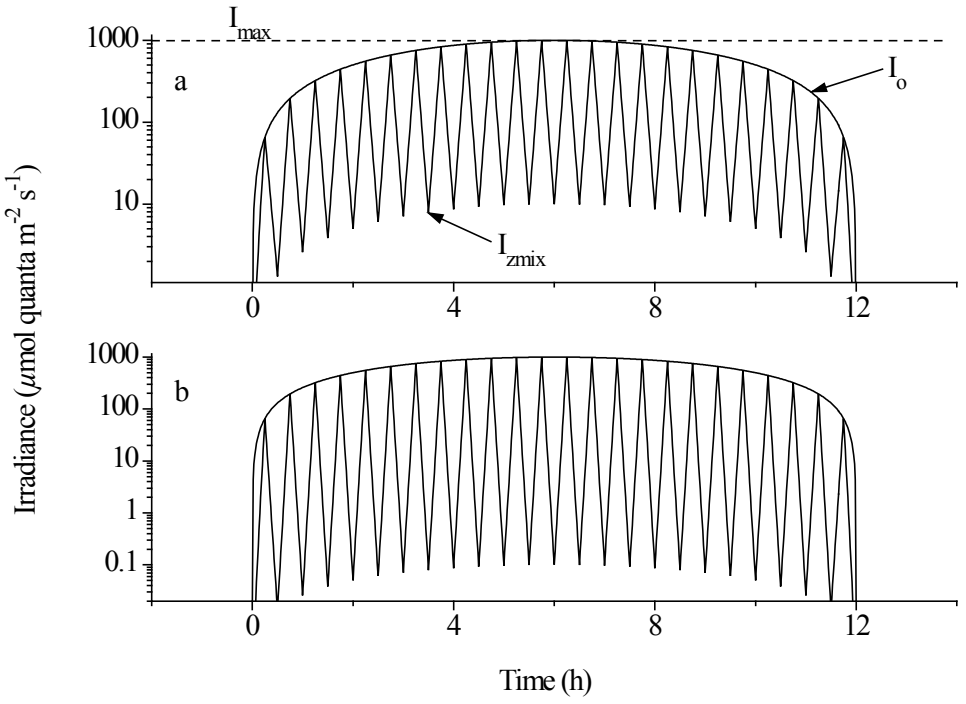

Figure 8: Structure of the fluctuating light regimes, here showing (a) the FL_{12} regime (12 h d^{-1} photoperiod, z_{eu}:z_{mix} = 1, such that I_{zmix}:I_o = 0.01) and (b) the $FL_{12}D$ regime (z_{eu}:z_{mix} = 0.5, such that I_{zmix}:I_o = 0.0001).

The different temperature, photoperiod and fluctuation treatments were always compared at the same daily light exposure (LE). Since it was difficult to adjust the total daily light exposure to exact predefined values in the experimental setup, and to increase statistical robustness, growth rates were measured over a range of light exposures from growth limitation to growth saturation and curves were fitted to the growth rates. The treatments were thus compared by comparing the respective curves. Accordingly, to obtain a range of daily light exposures while holding z_{eu}:z_{mix} constant, I_{max} was varied with the computer program in the range shown in Table 3, such that $I_{max} \approx 2038 \times LE / LP_{eff}$ (for units and abbreviations, see Table 1). The achievable range of light intensities with the experimental setup was about 0.06 – 1950 μmol quanta m^{-2} s^{-1}.

Cultures were first acclimated to the experimental conditions for one to two weeks, depending on the growth rates. During this phase and the subsequent experiments, biomass was measured as described in section 2.4 (p. 16). When cultures were in quasi-steady state and growth was balanced, the cultures were sampled every day or every second day in the middle of the photoperiod. Specific growth rates were then measured as described in section 2.5 (p. 17).

Table 3: Summary of experimental treatments and light regime names used. z_{eu}:z_{mix}: ratio of euphotic to mixed depth; LP: photoperiod, LP_{eff}: effective photoperiod; Imax: peak irradiance at the middle of the photoperiod.

Light regime	Description	z_{eu}:z_{mix}	LP (h d^{-1})	LP_{eff} (h d^{-1})	I_{max} (μmol m^{-2} s^{-1})	Temperatures (°C)
CL_{12}	Constant light, long photoperiod	∞	12	12	10-130	10, 15, 20
FL_{12}	Fluctuating light, long photoperiod	1	12	12	200-1300	10, 15, 20
CL_6	Constant light, short photoperiod	∞	6	6	30-200	15
FL_6	Fluctuating light, short photoperiod	1	6	6	620-1050	15
$FL_{12}D$	Fluctuating light, long photoperiod, simulating deep mixing	0.5	12	6	600-1000	15

Photosynthetically available radiation (PAR) in the constant light experiments was measured with a spherical sensor (QSL-101, Biospherical Instruments). In fluctuating light experiments, PAR was recorded at 1 minute intervals at each culture position under experimental conditions with a spherical sensor (Li-193A with a Li-1000 data logger, LI-COR). The two different light sensors were calibrated against each other in sunlight.

2.7 Phosphorus limitation experiments

2.7.1 Growth rate experiments

In P-limited growth experiments, cultures were grown at 10, 15, and 20°C with a photoperiod of 12 h d^{-1} to investigate temperature interactions, and under photoperiods of 6, 9, and 12 h d^{-1} at 15°C to investigate the photoperiod interactions. Light exposures were saturating or near-saturating for all experiments (see Table 8; all growth rates were ≥ 80% of the asymptotic maximum growth rates) as determined from the growth-irradiance curves for these species measured in section 3.1 and also in the literature (Kohl and Giersdorf, 1991, Nicklisch et al., 2008, Shatwell et al., 2012). First, nutrient replete cultures were acclimated to the desired

conditions of temperature, photoperiod and irradiance for 5 to 7 days. During this phase and the ensuing experiment, the biomass and growth rates were determined every day or every second day (at low growth rates) as described in section 2.4 (p. 16) and section 2.5 (p. 17). After acclimation when the cultures had reached balanced growth, as evident from absorbance and fluorescence measurements, the maximum specific growth rates were determined in turbidostat mode. In these experiments, cultures were diluted to a constant starting biomass each day and the dilution rate was adjusted accordingly. The growth rate was then determined from the dilution rate. The growth experiments were carried out for two to four weeks to obtain a mean of the specific growth rate. The longer measuring periods were needed for low growth rates at low temperatures or short photoperiods.

To determine P-limited growth rates, nutrient replete cultures which had been acclimated to the experimental conditions as described above were diluted with P-free medium so as to achieve a final concentration of 1.2 μM P, and subsequently allowed to starve for 2 to 5 days. The algae were then further cultivated semi-continuously with FW04 medium containing 1.2 μM P at a constant dilution rate (0.2 – 0.8 d^{-1}). The cultures reached a steady state within 1 to 2 weeks so that the specific growth rate was equal to the dilution rate, and biomass was constant at each dilution. It was assumed that the P added at dilution is absorbed very rapidly and that biovolume then increases practically linearly, so that the P-quota determined exactly midway between dilutions is representative of the growth rate measured between dilutions. The P-quota associated with the measured growth rate was then calculated as the total P concentration in the medium per biovolume (or cell number), which were measured using a cell counter (CASY, Modell TTC, Schärfe System, Germany). This investigation considered the actual short term growth rates measured between dilutions, rather than those derived from the applied dilution rates, which usually differed slightly. The maximum yield (reciprocal of the minimum quota Q_0) was determined by allowing the cultures to grow without dilution until they reached a maximum biomass (usually 1 – 2 weeks). The total P-content of cultures was checked at the end of the experiments by standard methods (DEV, 2007).

2.7.2 Competition experiments

In competition experiments, axenic, unialgal cultures of *S. minutulus* and *N. acicularis* were first acclimated to the desired conditions of temperature, photoperiod and irradiance and then grown under P-limitation at the dilution rate required for the later competition experiments. Once the cultures had reached balanced growth within 1 - 2 weeks, equal culture volumes of

the two species were mixed so that each species initially contained 50% of the total phosphorus, although occasionally different proportions were used. The mixed cultures were further cultivated semi-continuously for one to three weeks at a constant dilution rate of 0.4-0.5 d^{-1} at 10°C, 15°C and 20°C with a 12 h d^{-1} photoperiod and also at 15°C with a 6 h d^{-1} photoperiod. Irradiances were saturating or near-saturating (85 – 200 μmol PAR m^{-2} s^{-1} corresponding to daily light exposures of 3.7 – 5.2 mol PAR m^{-2} d^{-1}) and are given in the results section (Table 10, p. 61). The proportions of each species were measured in fixed samples (0.25 % glutaraldehyde final concentration) every one or two days using a flow cytometer (FACStar-Plus, Becton Dickinson, San Jose, USA) according to Nicklisch and Steinberg (2009). While there was some error in the absolute cell counts by the flow cytometer, the proportions of the species were accurate as verified by microscopic counts. Cells from the different species in the mixed cultures were distinguished based on their forward scatter signals and the Chl *a*-autofluorescence excited by a blue laser at 488 nm.

2.8 Silicon limitation experiments

2.8.1 Growth rate experiments in continuous culture

S. minutulus was grown in continuous chemostat culture under silicon limitation at 5°C, 10°C, 15°C and 20°C with a photoperiod of 12 h d^{-1} to investigate temperature interactions, and under photoperiods of 6 h d^{-1}, 9 h d^{-1} and 12 h d^{-1} at 15°C to investigate the photoperiod interactions. Light exposures were saturating for all experiments. First, nutrient replete cultures which had been acclimated to the experimental temperature and photoperiod in semi-continuous culture for at least one week were diluted with Si-free medium so as to achieve a final concentration of 60 μmol Si L^{-1} before being introduced into the chemostats under sterile conditions. The algae were then further cultivated with a nutrient solution containing 60 μmol Si L^{-1} at a constant dilution rate (0.2 – 0.9 d^{-1}) until cultures reached steady state (generally 1 week). Steady state conditions were determined by turbidity measurements at 880 nm using a sterilised self-made turbidity meter with 1cm path length at 30 minute intervals (Walz et al., 1997), as well as daily measurements of absorbance at 436 nm, chlorophyll fluorescence (F_o) and variable fluorescence (F_v) as described in section 2.4 (p. 16). At steady state the specific growth rate was equal to the dilution rate and biomass was constant at the same measuring time each day. Once cultures had reached steady-state, samples were taken at the same time each day in the middle of the light period for one week (4-5 samples per

dilution rate) for determination of DSi concentration as described in section 2.11 (p. 27), biomass as described in section 2.4 (p. 16), growth rates as described in section 2.5 (p. 17), and cell counts with a cell counter (CASY, Modell TTC, Schärfe System, Germany).

2.8.2 Growth rate experiments in batch culture

N. acicularis failed to grow in chemostats, presumably due to the increased turbulence from aeration, and was therefore grown in batch culture under silicon limited and silicon replete conditions at 10°C and 15°C under a 12 h d^{-1} photoperiod and also under a 9 h d^{-1} photoperiod at 15°C. Light was saturating for all experiments. Batch cultures of *N. acicularis* were inoculated to a concentration of 300 cells mL^{-1} from stock cultures maintained semi-continuously in FW04 medium with 60 μmol Si L^{-1} at a dilution rate of 0.2 d^{-1} which had been previously adapted for at least two weeks to the required temperature, light and photoperiod for the subsequent experiments. Silicon concentrations were measured at the start and at the end of batch culture experiments after 5 days and also once or twice in between. Cell numbers and volume were monitored during experiments at the same time each day in the middle of the photoperiod with a cell counter (CASY, Modell TTC, Schärfe System, Germany). After experiments, cultures were allowed to grow to stationary phase and silicon concentrations continued to be monitored until growth ceased to determine the minimum concentration required for growth. Silicon concentrations did not decrease by more than 10% during batch growth experiments except under 15°C / 12 h d^{-1}, when some concentrations decreased by up to 70%. However, this decrease probably occurred on the last day of the experiment, and did not visibly affect daily measurements of the growth rates until after the experiment, when Si was completely depleted. Growth rates were determined as described in section 2.5 (p. 17).

2.8.3 Competition experiments

Competition experiments between *S. minutulus* and *N. acicularis* were performed in semi-continuous culture under silicon limitation in duplicate at 10°C, 15°C and 20°C under a photoperiod of 12 h d^{-1}. Unialgal inoculum cultures were acclimated to the experimental conditions by cultivating them under Si-limitation with FW04 medium at 60 μmol Si L^{-1} for at least one week at the same temperature, photoperiod, irradiance and dilution rate required for the subsequent experiments. During this time, cultures were diluted and sampled daily, and absorbance at 436 nm as well as F_o and F_v were monitored as described in section 2.4 (p. 16) to ensure the cultures had reached steady state and growth was balanced. When the

unialgal cultures had reached steady state, they were mixed in equal proportions by volume and further cultivated semi-continuously. The applied dilution rates were 0.4 d^{-1} at 10°C and 0.5 d^{-1} at 15° and 20°C. The daily light exposure was saturating or near saturating at 5.2, 5.8, and 3.0 mol m^{-2} d^{-1} at 10°C, 15°C, and 20°C respectively. During the competition experiments, 10 mL samples were removed every day before dilution and immediately fixed at 1:100 with glutaraldehyde solution (25% for electron microscopy, Merck, Darmstadt Germany) and stored at 4°C in the dark until counting. The proportions of cells of each species were counted by microscope (200X – 400X). At least 400 cells were counted from each sample.

2.9 Measurement of pigment content

Pigment contents were measured by high performance liquid chromatography (HPLC) (Mehnert et al., 2012, Shatwell et al., 2012). Culture samples (30 - 50 mL) were filtered through 25 mm Whatman GF/F-filters. The filters were placed into 2 mL safety reaction vessels, frozen at -85°C, freeze dried within 2-4 weeks at controlled temperature below -20°C in the dark and thereafter stored at -25°C in the dark until analysis. Pigments were extracted with 1 mL dimethylformamide (Wright and Jeffrey, 1997) in a vibration shaker (VIBRAX-VXR, IKA-Labortechnik, Staufen, Germany) at a frequency of 2000 min^{-1} for 45 min with a supplement of glass beads (0.75–1 mm) in the dark. After the addition of 0.1 mL of 1 mol L^{-1} ammonium acetate in high-purity water, the extraction was continued for a further 45 min. Samples were handled under dim light at 4 °C. The extract was centrifuged for 20 min at 2500 g and 4 °C in a cooled centrifuge and 0.2 ml of the supernatant was carefully pipetted at dim light into vials and stored in an auto-sampler at 4 °C in the dark.

Pigments were separated, identified and quantified according to Woitke *et al.* (1994) with some modifications. The HPLC system (Waters Alliance, Millford, MA, U.S.A.) comprised a Waters 2695 separations module and a 2696 photo diode array detector. Pigments were separated at a flow rate of 1.0 mL min^{-1} at 30 °C through a Waters Symmetry C18 column (3 μm particle size, 15 cm), protected with a Symmetry C-18 pre-column. An optimised gradient from eluent A to eluent B was used: Eluent A consisted of methanol, acetonitril and 1 μmol L^{-1} ammonium acetate in high-purity water (45:45:10) + 3 % of 0.1 mol L^{-1} ammonium acetate. Eluent B consisted of acetonitril and acetone (45:55). The timetable of the linear gradient is given in Table 4.

Table 4: Timing of linear eluent gradients for HPLC measurements

Time	Eluent A (%)	Eluent B (%)
0	100	0
0.5	100	0
4.5	80	20
6.0	80	20
11.0	0	100
16.5	0	100
17.5	100	0
25	100	0

60 μL extract was injected with a water packing of 20 μL before and 10 μL after the sample (Wright et al., 1997, van Leeuwe et al., 2006). Peak areas were monitored at 440 nm (all pigments including chlorophyll *a*) and 410 nm (chlorophyll *a* and its derivatives only), and the pigment spectra were monitored in the range from 350 to 700 nm.

Pigments were identified by their relative retention times and by their absorption spectra. Unialgal cultures, standards and literature data were used for comparison. Peak area integration allowed quantification with factors determined by (Woitke et al., 1994) that were checked by standards supplied by Hoffmann-La Roche AG (Grenzach, Germany) or Carbon 14 Centralen (Hørsholm, Denmark) from time to time. Chlorophyll *a* from *Anacystis nidulans* (Sigma-Aldrich) was used as standard for frequent examination of performance. Chlorophyll *a* was determined as a mean of the readings at 440 and 410 nm and was calculated as the sum of the true chlorophyll *a*, its epimer, its allomer, chlorophyllide *a* and other detectable derivatives with the typical spectrum of chlorophyll *a*. Pheophytin *a* was calculated on the basis of the 410 nm readings.

2.10 Electron transport rates

Electron transport rates were measured using the variable fluorescence yield of PS II in rapid light curve measurements using a PAM fluorometer (PhytoPAM, Heinz Walz) and the method given in Nicklisch and Köhler (2001). A modified version of the model of Eilers and Peeters

(1988) was fitted to relative electron transport rates using the software provided with the fluorometer (PhytoWin v 2.11, Heinz Walz). The model parameters were fitted and then averaged for measuring wavelengths of 470 and 535 nm for *S. minutulus* and *N. acicularis* and 535 and 620 nm for *Limnothrix redekei*. Electron transport rates were expressed in relative units.

2.11 Silicate determination

To determine DSi concentrations, samples were filtered on 2.0 μm polycarbonate membranes (Whatman, 25mm diameter) immediately after being taken, and the filtrate was stored at 4ºC in the dark in plastic containers which had been pre-rinsed with a Si-reagent solution and double-distilled water. Silicate concentrations of the sample filtrates were measured using a modified silicomolybdate method according to DEV (2007) which was determined to be accurate to within 0.05 μmol Si L^{-1}. Samples were analysed at 810 nm (Shimadzu photometer type UV-2401 PC) using a 5cm cuvette for concentrations up to 7 μmol Si L^{-1} and a 1cm cuvette for higher concentrations. The silicon content of cells was determined as the difference in silicon concentration in the fresh medium and in the culture divided by the number of cells, or biovolume.

2.12 Lake data

Lake Müggelsee is a shallow (mean depth 4.9 m) polymictic lake in Berlin (Germany, 52.44°N 13.65°E), with a surface area of 7.3 km^2, a catchment area of 7000 km^2 and a theoretical mean retention time of about 6–8 weeks (Köhler et al., 2005). The lake analysis is described in detail in Nicklisch et al. (2008) and Shatwell et al. (2008). Global radiation, the underwater light attenuation of the scalar photosynthetically available radiation and the temperature were measured daily at a station close to the north shore (Köhler *et al.* 2005). The euphotic depth (z_{eu}) was calculated as the depth where the radiation reaches 0.8 % of net surface radiation (I_0') (Reynolds, 1984). The length of the effective photoperiod was calculated as the length of the solar day multiplied by the ratio of the volume of the euphotic zone to the volume of the whole lake (Foy et al., 1976, Nicklisch et al., 2008). Irradiance at the lake surface was calculated from gross incoming global radiation by subtracting 8% for reflection and backscattering and assuming that 50% of global radiation is photosynthetically

available radiation (PAR) (Nicklisch et al., 2008). The mean light exposure was calculated by integrating the exponentially decreasing PAR over the mixed depth according to the Beer-Lambert law, and then dividing it by the mixed depth (Nicklisch et al., 2008). Samples were taken weekly from spring to autumn and biweekly in winter according to a sampling procedure described in Shatwell et al. (2008). Phytoplankton samples were fixed with Lugol´s solution and analysed using an inverted microscope to obtain biovolumes of individual species or algal groups. Concentrations of dissolved silicon (DSi) and total phosphorus (TP) were analysed by standard methods (DEV, 2007).

2.13 Statistical models and analyses

2.13.1 The base model of nutrient replete growth

The starting point of this thesis is a model of phytoplankton growth developed by Nicklisch et al. (2008), for the phytoplankton species *Stephanodiscus minutulus*, *Nitzschia acicularis*, *Limnothrix redekei* and *Planktothrix agardhii*, which is summarised in this section and hereafter referred to as the "base model". The model accounts for the effects of and interactions between light exposure (LE), temperature (T) and photoperiod (LP) on the growth of algae, where light is considered to be the resource and the temperature and photoperiod are considered to be control factors which determine how the algae use this resource. It is based on the concept of an overall maximum specific growth rate ($\mu_{max,}$ biomass-specific) which is achievable under optimum conditions (extrapolated from measured rates), that is at light and nutrient saturation, under long photoperiods and at optimum temperature. This maximum growth rate is then decreased by a series of mathematical functions to account for the effects of suboptimal temperature (f(T)), suboptimal photoperiod (f(LP)) and suboptimal light exposure (f(LE)). The model begins with an exponential saturation equation to describe the nutrient replete specific growth rates, μ_{NR} (d^{-1}) as a function of the resource (LE, mol quanta $m^{-2}\,d^{-1}$):

$$\mu_{NR} = \mu_m\left(1-\exp\left(\frac{-\alpha_{LE}(LE-LE_{min})}{\mu_m}\right)\right) \quad (5)$$

where μ_m is the maximum specific growth rate (d^{-1}), which is light and nutrient saturated but at suboptimal temperature and photoperiod, α_{LE} is the initial slope of the curve (m^2 mol^{-1} quanta), and LE_{min} is the light compensation point (mol quanta m^{-2} d^{-1}).

The interactions between light exposure and temperature and between light exposure and photoperiod seem well-established: temperature and photoperiod do not influence the initial slope of the growth-light curve (α_{LE} in Eq. 5) but do influence the maximum growth rate (μ_m) (Paasche, 1967, Paasche, 1968, Yoder, 1979, Foy, 1983, Nicklisch and Kohl, 1989, Kohl and Giersdorf, 1991, Thompson, 1999, Nicklisch et al., 2008, Shatwell et al., 2012). Accordingly α_{LE} is a constant in the model, whereas μ_m is temperature and photoperiod dependent as follows:

$$\mu_m = \mu_{max} \times f(T) \times f(LP) \tag{6}$$

where μ_{max} (d^{-1}) is the overall maximum growth rate under optimum conditions, and f(T) and f(LP) are the functional temperature and photoperiod dependencies, respectively.

To describe the temperature dependence, a function after Lehman (1975) is used:

$$f(T) = \exp\left(-2.3\left(\frac{T_{opt} - T}{T_{opt} - T_{min}}\right)^2\right) \tag{7}$$

where T is the temperature, T_{opt} is the optimum temperature and T_{min} (all in °C) is the temperature at which the function takes on a value of 0.1. The influence of the photoperiod on μ_m can be described by an exponential saturation function of the same form as Eq. 5:

$$f(LP) = 1 - \exp\left(\frac{-\alpha_{LP}(LP - LP_{min})}{\mu_{mLP}}\right) \tag{8}$$

where α_{LP} is the initial slope of the curve (h^{-1}), LP_{min} is the minimum photoperiod for growth (h d^{-1}), and μ_{mLP} (d^{-1}) is the maximum specific growth rate when photoperiod is "saturating" (i.e. LP = 24 h d^{-1}) and is limited only by temperature.

Table 5: Parameters of the base model (Nicklisch et al., 2008)

Parameter	Units	*Stephanodiscus minutulus*	*Nitzschia acicularis*	*Limnothrix redekei*	*Planktothrix agardhii*
μ_{max}	d^{-1}	1.46	1.82	0.89	0.76
α_{LE}	$m^2\ mol^{-1}$	0.67	0.83	0.46	0.32
LE_{min}	$mol\ m^{-2}\ d^{-1}$	0.31	0.24	0	0.05
α_{LP}	h^{-1}	0.22	0.32	0.24	0.26
LP_{min}	$h\ d^{-1}$	0.4	2.0	2.0	1.4
T_{opt}	°C	20.7	21.7	23.6	27.2
T_{min}	°C	-0.6	1.0	0.4	5.5

Eqs. 5 to 8 describe the interactions between light exposure and temperature and between light exposure and photoperiod, but there still remains the interaction between photoperiod and temperature, which can be described by

$$\mu_{mLP} = \mu_{max} \tag{9}$$

which applies to *N. acicularis*, *L. redekei* and *P. agardhii* (Nicklisch et al., 2008) and apparently also to *Aphanizomenon flos-aquae* (Gibson, 1985) and *Schizothrix calcicola* (Tang and Vincent, 2000). On the other hand, *S. minutulus* had a more complex interaction, given by:

$$\mu_{mLP} = \mu_{max} \times f(T) \tag{10}$$

which also applied to *Thalassiosira pseudonana* (Thompson, 1999). Eq. 9 implies that α_{LP} is temperature dependent, whereas Eq. 10 implies that α_{LP} is independent of temperature. The parameters of the model of Nicklisch et al. (2008) are given in Table 5.

2.13.2 Fluctuating light experiments

The growth-light exposure function from the base model (Eq. 5, p. 28) was used to analyse growth rates in the fluctuating light experiments. When fitting the model, it was assumed that

the initial slope α_{LE} estimated at 15°C was independent of temperature and photoperiod and thus also applied at 10°C and 20°C where light-limited growth rates were not measured.

Model parameters under different treatments were compared using *t*-tests. The percentage reduction in μ_m due to different light treatments was estimated by non-linear regression and the estimates for different treatment combinations were compared with *t*-tests. Pigments and photosynthetic parameters from fluorescence measurements were analysed using one-way and two-way analysis of variance with temperature and/or type of light regime as factors. Differences between variables that were strongly dependent on light were also analysed using analysis of covariance with daily light exposure or mean irradiance as the covariates. The individual measurements (up to 5 per culture) were used in statistical analyses, whereas culture means are shown in the figures in the results for simplicity. Unless otherwise stated, means ± SD are given. Statistical analyses were performed with R (version 2.13.0, R Development Core Team, 2009) and non-linear growth models were fitted with SPSS for Windows (version 17).

2.13.3 Phosphorus limitation experiments

To analyse P-limited growth measurements, different types of rectangular hyperbolic (HYP) and exponential (EXP) saturation curves with and without a half-saturation constant (k_Q), were fitted to the experimental data and compared. Each curve describes the specific growth rate (μ) under P-limitation as a function of P-quota (Q):

$$\mu = \mu'_{NR}\left(1-\frac{Q_0}{Q}\right) \qquad \text{HYP, without } k_Q \text{ after Droop (1968)} \qquad (11)$$

$$\mu = \mu'_{NR}\frac{Q-Q_0}{k_Q+(Q-Q_0)} \qquad \text{HYP, with } k_Q \text{ after Caperon \& Meyer (1972)} \qquad (12)$$

$$\mu = \mu'_{NR}\left\{1-\exp\left[-\ln 2\left(\frac{Q}{Q_0}-1\right)\right]\right\} \qquad \text{EXP, without } k_Q \text{ after Fuhs (1969)} \qquad (13)$$

$$\mu = \mu'_{NR}\left[1-\exp\left(-\ln 2\frac{Q-Q_0}{k_Q}\right)\right] \qquad \text{EXP, with } k_Q \qquad (14a)$$

Here μ'_{NR} is the theoretical maximum nutrient replete specific growth rate at infinite Q, Q_0 is the subsistence or minimum cell quota and k_Q is the half saturation constant. The Droop and Fuhs equations are half-saturated when $Q = 2Q_0$. I refer to this curve property as the "Droop relation". Accordingly Eq. 12 simplifies to Eq. 11 and Eq. 14a simplifies to Eq. 13 when $k_Q = Q_0$, so that the curves are half-saturated when $Q = Q_0 + k_Q$. In other words, the Droop and Fuhs equations assume the "Droop relation", but the 3-parameters equations do not. Sometimes it is more convenient to express Eq. 14a in terms of the initial slope α_Q instead of the half saturation constant k_Q:

$$\mu = \mu'_{NR}\left[1 - \exp\left(-\alpha_Q \frac{Q - Q_0}{\mu'_{NR}}\right)\right] \tag{14b}$$

Eqs. 14a and 14b both describe the same model curve. Therefore in the following, I will refer to the model itself simply as Eq. 14 and only use the suffix a or b when it is necessary to differentiate between the specific parameter formulations. Eqs. 14a and 14b can be interchanged with the following relation:

$$\alpha_Q = \ln 2 \frac{\mu'_{NR}}{k_Q} \tag{15}$$

To analyse the effect of temperature and photoperiod on P-limited growth, Eqs. 14a and 14b were fitted to each experimental treatment and the effects of temperature and photoperiod on the fitted model parameters were examined by comparing the non-linear models according to Bates and Watts (1988). Nested models were compared using ANOVA (F-tests) allowing hypothesis testing, whereas non-nested models were compared with Akaike's Information Criterion (AIC). Although models using both cell P-quota and biovolume P-quota were fitted, only results for biovolume quota are shown since the fits were similar and the biovolume quota allows better comparisons between the species.

2.13.4 The Droop relation

Nutrient limitation data (generally chemostat experiments) from the literature were also analysed to investigate the Droop relation. Published growth rates and nutrient quotas were obtained by scanning the figures from printed journal material at 600 dpi on a flat scanner to avoid distortion, and digitising the figures with Plot Digitizer (version 2.6.0 Huwaldt and

Steinhorst, 2012). Data for the following marine and freshwater phytoplankton species were used (see Appendix 1, p. 120 for a table with more details): *Scenedesmus* sp. (Rhee, 1973, Rhee and Gotham, 1981b, Rhee and Gotham, 1981a), *Monochrysis lutheri* (Goldman, 1979, Goldman et al., 1979), *Scenedesmus quadricauda* (Ahlgren, 1987), *Limnothrix* (formerly *Oscillatoria*) *redekei* (Wernicke and Nicklisch, 1986), *Planktothrix* (formerly *Oscillatoria*) *agardhii* (Ahlgren, 1985), *Synechococcus linearis* (Healey, 1985), *Cyclotella nana* (Fuhs, 1969), *Ankistrodesmus falcatus* (Gotham and Rhee, 1981a, Gotham and Rhee, 1981b), *Anabaena flos-aquae*, *Asterionella formosa*, *Fragilaria crotonensis*, *Microcystis* sp. (Gotham and Rhee, 1981b, Gotham and Rhee, 1981a), *Cyclotella meneghiniana*, *Asterionella formosa* (Tilman and Kilham, 1976), *Thalassiosira fluviatilis* (Laws and Bannister, 1980), *Selenastrum minutum* (Elrifi and Turpin, 1985), *Staurastrum lueutkemuellerii*, *Microcystis aeruginosa* (Olsen, 1989), and *Scenedesmus acutus* (Sterner, 1993).

To make the data comparable despite the different units of measurement (e.g. quota by cell, biovolume, dry weight or molar ratios per carbon), the curves were normalised and fitted to dimensionless variables such as the relative growth rate (μ/μ_{NR}) and the relative quota (Q/Q_0). Furthermore, a normalised half-saturation coefficient, κ_Q (dimensionless), was introduced:

$$\kappa_Q = \frac{Q_0}{k_Q} \tag{16}$$

which yields the following dimensionless quota curve when introduced into Eq. 14a

$$\frac{\mu}{\mu'_{NR}} = 1 - \exp\left(-\ln 2 \times \kappa_Q \left(\frac{Q}{Q_0} - 1\right)\right) \tag{17}$$

The values of the parameters μ_{NR} and Q_0 depend on the model used to estimate them, so the actual measured values stated by the authors or estimated by me were used wherever possible. If this was not possible, all 4 curves (Eqs. 11-14) were fitted to the data and an arithmetic mean of the 4 parameter values was taken to try to get an unbiased parameter set. The data were analysed by fitting Eq. 17 to each experiment.

2.13.5 Silicon limitation experiments

In silicon limitation experiments, experimental treatments were compared by fitting the Monod model (Eq. 18) to the specific growth rates (μ):

$$\mu = \mu_{NR} \frac{S - S_0}{k_S + S - S_0} \quad (18)$$

S is the dissolved silicon concentration in the culture, S_0 is the minimum silicon concentration for growth, k_s is the half-saturation coefficient and μ_{NR} is the nutrient replete growth rate. Here S_0 is defined as the x-axis intercept when Si-limited growth rates are plotted against Si concentration, and was determined by fitting Eq. 18 to the measured data (Paasche, 1973). To improve the accuracy of the estimates of S_0, several cultures were allowed to grow to stationary phase in each growth experiment, and then the residual silica concentration in the filtered medium was measured. These measurements at stationary phase were then included in model fitting. The effects of temperature and photoperiod were investigated using the non-linear regression approach described by Bates and Watts (1988). In short, the Monod model (Eq. 18) was first fitted to the whole data set with all temperature or photoperiod treatments. Next, a more complex non-linear model, in which the Monod parameters (K, S_0, and/or the initial slope) were allowed to vary linearly with temperature or photoperiod, was fitted to the same data set. Then the simple and complex models were compared using ANOVA to determine whether the temperature or photoperiod dependence significantly improved the overall model fit. In this way I inferred whether temperature or photoperiod significantly affected Si-limited growth. Overfitting was avoided by preselecting the parameters likely to vary with temperature or photoperiod after inspecting their t-values in preliminary fits. Model fits were checked by inspecting residuals vs. fitted plots and normal quantile-quantile plots.

2.13.6 Statistical analysis of lake data

Lake data were analysed by multiple linear regression. Dependent variables were biovolumes of centric diatoms, pennate diatoms and total diatoms and the independent variables were water temperature, effective photoperiod, dissolved silicate concentration, global radiation, mean light exposure in the mixed layer, Julian day of the spring diatom peak, start concentrations of centric and pennate diatoms measured in mid-winter (end of January), and cladoceran abundance. The interactions of these variables with DSi and TP were also checked. TP (as opposed to SRP) and DSi were shown to be good predictors of phytoplankton

abundance (Teubner and Dokulil, 2002, Shatwell et al., 2008), also because phytoplankton can store P but not Si. For all variables except spring peak timing and the diatom start concentrations, means were taken over the spring growth period defined according to physical and biological parameters as described in Shatwell et al. (2008), rather than according to the calendar. In short, spring was defined as starting when the water temperature reached 3°C (generally coinciding with ice-thaw) and ending at the first cladoceran peak (generally coinciding with the clear water phase). The most important predictors were selected in a stepwise procedure based on probabilities (Crawley, 2007) and model residuals were checked against fitted values and predictors. Normal quantile-quantile plots were examined to check for non-normality or heteroscedasticity. Statistical analyses and model fitting were performed using R (version 3.0.0, R Core Team, 2013).

2.14 Dynamic models and simulations

The competition experiments under phosphorus and silicon limitation were analysed using simple dynamic models to simulate the algal growth in culture. In analysing the P-limited competition experiments, the aim was to estimate the relative P uptake rates of each species that would be required to produce the measured outcome (displacement rate) of competition given the growth-quota kinetics measured in the growth rate experiments. In analysing the Si-limited competition experiments, the aim was to test the overall model of factor interactions. All model simulations were performed using R as a platform for dynamic simulations and statistics, by means of the R packages deSolve (Soetaert et al., 2010) and FME (Soetaert and Petzoldt, 2010).

2.14.1 P-limited competition and relative P uptake rates

To estimate the P-uptake rates of *S. minutulus* and *N. acicularis*, the growth of these species in the competition experiments described in section 2.7.2 (p. 22) in semi-continuous P-limited culture was simulated with a small dynamic model. The simulation was run in steps, from one dilution to the next. Between dilutions the two species grew as in a batch culture, such that

$$\frac{dX}{dt} = \mu X \tag{19}$$

$$\frac{dQ}{dt} = -\mu Q \tag{20}$$

where X is the biovolume of each species, Q is the biovolume quota of P, and t is time. The specific growth rate, μ is given by Eq. 14 (p. 31) with the parameters in Table 8 (p. 56). Because the maximal uptake rate (V_m) is much higher than required to satisfy immediate needs for growth if cells are substantially P-limited (Cembella et al., 1984a, Riegman et al., 2000), it was assumed that the P added during dilution was absorbed instantly and completely, so that the dissolved P concentration in the medium was negligible. Furthermore, it was assumed that the added P was distributed between the two species (*i* and *j*) in fixed proportions, c_i and c_j, (dimensionless) such that $c_i+c_j = 1$. Therefore, at the end of each step the biovolume (X) and P-quota (Q) of each species were modified to account for dilution as follows:

$$X^* = fX \tag{21}$$

$$Q_i^* = Q_i + \frac{(1-f)S_m}{X_i^* + X_j^*\left(\frac{1}{c_i} - 1\right)} \tag{22}$$

where X* and Q* denote the new biomass and P-quota, respectively, at the start of the next simulation step directly following dilution, S_m is the P concentration in the fresh medium, and f is the dilution factor, given by:

$$f = e^{-D\Delta t} \tag{23}$$

where D is the applied dilution rate and Δt is the time until the next dilution. Note the subscripts, *i* and *j*, which have been introduced to Eq. 22 because the nutrient absorbed by one species depends on the biomass of the other. The variables c_i and c_j are biomass-specific and are therefore proportional to the P-uptake rates of the two species relative to each other. In effect, this approach assumes a linear relationship between external nutrient concentration and uptake rate. The slope of this linear relationship (c_i and c_j) is proportional to the uptake affinity, or the initial slope of the Michaelis-Menten uptake curve V_m/k_m, where k_m is the half-saturation coefficient (Button, 1978, Healey, 1980). In a calibration routine during the

simulations, c_i and c_j were fitted to the measured data in each competition experiment to investigate how the relative uptake rates change with temperature and photoperiod.

2.14.2 Silicon-limited competition

The competition experiments under silicon limitation (described in section 2.8.3, p. 24) were analysed by simulating the growth of *S. minutulus* and *N. acicularis* in semi-continuous culture. The simulations were then compared with the results of the competition experiments, specifically with the dynamics of dominance and competitive exclusion. Firstly the simulations were performed using the Monod model, which assumes that nutrient uptake matches biomass growth. Secondly simulations were repeated with a new cell cycle model in which biomass growth, increase in cell number and nutrient uptake are uncoupled.

2.14.2.1 Simulations with the Monod model

In these simulations, the specific growth rate, μ, is given by the model and parameters described in Table 12 (p. 68), which is based on the Monod model (Eq. 18, p. 34) and the base model (Section 2.13.1, p. 28). Thus specific biomass growth rates, cell number growth rates and specific nutrient uptake rates are all equal to μ. The simulation was run in steps from one dilution to the next, with batch growth between dilutions as described above, such that

$$\frac{dX_i}{dt} = \mu_i X_i \qquad (19, \text{p. } 35)$$

$$\frac{dS}{dt} = \sum_{i=1}^{2} -\mu_i Q_i X_i \qquad (24)$$

where Q is the cellular silicon content and subscript *i* refers to species *i*. At each dilution in the simulation, a certain amount of the mixed biomass is removed and fresh medium is added such that

$$X_i^* = f \times X_i \qquad (21, \text{p. } 36)$$

$$S^* = f \times S + (1 - f) S_m \qquad (25)$$

where X_i* and S* denote the new biomass and silicon concentration, respectively, directly after dilution, S_m is the silicon concentration in the fresh medium, and f is the dilution factor given by Eq. 23, determined from the dilution rate D.

2.14.2.2 Simulations with a cell-cycle model

In diatoms, silicon uptake is restricted to certain parts of the cell cycle (Azam, 1974, Martin-Jézéquel et al., 2000, Brzezinski, 1992, Hildebrand et al., 2007, Leynaert et al., 2009, Thamatrakoln and Hildebrand, 2007, Thamatrakoln and Hildebrand, 2008). The bulk of silicate for deposition of new valves is absorbed during the G2 cell phase just prior to mitosis (Brzezinski et al., 1990, Claquin et al., 2002). A cell cycle model was developed to account for rapid uptake of silicate during a restricted part of the cell cycle of duration τ_0 (duration of the uptake phase divided by the duration of the total cell cycle at the nutrient replete growth rate μ_{NR}), where the parameters can be derived directly from the Monod model (Eq. 18, p. 34). Therefore in steady-state, the cell cycle model is equivalent to the Monod model and the overall time required for one cell division is identical in both models for all silicon concentrations.

In the cell cycle model (Figure 9), the cell size (B) always increases at the maximal, nutrient replete rate (μ_{NR}) until the relative cell size (B/B_0) reaches a value of two, when cell size ceases to increase (Figure 10a):

$$\frac{dB}{dt} = \left(\frac{B}{B_0} < 2 \right) \times \mu_{NR} B \qquad (26)$$

where B_0 is the minimum cell size. Note the use of the Boolean operator, which takes on the value of 1 if TRUE and 0 otherwise. Silicate uptake can only begin when a certain amount of biomass has been produced (at point 2 in Figure 9) and the relative cell size has reached the value 2 - τ_0. The maximum uptake rate (V_m), when nutrients are replete, needs to be high enough to accumulate enough silicate for a new cell within the remaining time until the cell cycle is complete (i.e. when B/B_0 just reaches the value 2 when proceeding at rate μ_{NR}, see Figure 10b).

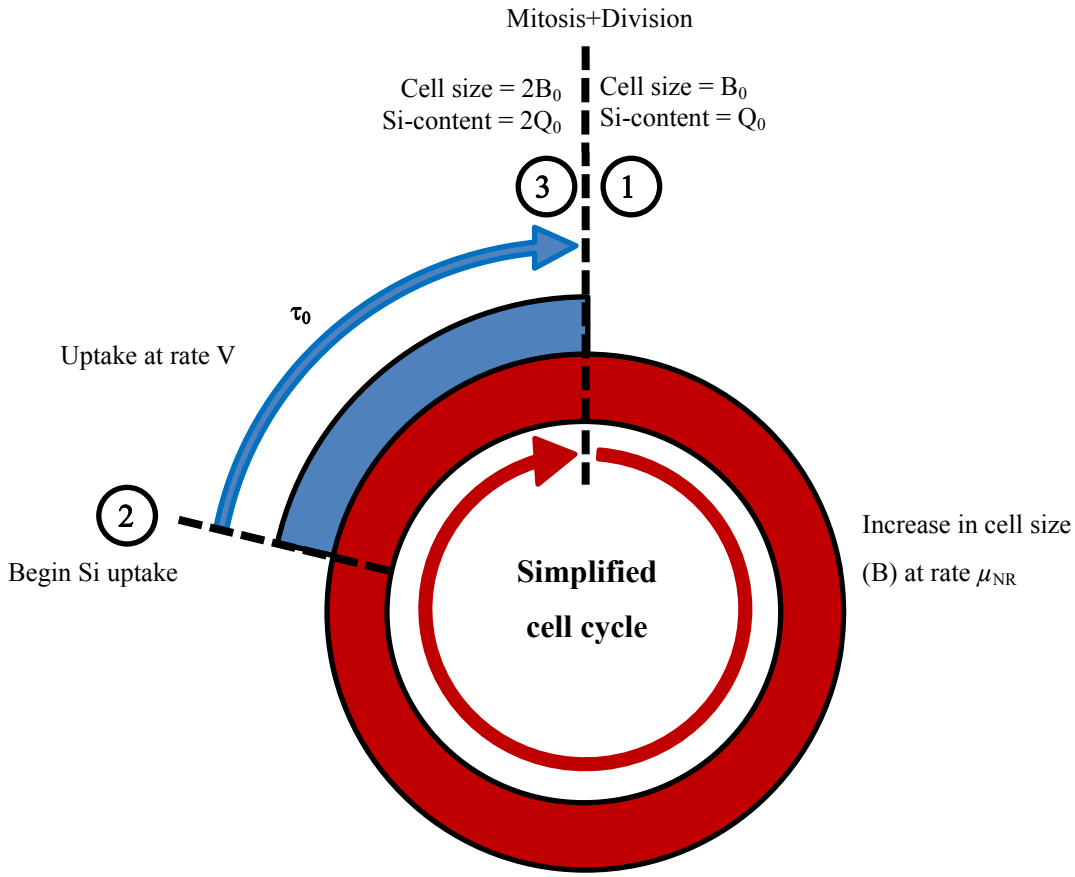

Figure 9: Schematic of the cell-cycle model showing biomass increase uncoupled from nutrient uptake. The cell cycle begins at point 1 where the newly formed cell has a minimum size B_0 and minimum cell Si-content (Q_0). Cell size (B) increases at a constant nutrient replete rate (μ_{NR}) until the cell size has doubled at point 3. Here cell size ceases to increase. Si-uptake begins at point 2 and proceeds at rate V. The cell is only allowed to divide at point 3 (mitosis and division are assumed instantaneous) when sufficient biomass has been formed ($B = 2B_0$) and enough Si has been absorbed ($Q = 2Q_0$) to form a new cell. Under Si-limitation, the length of the blue uptake phase is extended, thus increasing the duration of the cell cycle and decreasing the division rate.

Thus V_m, which is cell-specific and not biomass-specific, can be calculated from μ_{NR}, τ_0, and the minimum cellular silicon content (Q_0):

$$V_m = \left(\frac{B}{B_0} \geq 2 - \tau_0 \right) \times \frac{\mu_{NR} Q_0}{\ln\left(\frac{2}{2 - \tau_0} \right)} \qquad (27)$$

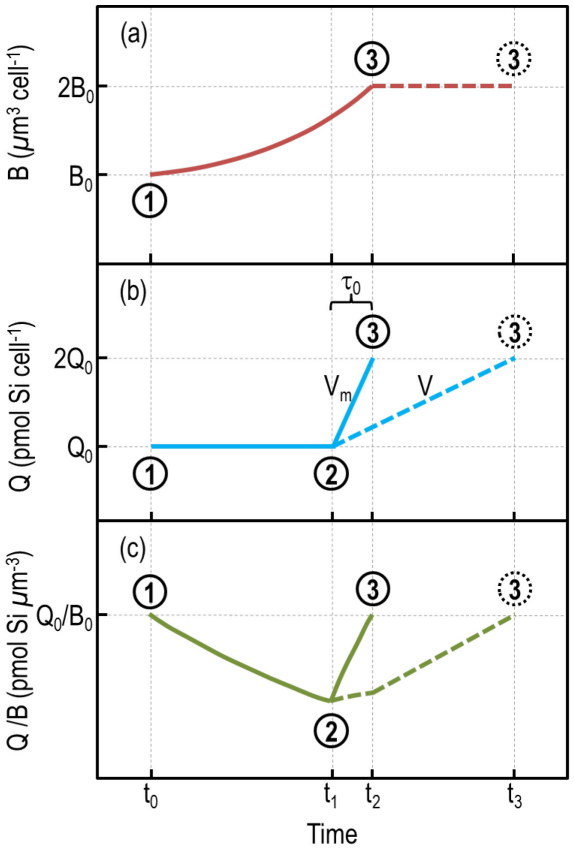

Figure 10: The change in cell volume, B (a), cell silicate content, Q (b) and silicate content per biovolume (Q/B) (c) over time assumed in the cell-cycle model. Numbers and definitions correspond to those in Figure 9. Under nutrient replete conditions, the cell divides at t_2. Dashed lines show the effect of silicate limitation, where cell division is delayed until t_3. τ_0 is defined as $(t_2\text{-}t_1)/(t_2\text{-}t_0)$. Silicate uptake proceeds at rate V_m under nutrient replete conditions and at rate V under silicate limitation (b).

A reduction of the growth rate under silicon limitation is achieved by extending the duration of the uptake phase (Figure 10). Here the cell-specific uptake rate (V) is given according to the Michaelis-Menten equation:

$$V = V_m \frac{S - S_0}{k_m + S - S_0} \tag{28}$$

where S is the nutrient concentration, S_0 is the minimum nutrient concentration and k_m is the half-saturation coefficient of uptake. k_m and S_0 need to be parameterised so that the silicate uptake phase is extended until one complete cell cycle has the same duration as the cell division rate given by the Monod equation.

Here S_0 is simply adopted from the Monod equation so that uptake ceases when growth ceases and k_m is scaled up from k_S as follows:

$$k_m = \frac{\ln 2}{\ln\left(\frac{2}{2-\tau_0}\right)} \times k_S \tag{29}$$

The cellular silicate content (Q) then increases at the rate V:

$$\frac{dQ}{dt} = V \tag{30}$$

When the uptake phase is complete (at point 3 in Figure 9 and Figure 10), the cell has accumulated enough biomass ($B = 2B_0$) and enough silicate ($Q = 2Q_0$) to produce a new cell, so the cell is allowed to divide. At this point the cell concentration (N) is doubled and both B and Q are halved, so that the daughter cells are at the beginning of the cycle where $B = B_0$ and $Q = Q_0$. The cell-cycle model is equivalent to the Monod model (Eq. 18, p. 34) when nutrient uptake is continuous and coupled to biomass growth, which can be seen by substituting $\tau_0 = 1$ into Eqs. 27 and 29 and noting in Eq. 28 that

$$\mu = \ln 2 \frac{V}{Q_0} \tag{31}$$

when V is cell-specific. The term ln(2) is required to convert the cell division rate to the specific growth rate. An apparent decrease in silicate content per biovolume (Figure 10c) does not imply that the valves (silicate shells) become thinner. Instead the existing valves move apart as the cell grows and the gap is filled by the formation of additional girdle bands (Pickett-Heaps et al., 1990), which are not explicitly considered in the model.

Growth in the competition experiments was simulated as the increase in cell number. At any point during the experiment, the total biomass of a species is given by $X = BN$. Silicate is consumed by each competing species (denoted with subscript *i*):

$$\frac{dS}{dt} = \sum_{i=1}^{2} -V_i N_i \tag{32}$$

In such a simulation with two species, the two populations are completely synchronised and all cells divide simultaneously, which is unrealistic. Therefore 1000 Monte Carlo simulations were performed where each simulation began with the initial populations at a randomly generated point in the cell cycle ($B_0 < B < 2B_0$ and $Q_0 < Q < 2Q_0$ when $B/B_0 \geq 2\text{-}\tau_0$). Furthermore, some random noise was added to the model parameters derived from their standard errors. The cultures were diluted in the simulations as described above in section 2.14.2.1. Q_0 and B_0 were chosen so that the average Si content and average cell size over the duration of all simulations matched the average of the measured values of Si content and cell size in the experiments.

3. Results

3.1 Fluctuating light and the effects of temperature and photoperiod

3.1.1 Effect of fluctuating light on growth

At light saturation, the specific growth rates of all three species at 15°C under the FL_{12} regime were lower than the growth rates under the CL_{12} regime at the same daily light exposure (Figure 11; for a description of the light regime names, see Table 3, p. 21). Fitting the growth-light model (Eq. 5, p. 28) showed that this decrease (μ_m) was significant (*t*-test, $t > 8$, $df \geq 11$, $p \leq 0.00001$ all species, Table 6).

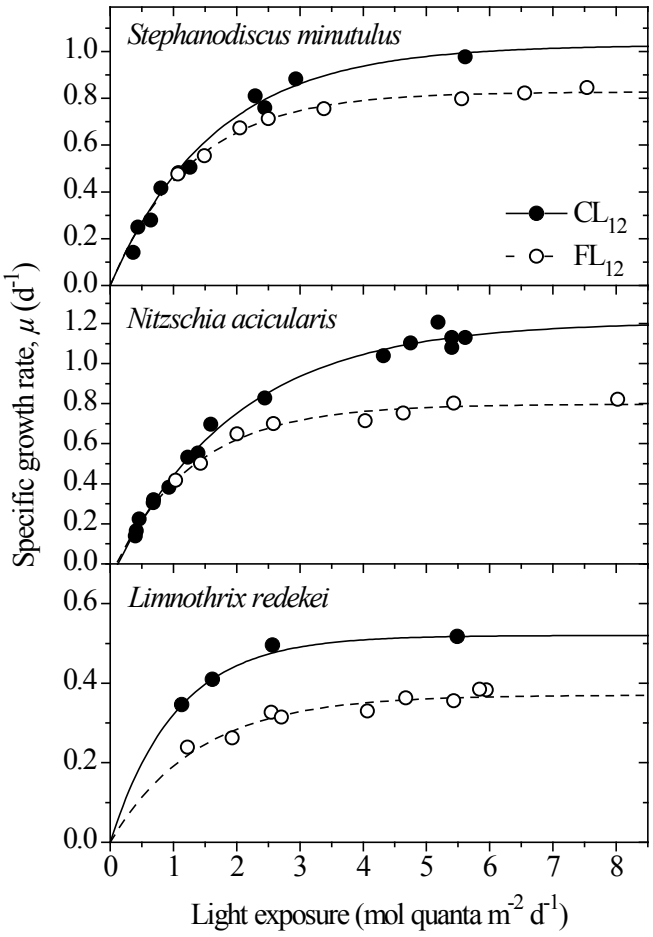

Figure 11: Specific growth rates (d^{-1}) of the three test species vs. light exposure (LE, mol quanta m^{-2} d^{-1}) under constant and fluctuating light under a long photoperiod at 15°C. Lines show individually fitted models (Eq. 5, p. 28) with parameters in Table 6.

Table 6: Model parameters (Eq. 5, p. 28) fitted to measured data for the three test species under the different light regimes at 15°C. μ_m: maximum specific growth rate, α_{LE}: initial slope of growth light curve, LE_{min}: minimum light for growth. For light regime descriptions, see Table 3 (p. 21). E_k, which is defined as $\mu_m : \alpha_{LE}$, is the light saturation parameter for growth expressed as average irradiance (μmol m^{-2} s^{-1}) over the photoperiod. Values in parentheses show 95% confidence intervals.

Light regime	μ_m (d^{-1})	α_{LE} (m^2 mol^{-1})	LE_{min} (mol m^{-2} d^{-1})	E_k (μmol m^{-2} s^{-1})	R^2
S. minutulus					
CL_{12}	1.03 (0.93-1.12)	0.62 (0.55-0.70)	0 (nf)	38	0.98
FL_{12}	0.83 (0.81-0.85)	0.64 (0.60-0.69)	0 (nf)	30	0.99
CL_6	0.74 (0.52-0.96)	0.69 (0.25-1.13)	0 (nf)	50	0.997
FL_6	0.48 (0.41-0.55)	0.64[b] (nf)	0 (nf)	-	0.56
$FL_{12}D$	0.59 (0.52-0.65)	0.64[b] (nf)	0 (nf)	-	0.74
N. acicularis					
CL_{12}	1.21 (1.14-1.28)	0.63 (0.52-0.73)	0.12 (0.01-0.23)	44	0.99
FL_{12}	0.80 (0.74-0.86)	0.63 (0.29-0.97)	0.10 (-0.56-0.75)	29	0.97
CL_6	0.67 (0.59-0.76)	0.71 (0.42-0.99)	0.12[a] (nf)	44	0.90
FL_6	0.39 (0.33-0.46)	0.63[b] (nf)	0.10[b] (nf)	-	0.40
$FL_{12}D$	0.46 (0.35-0.57)	0.63[b] (nf)	0.10[b] (nf)	-	0.36
L. redekei					
CL_{12}	0.52 (0.50-0.55)	0.50 (0.39-0.62)	0 (nf)	24	0.99
FL_{12}	0.37 (0.35-0.40)	0.27 (0.21-0.33)	0 (nf)	32	0.90
CL_6	0.31 (0.30-0.32)	0.53 (0.46-0.61)	0 (nf)	27	0.98
FL_6	0.21 (0.19-0.23)	0.27[b] (nf)	0 (nf)	-	0.30
$FL_{12}D$	0.22 (0.18-0.25)	0.27[b] (nf)	0 (nf)	-	0.30

[a] Assumed equal to value for CL_{12} (see section 2.13.2, p. 30); [b] assumed equal to value for FL_{12}; nf: not fitted

The initial slope, α_{LE}, at 15°C did not change between constant and fluctuating light for the diatoms but decreased significantly for *L. redekei* under fluctuating light. The light compensation point LE_{min} was not significantly different from zero for *S. minutulus* and *L. redekei* in initial model fits (in part because there were not much data at very low light), so it was set to zero for the final parameter estimates. In contrast, LE_{min} was significantly higher than zero for *N. acicularis* under constant light, and was thus included in the model. For consistency LE_{min} was also included in the model for fluctuating light. Interestingly, the growth curves of the two diatoms were almost identical under FL_{12} at 15°C, whereas the curves for these species under CL_{12} differed considerably (Table 6).

3.1.2 Effect of temperature

The maximum growth rates of all species under FL_{12} were also lower than under CL_{12} at 10°C and 20°C (*t*-test, $t > 4$, $df \geq 4$, $p < 0.001$, μ_m in Table 7). The decrease in light-saturated growth rates under the FL_{12} regime at 10°C, 15°C, and 20°C was smaller for *S. minutulus* (14-21%) than for *N. acicularis* and *L. redekei*, which were similar (31-34% and 27-31%, respectively).

Table 7: Maximum (light saturated) specific growth rates (μ_m) under constant (CL_{12}) and fluctuating (FL_{12}) light at 12 h d^{-1} photoperiod. Data for 15°C are given in Table 6. Values were estimated by model fitting (Eq. 5, p. 28) as described in the methods. CI: 95% confidence interval, *n*: number of cultures.

Temperature	Constant light (CL_{12})			Fluctuating light (FL_{12})		
(°C)	μ_m (d^{-1})	CI	*n*	μ_m (d^{-1})	CI	*n*
S. minutulus						
10	0.77	0.72-0.82	4	0.66	0.63-0.69	4
20	1.18	1.17-1.19	2	0.93	0.91-0.96	4
N. acicularis						
10	0.84	0.79-0.88	4	0.58	0.55-0.60	4
20	1.47	1.40-1.54	2	0.99	0.82-1.17	4
L. redekei						
10	0.32	0.30-0.35	3	0.22	0.21-0.24	4
20	0.70	0.58-0.82	4	0.51	0.38-0.64	4

Furthermore, the percentage decrease in growth rates was the same at 10°C, 15°C, and 20°C for *N. acicularis* and *L. redekei* ($p > 0.3$ all cases; Figure 12). In *S. minutulus*, the decrease in μ_m was slightly greater at 20°C than at 10°C ($p = 0.05$). The decrease at 15°C was not significantly different than at 10°C or 20°C. This indicates a marginally significant increasing tendency of the effect of fluctuating light with increasing temperature. Overall the mean decrease in growth rates of *S. minutulus*, *N. acicularis*, and *L. redekei* over all temperatures under fluctuating light at $z_{eu}:z_{mix} = 1$ was 18%, 33%, and 29%, respectively.

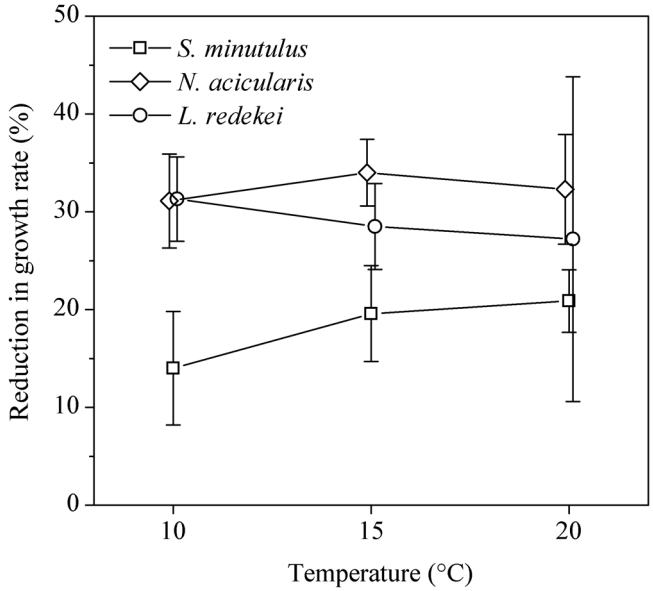

Figure 12: Reduction of maximum specific growth rate (in %) due to the FL_{12} regime compared to the CL_{12} regime as a function of temperature (°C). Measurements under light saturation (4-8 mol quanta m^{-2} d^{-1}). Temperatures were staggered slightly to avoid overlap. For explanation of regime abbreviations see Table 3, p. 21.

3.1.3 Effect of photoperiod

To separate the effects of the different temporal components of the light supply, growth rates were compared under constant and fluctuating light at a decreased photoperiod of 6 h d^{-1} (Table 6). At CL_6, growth rates were 28%, 45%, and 40% lower than at CL_{12} for *S. minutulus*, *N. acicularis*, and *L. redekei*, respectively. The initial slope α_{LE} did not change significantly between CL_{12} and CL_6 regimes for any species (Table 6). Under the FL_6 regime, maximum growth rates decreased by a further 35%, 42%, and 32% compared to CL_6 for *S. minutulus*, *N.*

acicularis, and *L. redekei*, respectively. With the exception of *S. minutulus* ($p < 0.01$), these decreases due to fluctuating light at 6 h d^{-1} were not significantly different from the decreases measured at 12 h d^{-1} ($p > 0.05$). Therefore the decrease in growth rate due to fluctuating light simulating mixing at $z_{eu}:z_{mix} = 1$ was independent of photoperiod.

3.1.4 Effect of $z_{eu}:z_{mix}$

The experiments described above showed that the percentage decrease in growth rate caused by fluctuating light was approximately the same at both 6 and 12 h d^{-1} photoperiods. Therefore fluctuating light experiments were repeated at 15°C under the $FL_{12}D$ regime. Growth rates were similar under the FL_6 and $FL_{12}D$ regimes (Figure 13), which both have an effective photoperiod of 6 h d^{-1}.

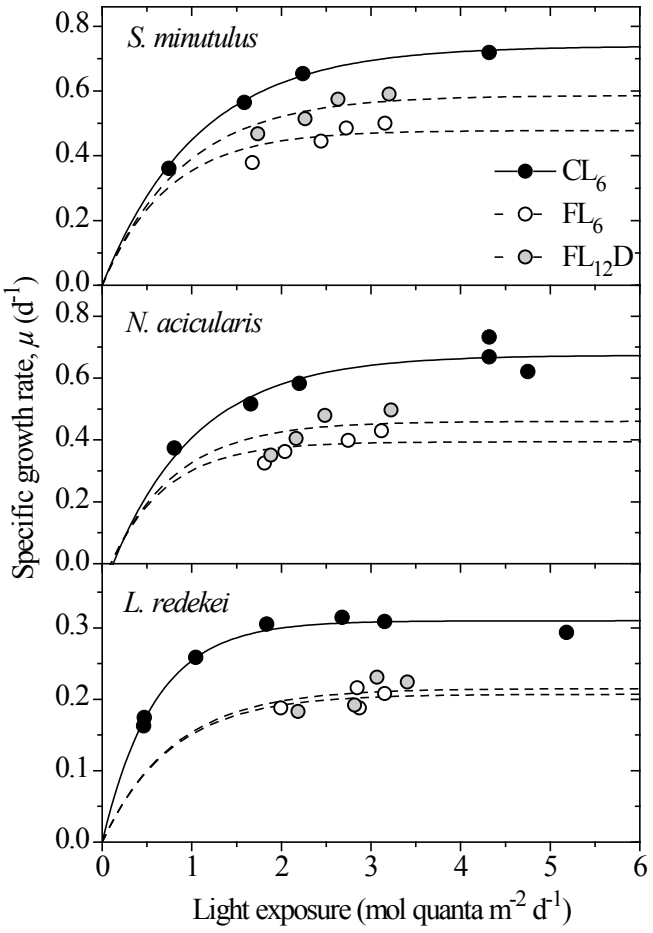

Figure 13: Specific growth rates (d^{-1}) vs. light exposure (mol quanta m^{-2} d^{-1}) under constant and fluctuating light at 15°C and 6 h d^{-1} effective photoperiod. Lines show individually fitted models (Eq. 5, p. 28) with parameters in Table 6.

For *N. acicularis* and *L. redekei* there was no significant difference between growth rates under these two regimes (*t*-test, $t < 1.7$, df = 6, $p > 0.1$, both cases), whereas for *S. minutulus*, growth rates under the $FL_{12}D$ regime were higher ($t = 3.7$, df = 6, $p = 0.01$, Table 6).

Compared to the CL_6 regime, the $FL_{12}D$ regime decreased the growth rates of *S. minutulus*, *N. acicularis*, and *L. redekei* by 20%, 31%, and 29%, respectively, which was not significantly different to the respective decreases at 12 h d^{-1} of 19%, 34%, and 29% (due to the FL_{12} regime compared to CL_{12} at 15°C in Table 6, $p > 0.5$). Comparing all treatments to a chosen set of reference conditions (CL_{12}) showed that a reduced photoperiod and light fluctuations had a cumulative effect on *N. acicularis* and *L. redekei*. In other words, the sum of effects of a reduced photoperiod alone (CL_6) and light fluctuations alone (FL_{12}) was equal to the combined effects of both decreased (effective) photoperiod and light fluctuations ($FL_{12}D$ and FL_6) as indicated by the solid bars in Figure 14.

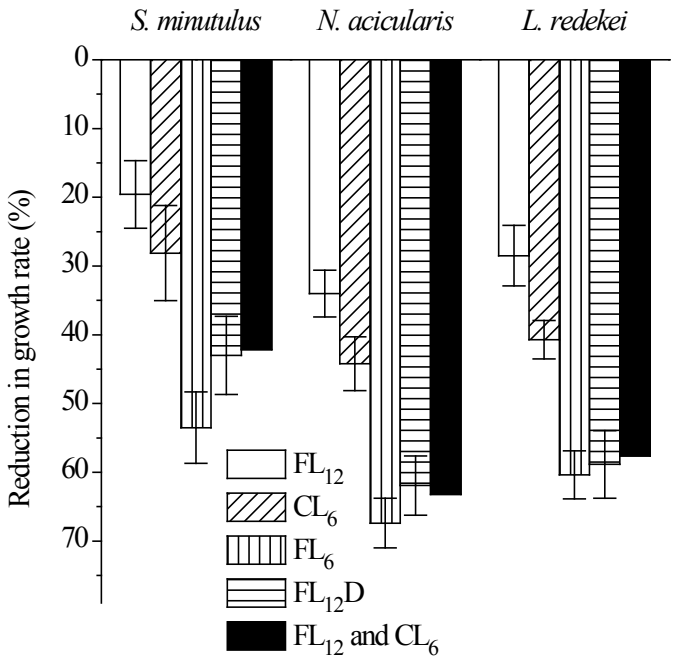

Figure 14: Reduction in maximum specific growth rate (in %) caused by different light regimes compared to the CL_{12} regime at 15°C. Black bars show estimated combined effects of FL_{12} and CL_6 calculated from the growth reduction for the corresponding treatments $(1 - (1-FL_{12})\times(1-CL_6))$. All measurements at 15°C. For explanation of regime abbreviations see Table 3, p. 21.

This relation can be generalised as follows:

$$LF = \frac{\mu_{mf}}{\mu_{mc}} \quad (33)$$

where LF is a light fluctuation factor, μ_{mf} and μ_{mc} are the maximum specific growth rates under fluctuating and constant light, respectively. LF is thus constant provided that μ_{mc} is given at the same *effective* photoperiod as μ_{mf}. In Figure 14, LF is defined as μ_{mf} (FL_{12}) : μ_{mc} (CL_{12}) and the effects of fluctuating light at the other photoperiods and ratios of z_{eu}:z_{mix} were estimated using Eq. 33. For *S. minutulus*, Eq. 33 applied only to the FL_{12}D regime while the reduction in growth rate under the FL_6 regime was stronger than the sum of individual effects of CL_6 and FL_{12}.

3.1.5 Pigments

The chlorophyll *a* content of all species decreased with increasing light in a typical hyperbolic fashion (Figure 15). At low light levels, the chlorophyll *a* content increased sharply, reaching around 8, 9, and 11 μg Chla mm^{-3} for *L. redekei*, *S. minutulus* and *N. acicularis* respectively. Comparing the chlorophyll *a* content under the different treatments at light levels above E_k (the light saturation parameter of growth in Table 6 given by μ_m/α_{LE}; note the term I_k = ETR_{max} : α_I* is used here for saturation of photosynthesis) showed that the diatoms decreased their chlorophyll *a* content in response to a shorter photoperiod ($p < 0.0001$ for *S. minutulus*, $p = 0.006$ for *N. acicularis*) but there was no significant difference between constant (CL_{12} and CL_6) and fluctuating light regimes (FL_{12} and FL_6). In contrast, *L. redekei* showed no difference between different photoperiods, but an increase in chlorophyll *a* content in response to fluctuating light ($p = 0.002$). The chlorophyll *a* content at 15 °C was higher than at 10 °C in all species ($p < 0.01$ in all cases). At 20 °C, the chlorophyll *a* content increased again for *N. acicularis* ($p < 0.0001$), did not change significantly for *S. minutulus* and measurements were unreliable for *L. redekei*. Under the deep mixing regime (FL_{12}D), the chlorophyll *a* content was not significantly different to that under the 12 h d^{-1} fluctuating regime (FL_{12}) in all species and was higher than the 6 h d^{-1} photoperiod regime (FL_6) for the two diatoms ($p < 0.001$ both cases). Here the chlorophyll *a* content was also higher for *L. redekei* but the difference was not significant. This indicates that the chlorophyll *a* content depends on the average irradiance in the overall solar photoperiod (LP), not the effective

photoperiod (LP_{eff}), otherwise the contents under $FL_{12}D$ would be similar to those under FL_6 and not FL_{12}.

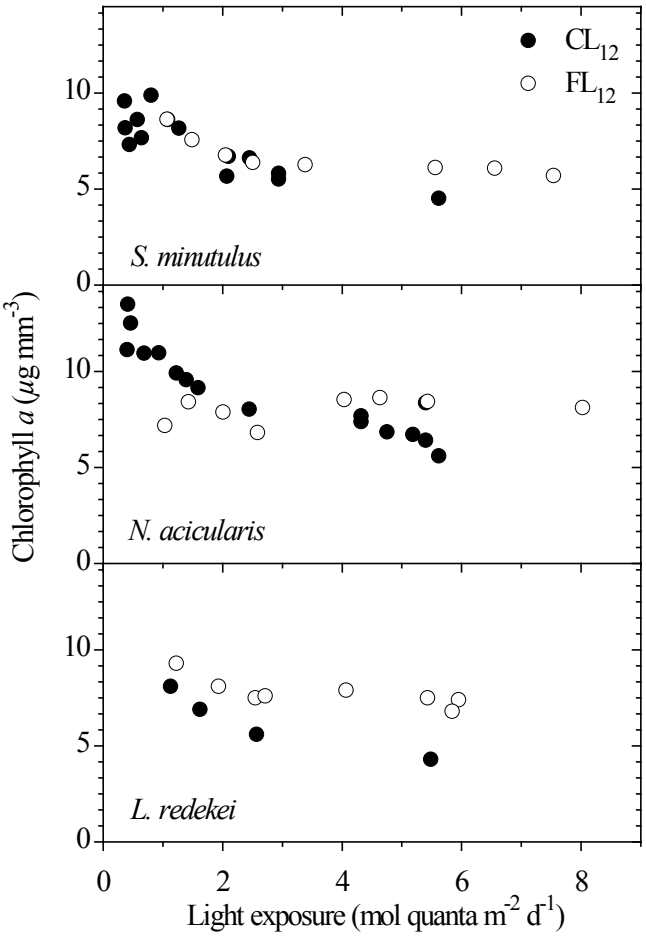

Figure 15: Biovolume quota of chlorophyll *a* (μg mm^{-3}) for the three test species at 15°C. Each point represents the average of up to 4 measurements for each culture.

Over most light intensities, the fucoxanthin : chlorophyll *a* ratio was relatively constant at 47-53% and 50-55% for *S. minutulus* and *N. acicularis* respectively (Figure 16). This ratio was higher under constant light than under fluctuating light for both diatoms ($p < 0.0001$) and increased with temperature, although the increase was marginal in *S. minutulus* ($p = 0.050$, Figure 16). In *S. minutulus* the fucoxanthin : chlorophyll *a* ratio increased at light exposures below 1 mol PAR m^{-2} d^{-1} under the CL regime or about 25 μmol PAR m^{-2} s^{-1}, indicating an increase in size of the photosynthetic antenna in adaptation to low light, and was lower under the FL_6 regime than under other regimes ($p < 0.0001$). The chlorophyll *c* : chlorophyll *a* ratio behaved in a very similar way to the fucoxanthin : chlorophyll *a* ratio (Figure 16).

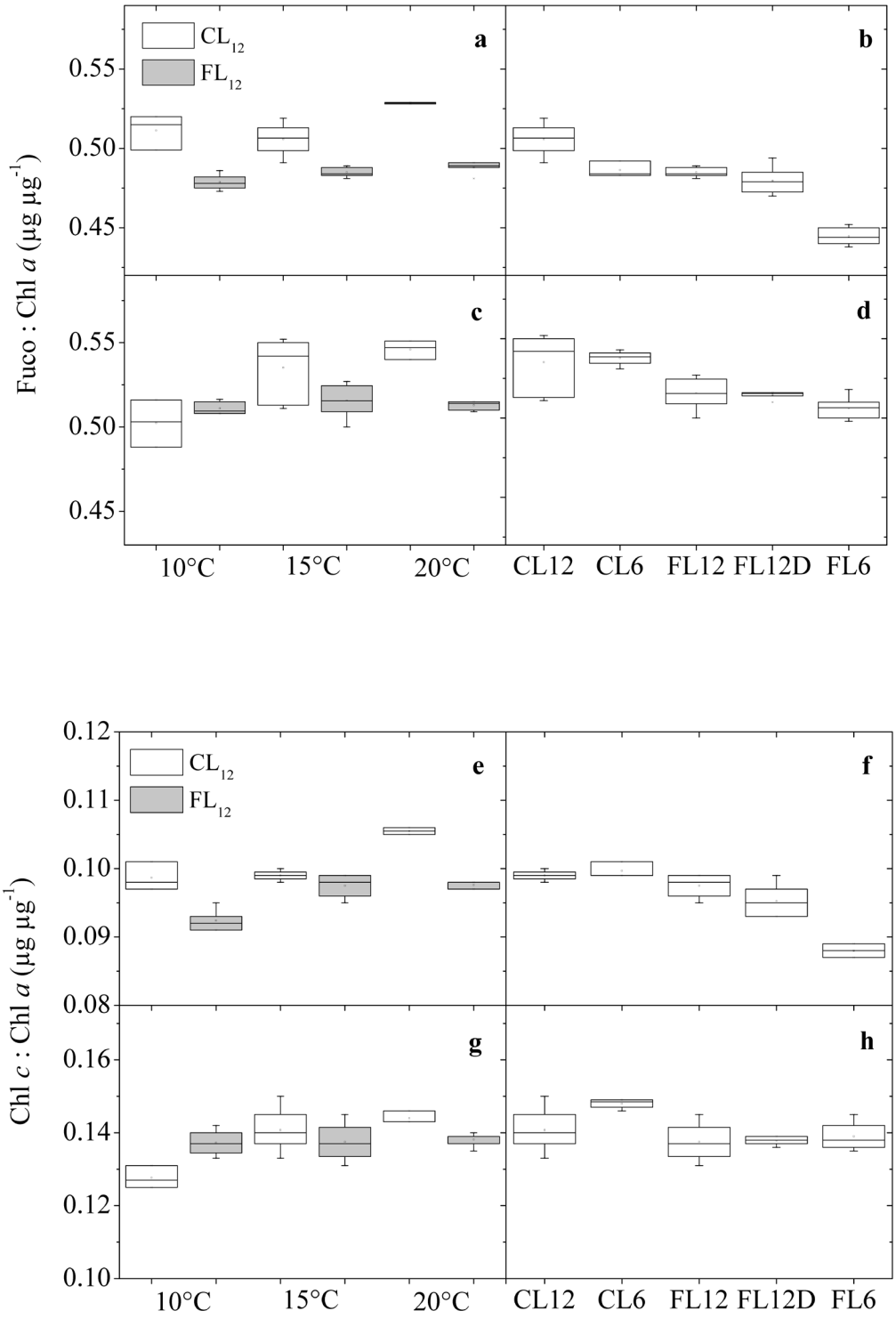

Figure 16: Ratio of fucoxanthin and chlorophyll *c* to chlorophyll *a* in the diatoms *S. minutulus* (a, b, e, f) and *N. acicularis* (c, d, g, h) at different temperatures at 12 h d^{-1} photoperiod (left panels) and under different light regimes at 15°C (right panels). Measurements at light saturation, values at mean light intensities under E_k were excluded.

3.1.6 Photosynthetic parameters

The Eilers and Peeters (1988) model was fitted to relative electron transport rates (ETR) and the model parameters, which are chlorophyll-specific (or more precisely F_o-specific), were analysed to provide information about photosynthesis and acclimation. All three species responded to low light exposures under CL_{12} by decreasing the maximum electron transport rate (ETR_{max}, $p \leq 0.0001$) and the light saturation parameter (I_k, $p \leq 0.01$), while the initial slope α_I* was constant ($p \geq 0.09$, Figure 17).

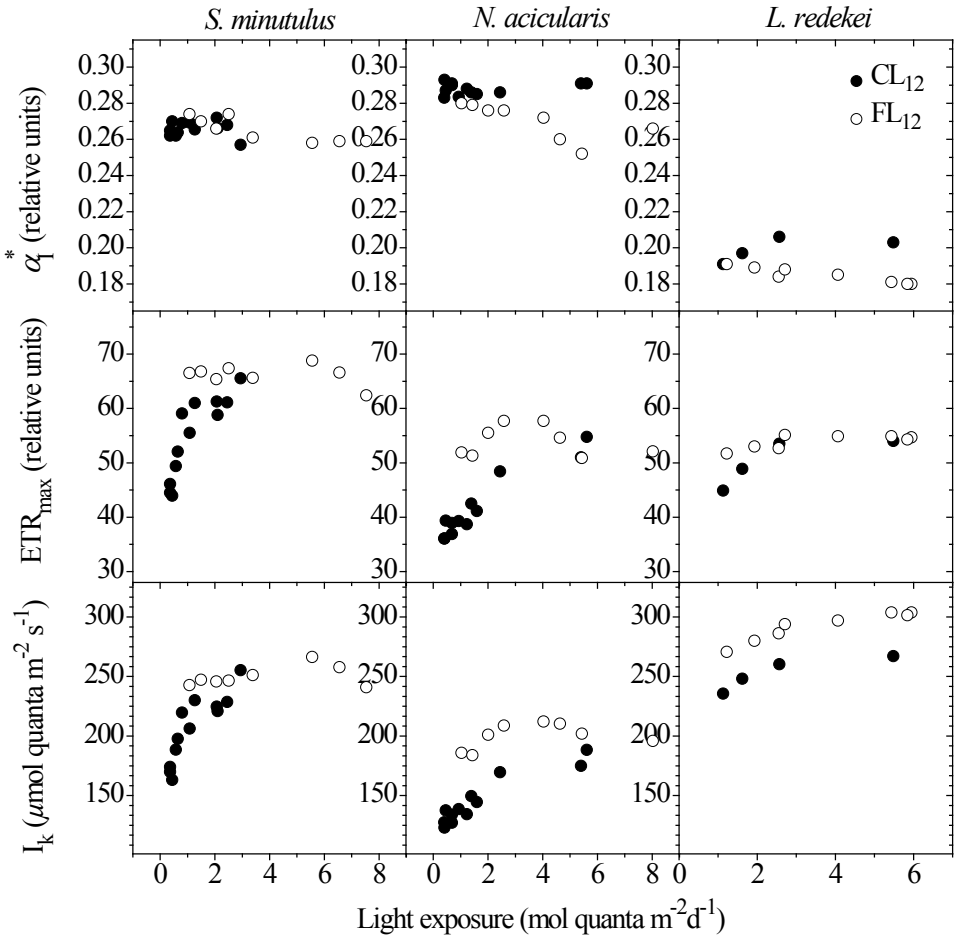

Figure 17: Parameters of the chlorophyll-specific ETR curves for the three test species at 15°C. α_I*: initial slope of curve, ETR_{max}: maximum electron transport rate (both in relative units), I_k: light saturation parameter (μmol quanta m^{-2} s^{-1}). Parameters were fitted to the Eilers and Peeters model (1988). Each point represents an average of up to 4 measurements for each culture.

In contrast, under FL_{12}, α_I* increased with decreasing light exposure in all species ($p \leq 0.05$), whereas ETR_{max} was constant for the diatoms and had a slight decreasing tendency in *L. redekei* ($p = 0.06$). I_k did not change with light exposure for the diatoms but increased in a saturation curve for *L. redekei* with increasing light exposure. Interestingly, each species' response to light exposure under CL_6 was the same in qualitative terms as the response to FL_{12}, with the exception that ETR_{max} in *L. redekei* decreased slightly but significantly with increasing light exposure, probably due to very slight photoinhibition visible in Figure 13. Considering now the overall effects of the different experimental treatments on photosynthesis, all species had a lower α_I* and higher I_k under fluctuating light than under constant light. ETR_{max} increased in the diatoms but did not change in *L. redekei* in comparison to constant light. In the $FL_{12}D$ regime, *S. minutulus* responded mainly by increasing α_I*, *N. acicularis* responded by increasing ETR_{max}, and *L. redekei* responded by decreasing ETR_{max}. The initial slope α_I* was significantly higher at 10°C than at 15°C or 20°C for the diatoms ($p \leq 0.03$), regardless of whether light was fluctuating or constant, whereas I_k was significantly higher at 20°C for *L. redekei*. One important point is that electron transport rates saturated at irradiances (I_k) of 235 ± 38, 182 ± 34 and 289 ± 22 μmol quanta m^{-2} s^{-1} for *S. minutulus*, *N. acicularis*, and *L. redekei*, respectively, whereas growth saturated at 24-44 μmol quanta m^{-2} s^{-1} (E_k in Table 6). Therefore at 12 h d^{-1} photoperiod, electron transport was light saturated at irradiances 3-8 times higher than the irradiances required to saturate growth. At a 6 h d^{-1} photoperiod, this difference was even higher (9-11 times). For reference purposes, *S. minutulus* and *N. acicularis* had cell sizes of 158 ± 42 and 100 ± 19 μm^3 $cell^{-1}$, respectively.

3.2 Phosphorus and its interactions with temperature and photoperiod

3.2.1 Phosphorus-replete growth

The different models (Eqs. 11-14, p. 31) were fitted to the growth rates of *N. acicularis* and *S. minutulus* under P-limited and P-replete conditions. Since Eq. 14 produced the best fit in 8 of 10 cases, it was used to compare temperature and photoperiod treatments for the following analysis (Figure 18).

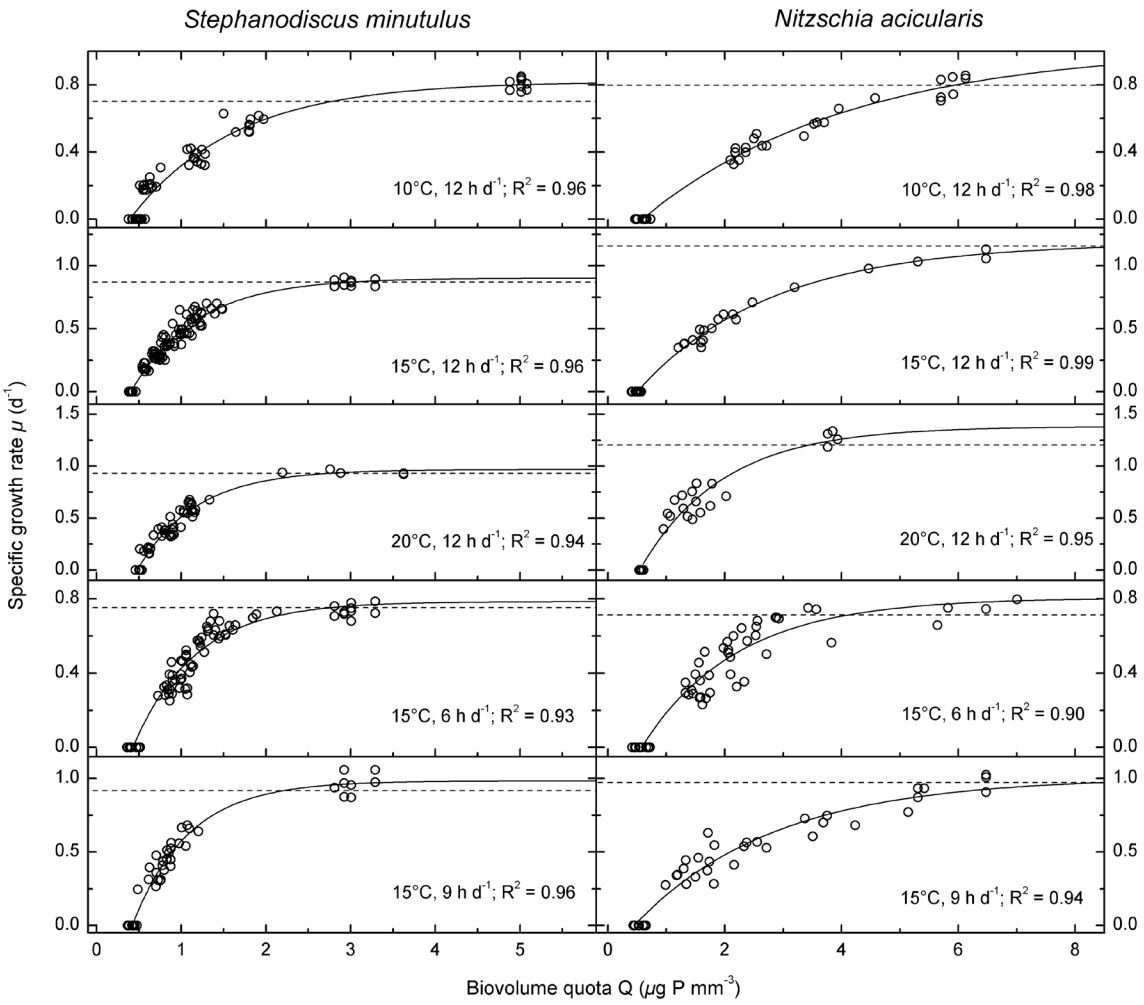

Figure 18: Specific growth rates as a function of biovolume P-quota at different temperatures and photoperiods for *S. minutulus* (left panels) and *N. acicularis* (right panels). Daily light exposure was saturating or near saturating. Points show measured values, solid lines show the fitted model (Eq. 14, p. 31) with the parameters in Table 8. The dotted lines show the nutrient replete specific growth rates (μ_{NR}) predicted by the base model (section 2.13.1, p. 28) at the respective temperature, photoperiod and light exposure.

The nutrient replete specific growth rates increased with increasing temperature and photoperiod for both species as expected (Figure 19), with exception of the treatment with *S. minutulus* at 15°C and 12 h d^{-1} photoperiod, where the maximum growth rate was lower than in the treatment at 15°C and 9 h d^{-1} photoperiod.

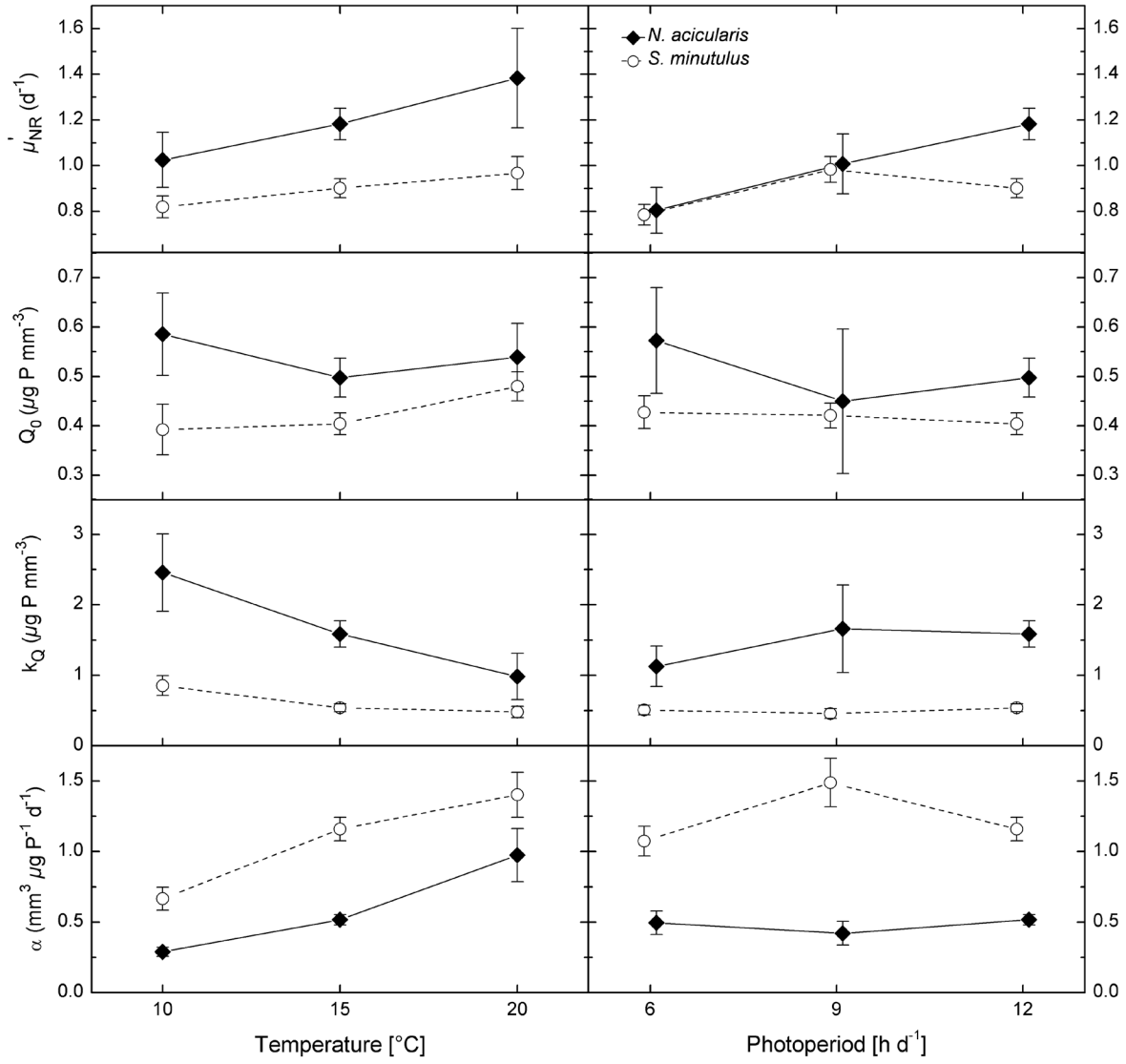

Figure 19: Temperature dependence (at 12 h d^{-1} photoperiod) and photoperiod dependence (at 15°C) of the physiological parameters fitted using (Eqs. 14a or 14b, p. 31): maximum specific growth rate (μ'_m), minimum P-quota (Q_0), half saturation constant (k_Q – Eq. 14a), and initial slope (α_Q – Eq. 14b) for *S. minutulus* and *N. acicularis*. Photoperiods have been staggered slightly to avoid overlap.

N. acicularis had a higher maximum (nutrient replete and light saturated) specific growth rate (μ'_{NR}) than *S. minutulus* at 10-20°C and 12 h d^{-1} photoperiod but growth rates were similar under shorter photoperiods, although the nutrient replete growth rates are not entirely comparable due to different light exposures as mentioned above. The maximum growth rates measured under P-replete conditions were compared with the base model (section 2.13.1, p. 28) and agreed very well with the model predictions (μ_{NR}, dotted line in Figure 18) for both species.

Table 8: Fitted parameters Eq. 14a or 14b (p. 32) for *S. minutulus* and *N. acicularis*. T: temperature, LP: photoperiod, LE: daily light exposure, Q_m: maximum P-quota measured under nutrient replete conditions, μ_{NR}: maximum (nutrient replete) specific growth rate, RSE: residual standard error, 95% confidence intervals are shown in parentheses.

Experimental conditions				Measured parameters			Fitted model parameters (Eqs. 14a or 14b)				
T (°C)	LP ($h\ d^{-1}$)	LE ($mol\ m^{-2}\ d^{-1}$)	I ($\mu mol\ m^{-2}\ s^{-1}$)	Cell size ($\mu m^3\ cell^{-1}$)	Q_m ($\mu g\ P\ mm^{-3}$)	μ_m (d^{-1})	μ_m' (d^{-1})	Q_0 ($\mu g\ P\ mm^{-3}$)	k_Q ($\mu g\ P\ mm^{-3}$)	α_Q ($mm^3\ \mu g\ P^{-1}\ d^{-1}$)	RSE (d^{-1})
S. minutulus											
10	12	2.98	66-75	185	4.99	0.80	0.82 (0.77-0.87)	0.39 (0.34-0.44)	0.85 (0.73-1.01)	0.67 (0.58-0.75)	0.059
15	12	2.94	65-73	175	3.01	0.87	0.90 (0.86-0.94)	0.40 (0.38-0.43)	0.54 (0.49-0.60)	1.16 (1.08-1.24)	0.052
20	12	2.98	66-75	164	3.09	0.94	0.97 (0.90-1.04)	0.48 (0.45-0.51)	0.48 (0.41-0.57)	1.40 (1.24-1.56)	0.066
15	6	4.21	180-200	184	-	0.74	0.78 (0.74-0.83)	0.43 (0.39-0.46)	0.51 (0.45-0.58)	1.07 (0.97-1.18)	0.063
15	9	4.54	133-145	189	-	0.96	0.98 (0.93-1.04)	0.42 (0.39-0.44)	0.46 (0.40-0.53)	1.49 (1.32-1.66)	0.068
N. acicularis											
10	12	4.10	92-98	109	5.91	0.79	1.03 (0.92-1.17)	0.59 (0.50-0.66)	2.46 (2.01-3.12)	0.29 (0.26-0.32)	0.039
15	12	5.62	95-105	107	5.89	1.09	1.18 (1.12-1.26)	0.50 (0.46-0.54)	1.59 (1.42-1.79)	0.52 (0.48-0.55)	0.036
20	12	3.89	86-95	94	3.85	1.27	1.38 (1.20-1.64)	0.54 (0.46-0.60)	0.98 (0.73-1.39)	0.98 (0.80-1.17)	0.103
15	6	4.32	190-205	93	6.44	0.80	0.80 (0.72-0.91)	0.57 (0.45-0.67)	1.13 (0.88-1.46)	0.50 (0.42-0.58)	0.087
15	9	4.21	125-140	99	5.73	0.95	1.01 (0.89-1.20)	0.45 (0.26-0.58)	1.66 (1.22-2.46)	0.42 (0.33-0.52)	0.082

The maximum P-quota (Q_m) when cells were growing at their maximum rate (μ_{NR}) under luxury consumption decreased with increasing temperature from about 5 μg P mm^{-3} at 10°C to 3 μg P mm^{-3} at 15°C and 20°C for *S. minutulus* ($p < 0.001$, Table 8). Overall *N. acicularis* could store more P than *S. minutulus* ($p < 0.001$), with Q_m decreasing significantly ($p < 0.001$) from 6 μg P mm^{-3} at 10°C to 4 μg P mm^{-3} at 20°C.

3.2.2 Temperature and photoperiod effects on P-limited growth

The minimum P-quota required for growth (Q_0) was lower for *S. minutulus* than for *N. acicularis*, whereas the initial slope (α_Q), which represents the efficiency of P usage, was higher for *S. minutulus* (Figure 19). This shows that *S. minutulus* is more efficient and can produce more biomass from a given amount of internal P than *N. acicularis*. Q_0 was independent of both temperature and photoperiod for both species. Although model fits suggested that Q_0 was significantly higher for *S. minutulus* at 20°C than in the other experiments (Table 8), this result was an artefact of model fitting because there was no significant difference between temperature treatments when the quotas measured in cultures grown to stationarity ($\mu = 0$) were compared directly by ANOVA ($p = 0.43$).

The half saturation coefficient k_Q did not change significantly with photoperiod for either *S. minutulus* ($p = 0.80$) or *N. acicularis* ($p = 0.06$). k_Q increased significantly with decreasing temperature in *N. acicularis* ($p < 0.001$). In *S. minutulus*, k_Q was not significantly different at 15°C and 20°C ($p = 0.19$) but was significantly higher at 10°C ($p < 0.001$). The initial slope α_Q increased significantly with increasing temperature for both species ($p < 0.001$), but did not change with photoperiod ($p \geq 0.08$). This suggests that the growth efficiency (α_Q) has the same temperature dependence as the nutrient replete growth rate (μ_{NR}) for *S. minutulus* but not for *N. acicularis*. In *N. acicularis*, α_Q increased faster than μ_{NR} with increasing temperature. In *S. minutulus*, k_Q was approximately equal to Q_0 (except at 10°C, where k_Q = 2.2 Q_0), whereas in *N. acicularis* k_Q was higher than Q_0 by a factor of 2 to 4 (Table 8). Therefore the simpler Droop (Eq. 11) and Fuhs (Eq. 13) models, which are half saturated at $2Q_0$ (i.e. such that $k_Q = Q_0$), provided a good description of the growth of *S. minutulus* but not of *N. acicularis*. Consequently a more complex model with a half-saturation coefficient was required for *N. acicularis*.

3.2.3 Model of factor interactions under P-limitation

To describe the interactions between temperature, photoperiod and P-limited growth, the temperature and photoperiod dependencies of the model parameters shown in Figure 19 were formulated in model terms. Because Q_0 was independent of photoperiod and temperature in both species, it was assumed constant in the model formulations. The Fuhs model (Eq. 13, p. 31) was adopted to describe P-limited growth rates of *S. minutulus* because k_Q was almost constant over the temperature range from 10 to 20 °C and over the photoperiod range from 6 to 12 h d^{-1}, and because the Droop relation of $k_Q = Q_0$ applied for this species as described above. Although a model with a half-saturation coefficient (Eq. 14a, p. 31) provided a significantly better fit ($p < 0.00001$), I think that the simpler Fuhs model is adequate based on visual inspection of the data and recommend this model due to its simplicity. The Droop model was not used because of a poorer fit and non-random residuals. Coupled to the base model of Nicklisch et al. (2008) to calculate μ'_{NR}, the Fuhs model accurately described the P-limited growth rates of *S. minutulus* under all tested conditions (Table 9).

For *N. acicularis*, a more complex model with k_Q or α_Q was necessary since the Droop relation did not apply. k_Q and α_Q, which can be used interchangeably, were dependent on temperature but independent of photoperiod in this species (Figure 19), so the simplest model formulation was to apply a temperature function to α_Q in Eq. 14b (p. 32) as follows:

$$\alpha_Q = \alpha_{Qm} \cdot g(T) \tag{34}$$

$$g(T) = \exp\left\{-2.3 * \left(\frac{T_{opt} - T}{T_{opt} - T_{minQ}}\right)^2\right\} \tag{35}$$

Where α_{Qm} is the initial slope at optimum temperature and $g(T)$ is the temperature function after Lehmann *et al.* (1975) with temperature T, optimum temperature T_{opt} and minimum temperature T_{minQ} (all °C). Note that $g(T)$ is identical to $f(T)$ in the base model (Eq. 7, p. 29) in terms of the equation and parameters, except that T_{min} in *f(T)* has been replaced by T_{minQ} in *g(T)*. This combined model for *N. acicularis* (Table 9) overall produced a good fit to the measured data under all temperatures and photoperiods, which was significantly better than model formulations without a temperature-dependent α_Q ($p < 0.001$, ANOVA).

Table 9: Model of factor interactions and corresponding parameters for P-limited growth of *S. minutulus* and *N. acicularis*. 95% confidence intervals shown in parentheses.

Parameter	Description	Units	*S. minutulus* (Eq. 13, p. 31)	*N. acicularis* (Eq. 14b p. 32, Eq. 34, Eq. 35)
μ'_{NR}	Nutrient replete (maximum) specific growth rate	d^{-1}	Base model (Eq. 5, p. 28)	Base model (Eq. 5, p. 28)
Q_0	Minimum P-quota	$\mu g\ P\ mm^{-3}$	0.452 (0.445 – 0.458)	0.532 (0.491 – 0.569)
k_Q	Half-saturation coefficient at optimum temperature	$\mu g\ P\ mm^{-3}$	-	-
α_{Qm}	Initial slope at optimum temperature	$mm^3\ \mu g\ P^{-1}\ d^{-1}$	-	0.898 (0.815 – 0.988)
T_{opt}	Optimum temperature	°C	-	21.7[a]
T_{minQ}	Minimum temperature	°C	-	6.6 (5.2 – 7.6)
RSE	Residual standard error	d^{-1}	0.069	0.089
df	Degrees of freedom	-	331	184

[a] Value adopted from the base model (Table 5, p. 30).

The models were used to plot the growth isoclines under combined limitation by phosphorus and temperature or photoperiod (Figure 20). *S. minutulus* could achieve the same growth rate as *N. acicularis* at considerably lower temperatures, photoperiod and P-quota combinations. The curved regions of these interaction diagrams indicate that an increase in photoperiod and temperature can compensate for a decrease in P-quota, and the regions of interaction correspond to the prevailing spring conditions for these species (roughly 8-15°C and 4-8 h d^{-1} photoperiods).

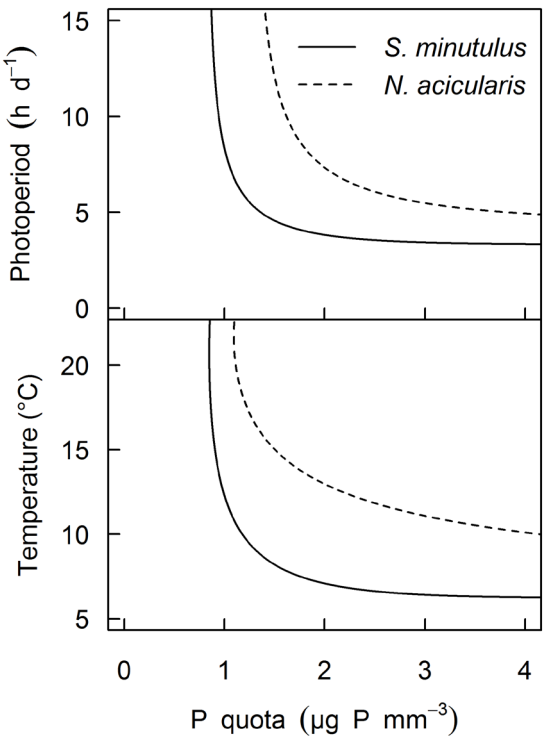

Figure 20: Interaction diagrams showing lines of constant growth rate (0.5 d^{-1}) in response to photoperiod and P-quota at 15°C (top panel), temperature and P-quota at 12 h d^{-1} photoperiod (bottom panel).

3.2.4 Competition experiments under P-limitation

In competition experiments under P-limitation, *N. acicularis* was the stronger competitor at all temperatures (10°C, 15°C, 20°C) and all photoperiods tested (6 h d^{-1} and 12 h d^{-1}). The competitive ability of the weaker species (*S. minutulus*) relative to the stronger species (*N. acicularis*) can be quantified by

$$\text{Competitive ability} = 1+\mu_{net}/D \qquad (36)$$

where μ_{net} is the net specific growth rate (≤ 0) and D is the applied dilution rate. The competitive ability is thus 1 when the two species coexist and 0 when the weaker species does not grow and is washed out at the dilution rate.

Table 10: Cultivation conditions and growth rates for P-competition experiments between *N. acicularis* and *S. minutulus*. T: temperature, LP: photoperiod, LE: daily light exposure, I: irradiance; df: degrees of freedom, D: applied dilution rate, μ_{net} net growth rate of the weaker competitor (*S. minutulus* in all cases), SE: standard error, μ: specific growth rate of the weaker competitor, CA: competitive ability of the weaker competitor (Eq. 36).

T (°C)	LP ($h\ d^{-1}$)	LE ($mol\ m^{-2} d^{-1}$)	I ($\mu mol\ m^{-2}\ s^{-1}$)	No. cultures	*df*	D (d^{-1})	μ_{net} (d^{-1})	SE (d^{-1})	μ (d^{-1})	CA
15	6	4.32	200	4	40	0.4	-0.127	0.012	0.273	0.683
10	12	5.18	120	4	32	0.4	-0.048	0.003	0.352	0.880
15	12	3.67	85	4	26	0.5	-0.250	0.013	0.250	0.500
20	12	3.67	85	2	10	0.5	-0.298	0.024	0.202	0.404

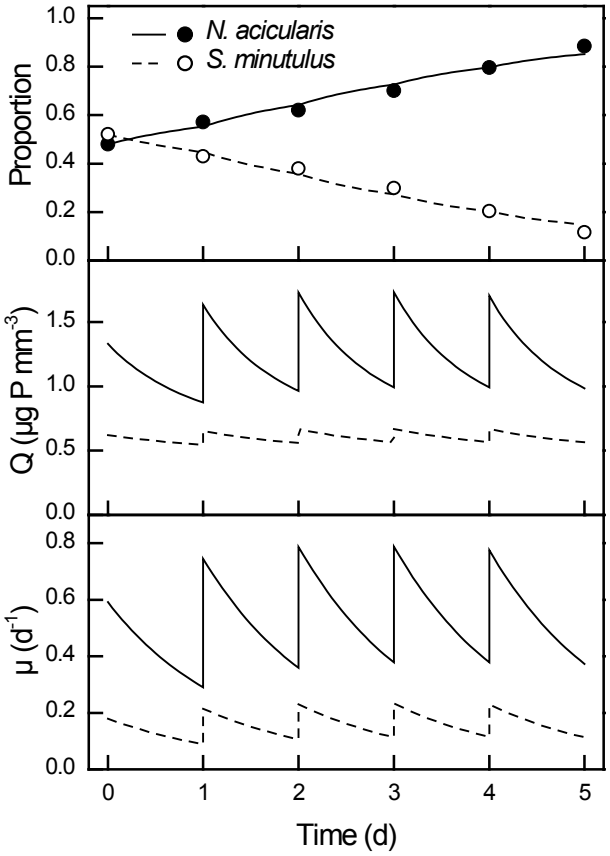

Figure 21: Simulation of P-competition experiments between *N. acicularis* (stronger competitor, solid line) and *S. minutulus* (dashed line), here at 15°C, 12 h d^{-1} photoperiod and 85 μmol PAR $m^{-2}\ s^{-1}$. a) Proportions of each species by biovolume; b) biovolume P-quota; c) specific growth rates. Points show measured values.

The experiments showed that, relative to *N. acicularis*, the competitive ability of *S. minutulus* increased with decreasing temperatures under a 12 h d^{-1} photoperiod (Table 10, $p < 0.001$, multiple linear regression on time and temperature) and was higher at 6 h d^{-1} photoperiod than at 12 h d^{-1} photoperiod at 15°C ($p < 0.001$, t-test on linear regression slopes).

3.2.5 Relative P uptake rates

The relative uptake rates were estimated from the model simulations, which accurately described the measured cell proportions of the two species in the competition experiments (Figure 21). The estimated relative uptake rates (Figure 22) showed a similar pattern to the competitive ability results shown in Table 10.

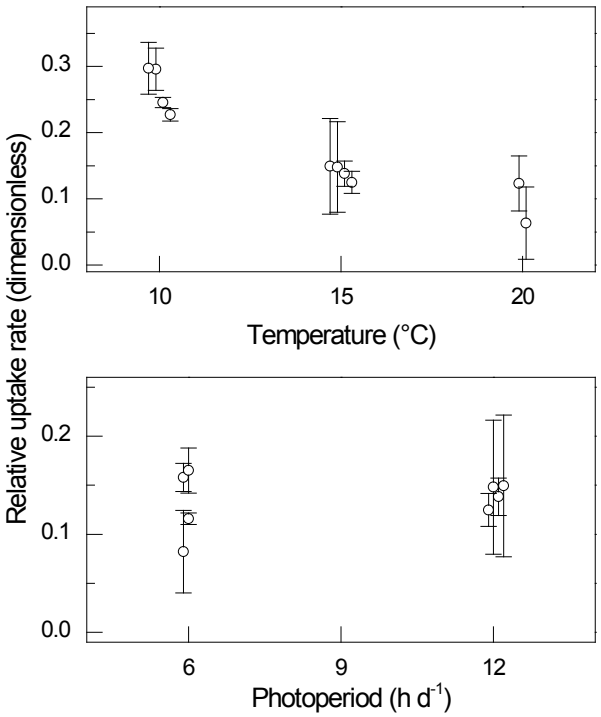

Figure 22: P-uptake rates of *S. minutulus* relative to *N. acicularis* at different temperatures with a 12 h d^{-1} photoperiod (top panels) and at different photoperiods at 15°C (bottom panels). Open circles show the fitted values of parameter c for *S. minutulus*, error bars show 95% confidence intervals of the fitted values.

The simulations showed that the uptake rate of *S. minutulus* relative to *N acicularis* was higher at 10°C compared to 15°C and 20°C (Figure 22, p = 0.0004, ANOVA). At 10°C under a photoperiod of 12 h d^{-1}, *S. minutulus* absorbed about 25-30% of the added P, whereas at 20°C it absorbed around 10%, while *N. acicularis* absorbed 90%. There was no significant difference between the relative uptake rates at 6 h d^{-1} and 12 h d^{-1} photoperiod (p = 0.6),

where *S. minutulus* and *N. acicularis* absorbed on average 14% and 86% of added P, respectively.

3.3 Silicon and its interactions with temperature and photoperiod

3.3.1 Chemostat experiments under silicon limitation

Interactions of photoperiod and temperature with silicon limited growth were investigated with *S. minutulus* in continuous chemostat culture (Shatwell et al., 2013). *N. acicularis* failed to grow in the chemostat, presumably due to turbulence from aeration, so experiments with this species were only performed under some selected conditions in batch culture as described below. Nutrient replete growth rates (μ_{NR}) for *S. minutulus* were taken from the previous results on fluctuating light (Table 6, p. 44 and Table 7, p. 45) and phosphorus limitation (Table 8, p. 56), except for the experiment at 5°C, where nutrient replete growth was measured in turbidostat mode. Therefore, the asymptotic maximum growth rate (μ_{NR}) in the Monod equation (Eq. 18, p. 34) was not fitted to the data but set to these measured nutrient replete rates. As described in sections 3.1 and 3.2.1, the nutrient replete growth rates increased with increasing temperature and photoperiod as expected, and agreed very well with the base model. The transition from nutrient saturated growth to nutrient limitation was quite abrupt, and growth was only substantially silicon limited at concentrations below 1 μmol L^{-1} (Figure 23), also evident from the half-saturation constants, k_S (Table 11). There was no relationship between cellular silicon content and dilution rate.

Comparing the fitted Monod model parameters showed that there was no temperature dependence in the minimum silicon concentration for growth, S_0 ($p = 0.19$, Figure 24), although there were some significant differences in S_0 at 10°C and 15°C. The apparent half saturation constant k_S+S_0 increased significantly with temperature ($p = 0.04$), as did K itself. The initial slope of the Monod curve ($\alpha_s = \mu_{NR}/k_S$) did not change significantly with temperature ($p = 0.54$). S_0 was significantly higher at 9 h d^{-1} photoperiod ($p < 0.001$) than at 6 or 12 h d^{-1} photoperiod, which did not differ significantly. Overall S_0 did not depend on photoperiod ($p = 0.34$) but k_S decreased significantly with increasing photoperiod ($p = 0.01$) according to model fits with all photoperiod treatments. There was a significant increasing trend of the initial slope (μ_{NR}/k_s) with increasing photoperiod ($p = 0.01$, Figure 24d). However, the initial slope at 6 and 9 h d^{-1} (at 15°C) in Figure 24d was very similar to the

initial slope at 5, 10 and 20°C (at 12 h d^{-1}) in Figure 24c, so it might be reasonable to assume that the initial slope is relatively constant for this species.

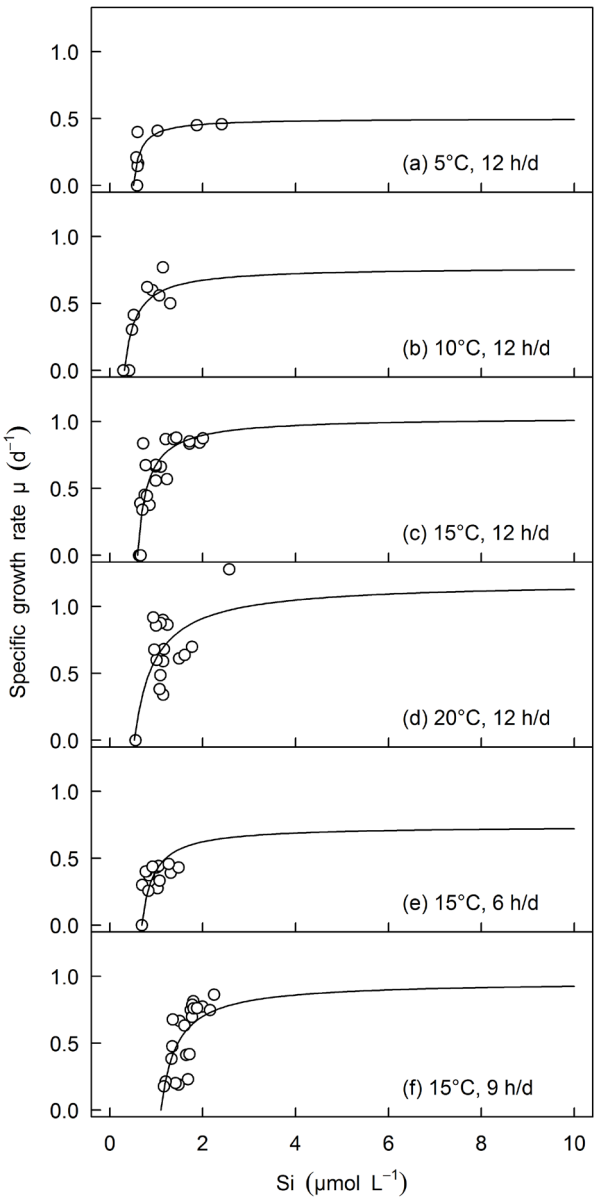

Figure 23: Growth rates of *S. minutulus* as a function of dissolved silicon concentration, grown in chemostats at different temperatures (a – d) and different photoperiods (c, e, f). Curves show the fitted Monod model (Eq. 18, p. 34) with the parameters in Table 11.

Table 11: Measured and fitted parameters for the growth of *S. minutulus* and *N. acicularis* under Si-limitation. T = temperature, LP = photoperiod, LE = light exposure, RSE = residual standard error; 95% confidence intervals are given in parentheses.

Experimental conditions					Measured parameters			Fitted parameters				
Culture method	T (°C)	LP (h d^{-1})	LE (mol m^{-2} d^{-1})	I (μmol m^{-2} s^{-1})	Cell size (μm^3 $cell^{-1}$)	Si content (fmol $cell^{-1}$)	Si content (μmol mm^{-3})	μ_{NR} (d^{-1})	k_S+S_0 (μmol L^{-1})	S_0 (μmol L^{-1})	μ_{NR}/k_S	RSE (d^{-1})
S. minutulus												
Chemostat, turbidostat	5	12	4.1	95	243 (219-267)	187 (174-200)	0.77 (0.75-0.80)	0.50 (0.32-0.77)	0.65 (0.45-0.84)	0.51 (0.24-0.77)	3.6 (-)	0.12
Chemostat	10	12	4.0	93	236 (196-277)	170 (154-187)	0.74 (0.65-0.83)	0.77[a]	0.55 (0.39-0.71)	0.31 (0.24-0.38)	3.2 (1.0-5.5)	0.13
Chemostat	15	12	4.4	102	251 (231-271)	199 (167-232)	0.79 (0.68-0.91)	1.03[b]	0.80 (0.73-0.88)	0.59 (0.52-0.66)	5.0 (2.4-7.6)	0.16
Chemostat	20	12	4.6	106	209 (181-238)	198 (171-225)	0.95 (0.88-1.03)	1.18[a]	0.96 (0.77-1.15)	0.53 (0.33-0.73)	2.7 (1.2-4.2)	0.22
Chemostat	15	6	4.0	185	164 (159-170)	121 (114-129)	0.74 (0.69-0.78)	0.74[c]	0.93 (0.82-1.13)	0.69[d]	3.0 (1.4-4.6)	0.14
Chemostat	15	9	4.5	140	193 (181-206)	131 (125-137)	0.70 (0.64-0.76)	0.96[c]	1.43 (1.30-1.56)	1.10 (0.94-1.26)	2.9 (1.2-4.5)	0.18
N. acicularis												
Batch	10	12	4.3	100	127 (117-137)	297 (259-335)	2.34 (2.04-2.64)	0.86 (0.78-0.94)	1.57 (1.27-2.01)	0.74 (0.67-0.79)	1.03 (0.72-1.53)	0.066
Batch	15	12	4.3	100	135 (124-145)	378 (234-522)	2.80 (1.73-3.87)	1.16 (1.07-1.26)	1.61 (1.13-2.2)	0.22 (0.13-0.29)	0.84 (0.62-1.21)	0.062
Batch	15	9	4.2	130	179 (161-197)	305 (274-335)	1.70 (1.53-1.87)	0.78 (0.72-0.84)	1.77 (1.34-2.33)	0.18 (0.13-0.22)	0.49 (0.38-0.64)	0.044

[a] from Table 7, p. 45; [b] from Table 6, p. 44; [c] from Table 8, p. 56; [d] not fitted, lowest measured value adopted

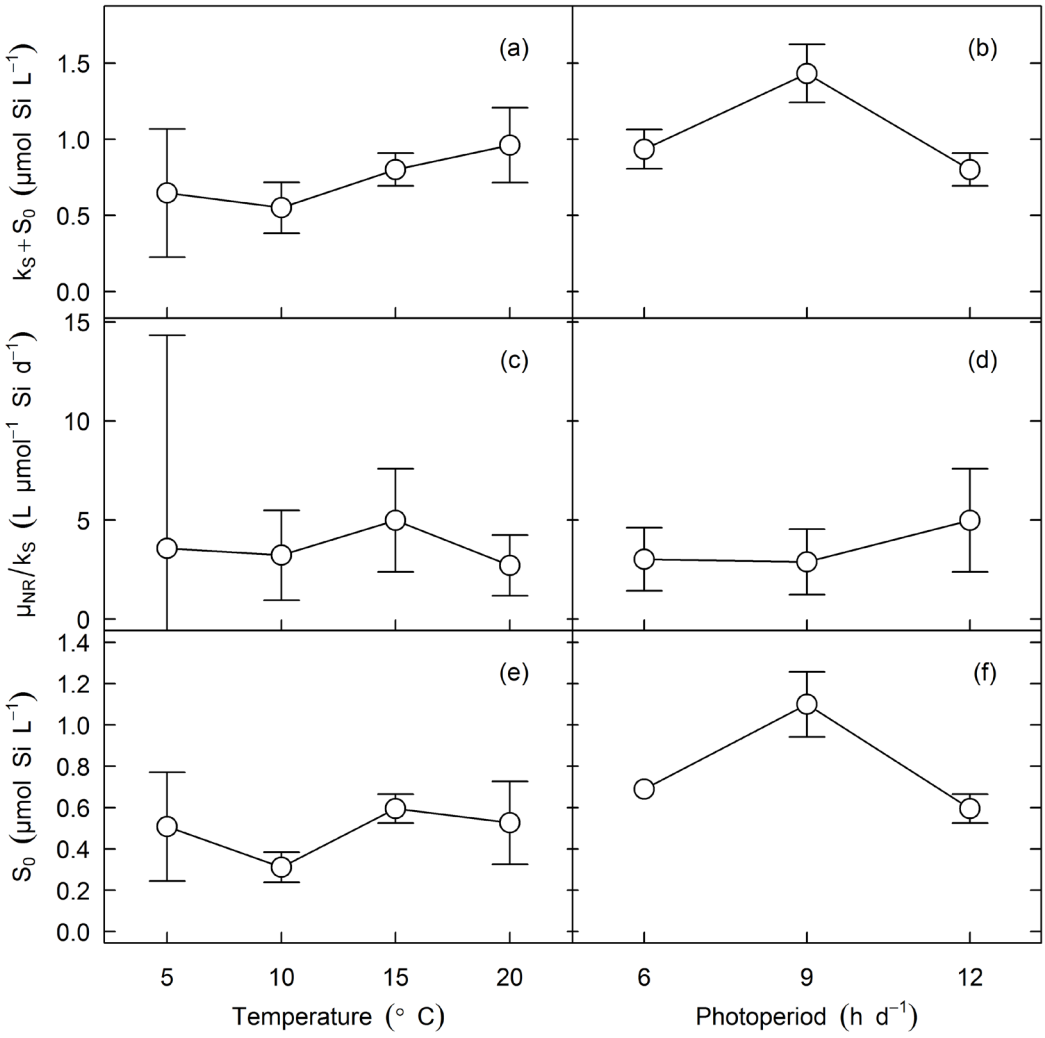

Figure 24: Parameters of the Monod model for Si-limited growth (Eq. 18, p. 34) (apparent half-saturation constant, k_S+S_0, initial slope $\alpha_s = \mu_{NR}/kS$ and minimum concentration, S_0). The points show the fitted parameter values that describe the curves in Figure 23 as a function of temperature (at 12 h d^{-1} photoperiod, left panels) and photoperiod (at 15°C, right panels) for *S. minutulus*. Error bars show the 95% confidence intervals of the parameter estimates (*n* ranges from 7 to 20 for each curve, see Figure 23). Maximum growth rates were not fitted.

3.3.2 Batch experiments under silicon limitation

Batch experiments were performed with *N. acicularis* under silicon limitation at 10°C and 15°C at 12 h d^{-1} and at a photoperiod of 9 h d^{-1} at 15°C (Figure 25). The maximum specific growth rates obtained by fitting the Monod model agreed well with the base model, except at 9 h d^{-1}. Here the fitted growth rates (0.78 d^{-1}) were somewhat lower than the rates measured in the phosphorus limitation experiments (0.95 d^{-1}, see Table 8, p. 56) or estimated by the base

model (0.97 d^{-1}). Growth of *N. acicularis* only became limited by silicon at concentrations below about 3 μmol L^{-1}, which is somewhat higher than *S. minutulus*. Whereas S_0 was significantly lower for *N. acicularis* than for *S. minutulus* at 15°C ($p < 0.0001$), k_S was significantly higher ($p = 0.0001$, Table 11). This was not the case at 10°C, where k_S and S_0 were both significantly higher for *N. acicularis* than for *S. minutulus* ($p \leq 0.01$).

For *N. acicularis*, there was no significant difference in k_S between 10°C and 15°C ($p = 0.39$) but S_0 was higher at 10°C than at 15°C ($p < 0.0001$, Table 11). Comparing photoperiod treatments at 15°C showed that neither k_S nor S_0 differed between 9 h d^{-1} and 12 h d^{-1} photoperiod treatments ($p = 0.57$ and $p = 0.34$ respectively).

The silicon content of silicon limited cells of *N. acicularis* increased with increasing growth rate and this also applied when the cultures were grown to stationary phase: cells that were exposed to higher start concentrations had a higher silicon content when this nutrient was depleted.

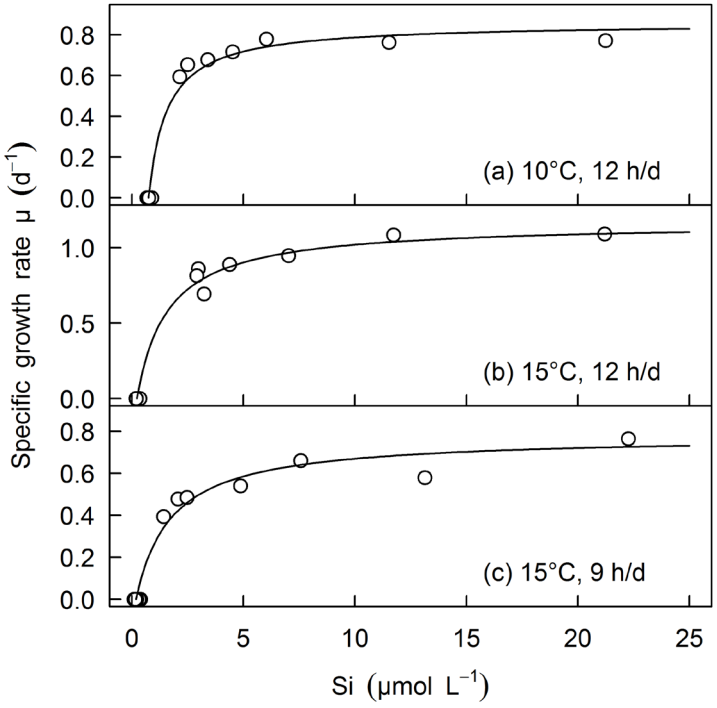

Figure 25: Growth rates of *N. acicularis* as a function of dissolved silicon concentration, grown in batch culture. Curves show the fitted model (Eq. 18, p. 34) with the parameters in Table 11.

3.3.3 Model of factor interactions under silicon limitation

To investigate interactions of temperature and photoperiod with silicon limited growth, the Monod model of silicon limited growth was coupled to the base model. The base model was used to describe the nutrient replete growth rates (μ_{NR}) of *S. minutulus* and *N. acicularis*, accounting for co-limitation of temperature, photoperiod and light exposure. For *S. minutulus*, k_S was dependent on temperature and may also have been dependent on the photoperiod. Alternatively, since k_S increased with temperature in parallel with μ_{NR}, the initial slope seemed to be constant over most temperatures and photoperiods, with the exception of an increase at 15°C / 12 h d^{-1}, and was adopted as a model parameter in the Monod equation (Eq. 18, p. 34) by substituting:

$$k_S = \frac{\mu_{NR}}{\alpha_S} \tag{37}$$

Table 12: Parameters of the model of temperature and photoperiod interactions with silicon limited growth. The parameters are for the Monod model (Eq. 18, p. 34). The Monod model was coupled here to the base model (section 2.13.1), which was used to calculate μ_{NR}; 95% confidence intervals are given in parentheses. For *S. minutulus*, the Monod model formulation with constant initial slope (α_S) is used.

Parameter	Description	Units	*S. minutulus*	*N. acicularis*
μ_{NR}	Nutrient replete growth rate	d^{-1}	Calculated with the base model	Calculated with the base model
S_0	Minimum nutrient concentration	μmol Si L^{-1}	0.55† (0.41-0.68)	0.24 (0.16-0.32)
k_S	Half saturation coefficient	μmol Si L^{-1}	μ_{NR}/α_S‡	1.87 (1.44-2.41)
α_S	Initial slope of Monod curve	L μmol^{-1} d^{-1}	3.14 (2.45-3.98)	-
df	Degrees of freedom	-	48	46
RSE	Residual standard error	d^{-1}	0.28	0.10

† Not fitted but set as the mean of all values measured at $\mu = 0$
‡ See Eq. 37

For *N. acicularis*, the interactions under silicon limitation can be described by the Monod model with constant k_S, since this parameter was not affected by temperature or photoperiod over the tested range. S_0 was higher at 10°C than at 15°C, but there were insufficient data to characterise a possible temperature dependency, thus S_0 was also assumed to be a model constant.

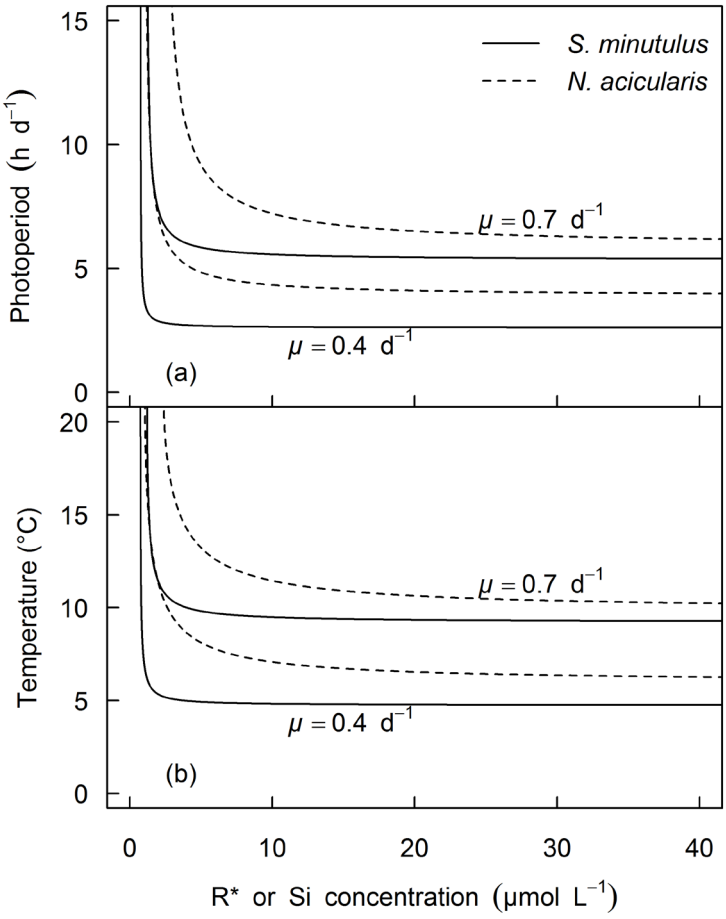

Figure 26: Interaction diagrams depicting the interactions of photoperiod (a) and temperature (b) with silicon concentration for *S. minutulus* (solids lines) and *N. acicularis* (dashed lines). Lines are isoclines of constant growth rate, here $\mu = 0.7$ d^{-1} for the upper two curves of each panel and $\mu = 0.4$ d^{-1} for the lower two curves of each panel. Photoperiod interactions (a) are shown at 15°C and light saturation and temperature interactions (b) are shown at 12 h d^{-1} photoperiod and light saturation. R* after Tilman (1982) is the Si concentration that supports the given growth rate at equilibrium (see text). The isoclines were calculated with the model described in Table 12.

Thus the complete coupled model, summarised in Table 12, accounts for the interactions of temperature and photoperiod with silicon limited and silicon replete growth, and was used to generate interaction diagrams (Figure 26) after Tilman (1980, 1982). Interactions between growth factors are evident as curved regions in the growth isoclines and indicate co-limitation of the two factors. There were only narrow ranges of interaction between silicon and the physical factors for *S. minutulus* at moderate to low growth rates as evident from a relatively sharp "L-shaped" curve (tending to Liebig's Minimum Law), whereas the interaction ranges were slightly broader and more curved for *N. acicularis* (Figure 26). The interaction ranges broadened for both species at higher growth rates, but nevertheless suggest that silicon co-limitation does not occur at concentrations above about 10-15 μmol L^{-1} for these species. The model suggests that *S. minutulus* is generally more competitive than *N. acicularis* under Si limitation, but *N. acicularis* can coexist at temperatures above 15°C and photoperiods longer than 10 h d^{-1} under strong silicon limitation ($\mu < 0.4$ d^{-1}). Also, at higher Si concentrations and slight Si limitation ($\mu > 0.7$ d^{-1}) the difference between the two species becomes smaller (Figure 26), because *N. acicularis* has a higher maximum specific growth rate above 12-13°C.

3.3.4 Competition experiments in semi-continuous culture

Competition experiments with *S. minutulus* and *N. acicularis* under silicon limitation were performed in semi-continuous culture to investigate the effect of temperature on competitive ability and test the model predictions described above. In these experiments *S. minutulus* displaced *N. acicularis* at 10°C and 15°C and both species coexisted for the duration of the experiment at 20°C (Figure 27). The competitive superiority of *S. minutulus* decreased with increasing temperature, so that *N. acicularis* was displaced more slowly at 15°C than at 10°C. At 20°C it is remarkable that *N. acicularis* was not displaced when cultures were diluted daily but was outcompeted under the stronger dilution at intervals of 2 or 3 days (Figure 27c). The stronger dilution increases the Si-concentration above limiting values and *N. acicularis* should then profit since it has a higher μ_m. However this was not the case, which indicates that *S. minutulus* has a higher uptake rate and perhaps can store some Si. Obviously, under such conditions uptake and growth are uncoupled and the Monod model cannot describe the behaviour correctly.

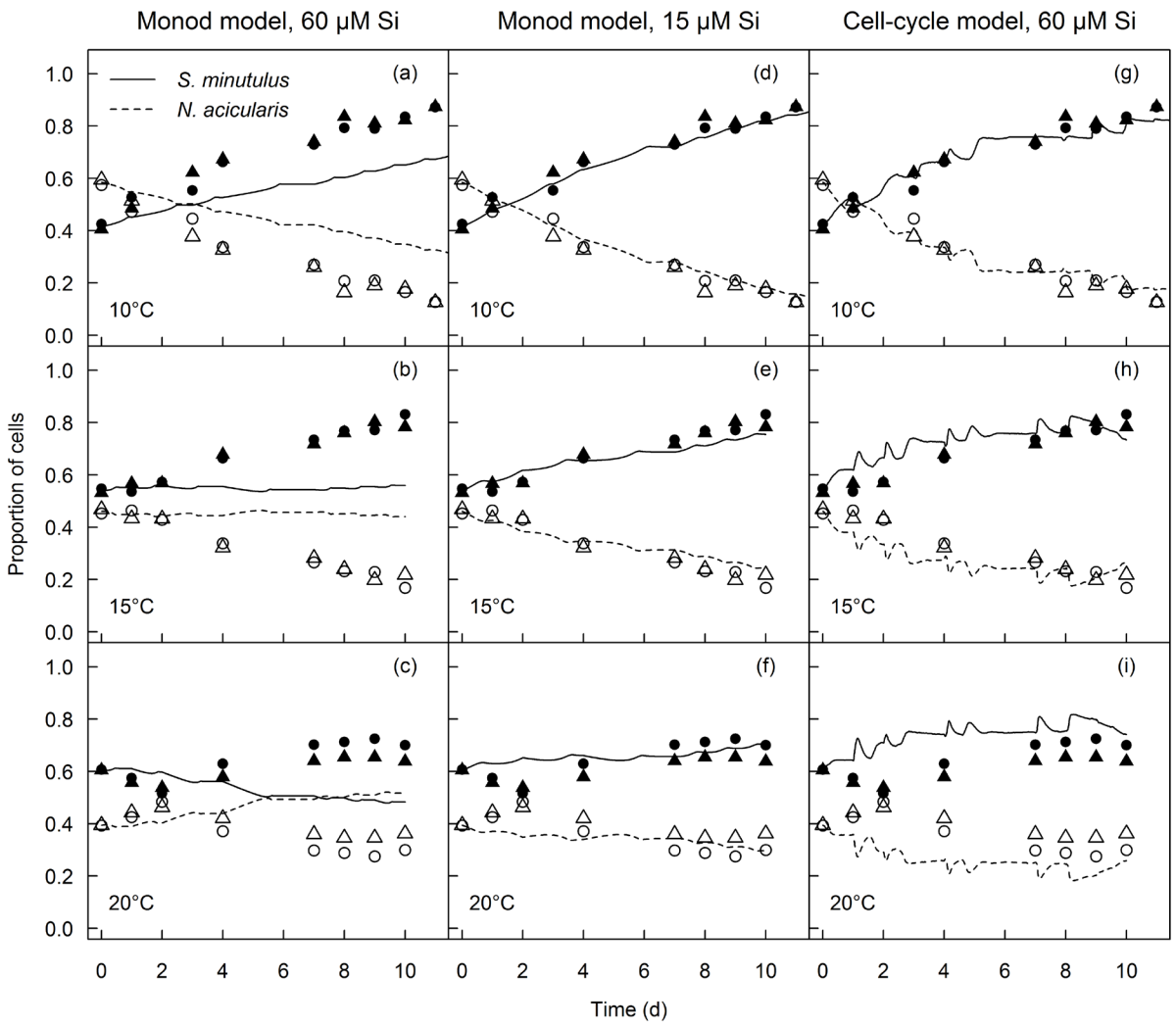

Figure 27: Results of Si-competition experiments (symbols) and model simulations (lines) at 10°C (a, d, g), 15°C (b, e, h) and 20°C (c, f, i) under a photoperiod of 12 h d^{-1}. The right hand panels (g – i) show simulations with the cell-cycle model, other panels with the Monod model; parameters are given in Table 12. The simulations in d – f assumed a decreased silicate concentration of 15 μmol Si L^{-1} in the medium. Filled symbols: *S. minutulus*, open symbols: *N. acicularis*; circles: experiment 1; triangles: experiment 2. Applied dilution rates were D = 0.4 d^{-1} at 10°C and D = 0.5 d^{-1} at 15°C and 20°C.

This was evident from the Monod model simulations (Figure 27 a – c) where simulations were in poor agreement with the measured rates of exclusion. Therefore I simulated the growth of *S. minutulus* and *N. acicularis* in competition experiments with the silicate concentration in the medium decreased from 60 to 15 μmol Si L^{-1} and the initial biomass concentration reduced proportionately (Figure 27 d – f). At these concentrations growth in situ is typically Si limited and biovolumes are close to naturally occurring concentrations below 100 mm^3 L^{-1}. Furthermore, the simulation very closely matched the observed dynamics of the competition experiments. In addition, I simulated the course of the competition experiments

using the cell-cycle model (Figure 27 g – i) with the medium concentration actually used in the experiments (60 μmol Si L^{-1}). The cell-cycle model reproduced the competition experiments quite accurately and much better than the Monod simulations at the same medium concentration (Figure 27 a – c).

The competition results were in agreement with model predictions described above, in particular that *S. minutulus* is the stronger competitor under Si-limitation, and that the competitive ability of *N. acicularis* relative to *S. minutulus* should increase with increasing temperature. According to Tilman (Tilman, 1982), R* is the limiting resource concentration at which the growth rate of a particular species just balances its loss rate at equilibrium (cf. isoclines in Figure 26). The lower the value, the more competitive the species is for that resource. R* values calculated for the experimental conditions in competition experiments were quite constant with temperature at 0.82, 0.88, and 0.85 μmol L^{-1} for *S. minutulus* at 10, 15, and 20°C respectively, but decreased with temperature for *N. acicularis*, with values of 2.63, 1.80, 1.41 μmol L^{-1} at 10, 15, and 20°C respectively.

3.4 Nutrient interactions in situ

To determine whether the interactions are meaningful *in situ*, data from a eutrophic temperate lake were examined as an example (Lake Müggelsee, Berlin). Silicon was potentially a limiting nutrient in the lake during a period of high P-loading until it returned to a eutrophic state in 1997 after a reduction in P-loading (Köhler et al., 2005). During the spring diatom blooms in years when silicate was likely to be growth limiting, silicate concentrations fell below 15 μmol L^{-1} on average for 6 weeks and below 5 μmol L^{-1} for 2.9 weeks. During periods when silicate levels were below 15 μmol L^{-1} the mean temperature in the lake was 10.1°C ± 3.3°C (mean ± SD), the mean effective photoperiod was 6.4 ± 1.2 h d^{-1} and the mean daily light exposure in the mixed layer was 2.9 ± 1.0 mol PAR m^{-2} d^{-1}. An interaction diagram drawn for these conditions showed that *S. minutulus* could achieve higher growth rates than *N. acicularis* and is likely to be silicon limited only below about 2 μmol L^{-1} (Figure 28). By comparison, *N. acicularis* is likely to be affected by silicon limitation below 5-10 μmol L^{-1}.

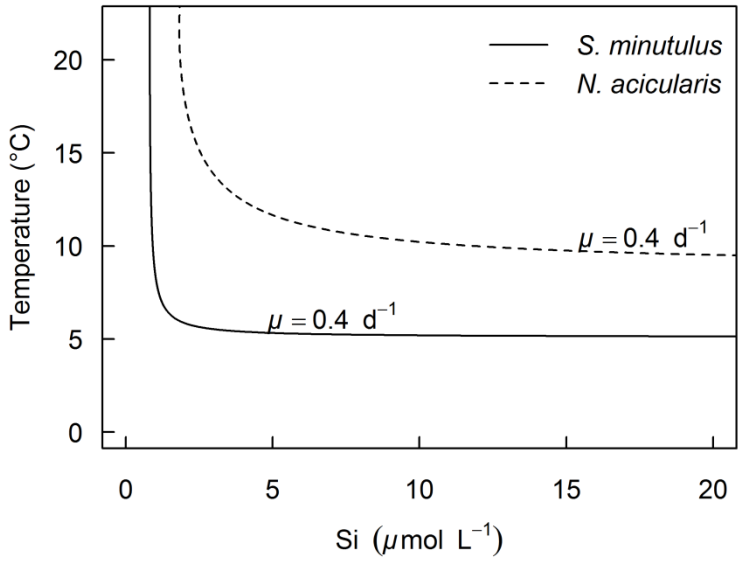

Figure 28: Interaction diagram for temperature and silicon concentrations under mean conditions during spring silicon limitation in Lake Müggelsee (photoperiod = 6.4 h d^{-1}; light exposure = 2.9 mol PAR m^{-2} d^{-1}). Growth isoclines were calculated with the model in Table 12.

A multiple linear regression analysis on the field data from Lake Müggelsee revealed that the mean spring biomass of centric diatoms (X_{cen} in mm^{-3} L^{-1}) could be best described as a function of mean silicate concentration (DSi in μmol L^{-1}, $p < 0.001$), mean water temperature (T in °C, $p < 0.001$), mean effective photoperiod (LP in h d^{-1}, $p = 0.006$), and mean total phosphorus concentration (TP in μg L^{-1}, $p = 0.02$) according to:

$$X_{cen} = 20.7 - 0.92 \times T - 0.82 \times LP - 1.76 \times DSi + 0.049 \times TP \quad (38)$$

Eq. 38 ($R^2 = 0.83$, $n = 25$, $p < 0.000001$) shows that centric diatoms in the lake, which are dominated by *Stephanodiscus neoastraea*, are favoured by low DSi, low temperature, short effective photoperiods and high phosphorus concentrations. The interaction terms of the physical factors (T, LP) with the nutrients (DSi, TP) as well as other variables such as mean light exposure, starting population size and grazer (cladoceran) abundance did not significantly improve the model and were dropped. The biomass of pennate diatoms (X_{pen} in mm^3 L^{-1}), of which the dominant form is *Synedra acus*, could be described in terms of the mean underwater light exposure (LE in mol m^{-2} d^{-1}), the starting population size (startpop in mm^3 L^{-1}), the cladoceran abundance (G in ind×10^3 L^{-1}), T and LP by the following model:

$$X_{pen} = 6.57 - 0.58 \times T - 1.73 \times LP + 3.97 \times LE + 3.11 \times startpop + 0.45 \times G \quad (39)$$

($R^2 = 0.76$, n = 25, $p < 0.0001$)

where the pennate diatom biomass increases with lower temperature, shorter effective photoperiods, higher underwater irradiance, larger start populations and more abundant grazers. Other variables and the interactions tested did not significantly improve the model. The biomass of total diatoms (X_{dia}) depended significantly on the physical factors and silicate:

$$X_{dia} = 41.2 - 1.58 \times T - 4.50 \times LP + 6.66 \times LE - 1.94 \times DSi \quad (40)$$

($R^2 = 0.80$, n = 25, $p < 0.000001$)

where low temperatures, short photoperiods, low silicate concentrations and high light exposures favour higher diatom concentrations.

4. Discussion

The interactive effects of physical factors and nutrients on phytoplankton growth are non-linear and species specific. Consequently, a shift in the relationship between the important growth factors should have an effect on the species composition, particularly in spring. Knowledge of the interactions should help untangle the combined effects of climate and trophic change. Therefore, the main objectives of this thesis were to characterise the interactive effects of temperature and photoperiod on growth limited by 1) fluctuating light, 2) phosphorus, and 3) silicon. These interactions were then to be characterised mathematically in model terms to enable the results to be generalised and formally compared. Finally the thesis aimed to draw inferences about the role of interactions in phytoplankton ecology, in particular, niche differentiation, with the hope of unravelling some of the complexity that contributes towards Hutchinson's Paradox of the Plankton (Hutchinson, 1961).

4.1 Hypotheses

The fluctuating light experiments confirmed that phytoplankton respond to fluctuating light with decreased growth rates (Shatwell et al., 2012). The results demonstrated that the combined effects of a shorter photoperiod and fluctuating light on growth were equal to the sum of individual effects. I showed that the percentage decrease in growth rate caused by fluctuating light was independent of temperature (at a photoperiod of 12 h d^{-1}) and photoperiod (at a temperature of 15°C) in all tested species, with only one significant exception in *S. minutulus*. I therefore reject hypothesis (1) which states that temperature and photoperiod alter the response of phytoplankton to fluctuating light.

The phosphorus limitation experiments demonstrated that temperature influenced the relationship between growth and P-quota of *S. minutulus* and *N. acicularis*, but the effect of photoperiod length was not significant. Moreover the effect of temperature differed between species in a way that a fixed quota curve such as the Droop model could not entirely account for. Similarly, temperature also influenced the relative phosphorus uptake rates of the two species, but the photoperiod apparently had no influence here. I therefore confirm hypothesis (2) that there is a complex interaction between temperature and phosphorus limitation but reject the claim that the photoperiod has an effect.

In the silicon limitation experiments, the results showed that temperature influenced silicon-limited growth of *S. minutulus* and *N. acicularis* in a species-specific way and altered the outcome of competition under silicon limitation (Shatwell et al., 2013). The effect of the photoperiod was more difficult to characterise but seemed to have a similar effect to temperature for each species. Thus the initial slope of the Monod curve was constant for *S. minutulus*, whereas in *N. acicularis* the half-saturation coefficient appeared to be constant. Therefore, I confirm hypothesis (3) that temperature influences the kinetics of silicon limited growth in a species-specific way, but can neither confirm nor reject with certainty the proposition that the photoperiod has an effect.

The statistical analysis of field data showed that the physical factors and nutrients in question (temperature, photoperiod, silicon, phosphorus) all significantly contributed to the biovolume of centric diatoms and total diatoms. Moreover, the direction (sign) of the regression coefficients pointed towards the interaction type predicted by the experiments, such as increased competitiveness of the centric diatom *Stephanodiscus minutulus* under silicon limitation at low temperature. Furthermore, interaction diagrams after Tilman (1982) constructed using models of factor interactions (the base model coupled to nutrient limitation models) showed that factor interactions occurred at conditions and growth rates typical for spring. I therefore confirm hypothesis (4) that the factor interactions are relevant in situ during spring.

Stephanodiscus minutulus is a centric diatom and an early spring species and thus typically reaches its highest biomasses at low temperatures, short daylengths, and under more intense mixing (Nicklisch et al., 2008, Shatwell et al., 2008, Sommer et al., 1986). *Nitzschia acicularis* is a pennate diatom which occurs in late spring (Teubner, 1996), at higher temperatures with a more stable water column. It is a "velocity" species (Sommer, 1985) with a higher optimum temperature than *Stephanodiscus minutulus* (Giersdorf, 1988, Kohl and Giersdorf, 1991, Nicklisch et al., 2008). *Nitzschia acicularis* occurs more frequently under high Si:P ratios (Kilham et al., 1986, Sommer, 1989), whereas the genus *Stephanodiscus* occurs at low Si:P ratios (Kilham, 1971, Mechling and Kilham, 1982, Sommer, 1985, Kilham et al., 1986, van Donk and Kilham, 1990). In summary, *Stephanodiscus minutulus* posesses interaction types which mean that it is relatively more competitive at low temperatures combined with short photoperiods, and is less inhibited by a variable light supply, either due to mixing induced fluctuations or short effective daylengths. Furthermore, its interaction types allow it to become relatively more competitive under fluctuating light, phosphorus limitation

and silicon limitation when temperatures are low. *Nitzschia acicularis* on the other hand possesses interaction types with phosphorus and silicon which make it relatively more competitive at higher temperatures and less intense light fluctuations. *Limnothrix redekei*, also a late spring species, responded to fluctuating light in a similar way to *Nitzschia acicularis*, but, rather than velocity, invests more in competitiveness under phosphorus limitation (Nicklisch, 1999) and grazing resistance (Teubner et al., 1999), which become important at the end of spring. The interaction types therefore are species-specific and appear to be tuned to optimise growth rates in their ecological niche with particular emphasis on the optimum temperature. I therefore confirm hypothesis (5) that the interaction types contribute to niche differentiation and the structure of the phytoplankton community. In the following sections, I discuss the results in more detail.

4.2 Fluctuating light interactions

4.2.1 Effect of fluctuating light

The results obtained in the fluctuating light experiments corroborated the results of previous studies which showed that fluctuating light, which simulated the changing irradiance experienced by algae in the mixed zone of a lake, decreased growth rates in comparison with constant light of the same daily light exposure (Nicklisch, 1998, Nicklisch and Fietz, 2001, van de Poll et al., 2007). The reason for the decreased growth rates observed under fluctuating light is likely to be that the peak intensities of fluctuating light are used less efficiently when photosynthesis is saturated (Nicklisch, 1998). Consequently, no effect of fluctuating light on growth rates of the diatoms was observed at low light (LE ~ 1 mol quanta m^{-2} d^{-1}, I_{max} ~ 170 μmol quanta m^{-2} s^{-1}) when the peak irradiances were never high enough to saturate electron transport rates (see light saturation parameter I_k in Figure 17, p. 52). *L. redekei* did not follow this pattern since growth rates were also significantly lower at low light despite having a higher I_k value than the diatoms. This may indicate a general pattern between diatoms and cyanobacteria since light-limited growth of *Stephanodiscus neoastraea* was only slightly affected, whereas that of *Planktothrix agardhii* (cyanobacterium) was strongly affected by fluctuating light (Nicklisch and Fietz, 2001).

If the photosynthesis-irradiance (P-I) curve does not change, then integrated photosynthesis is inherently lower under fluctuating light than under sinusoidal or constant light of the same average irradiance (Flameling and Kromkamp, 1997) provided that the maximum intensity

exceeds I_k. However, my results showed that *S. minutulus*, *N. acicularis*, and *L. redekei* did change their P-I curves under fluctuating light to compensate this. Enhanced rates of photosynthesis would also lead to higher maintenance costs (van Leeuwe et al., 2005, Dimier et al., 2009), which could also contribute to a decrease in growth rates. Accordingly, the reason that some authors found no change in growth rates under fluctuating light compared to a constant or sinusoidal regime of the same average irradiance and photoperiod (Litchman, 2000, Havelkova-Dousova et al., 2004, Dimier et al., 2009) may have been that the degree of saturation of photosynthesis was similar in the respective regimes.

The decrease in growth rates of diatoms measured under fluctuating light was much stronger than the decrease Mitrovic et al. (2003) observed in situ. Rather than any effect of temperature or photoperiod, this smaller effect of fluctuating light in the study of Mitrovic et al. (2003) was most likely due to the fact that phytoplankton samples were acclimated to naturally fluctuating light before growth was measured under constant light. Cells thus had to acclimate to different light conditions during the experiments.

4.2.2 Temperature

The growth experiments performed at different temperatures showed that the percentage decrease in light-saturated growth rates caused by fluctuating light was not significantly affected by temperature in *N. acicularis* and *L. redekei*. This implies that growth under fluctuating light has the same temperature dependence as under constant light. There was a marginal tendency for the effect of fluctuating light to decrease at lower temperature in *S. minutulus,* which would increase this species' competitiveness under highly fluctuating light in early spring or autumn when temperatures are low and mixing is more intense. I did not measure temperature effects on growth under fluctuating light at light limitation but I assume that temperature has no effect. This seems reasonable since temperature has no effect on either light limited photosynthesis (Davison, 1991) or light limited growth measured under constant light (Foy, 1983).

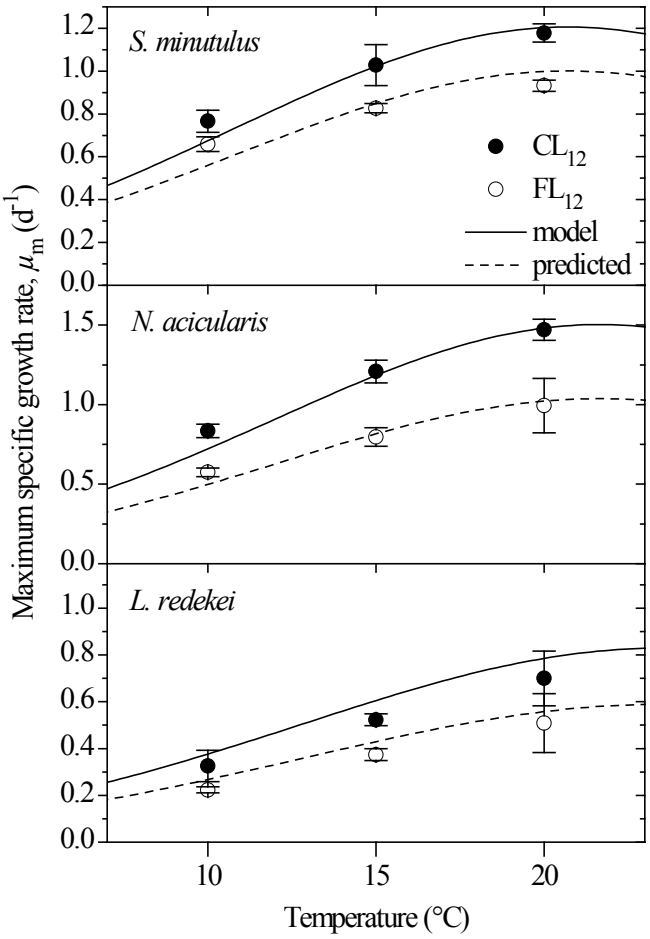

Figure 29: Comparison of temperature dependence of maximum growth rates (d^{-1}) measured in this study with the base model (Eq. 5, p. 28) for constant saturating light with a 12 h d^{-1} photoperiod. The points are values of μ_m from Table 6 (p. 44). Dashed lines show a simple reduction of the model estimates by 18%, 33%, and 29% for *S. minutulus*, *N. acicularis*, and *L. redekei*, respectively (see Results, section 0, p. 45).

The maximum specific growth rates at 10°C, 15°C, and 20°C measured under constant light are in close agreement with values independently predicted by the base model (Nicklisch et al., 2008) for *S. minutulus*, *N. acicularis*, and *L. redekei* (Figure 29). The maximum growth rates under fluctuating light at the same temperatures could also be estimated at a high accuracy by simply decreasing the light saturated growth rate μ_m in the base model according to the average decrease measured for each species in this study, in which the slightly altered temperature dependence of *S. minutulus* under fluctuating light was neglected without a great loss of accuracy.

4.2.3 Photoperiod and z_{eu}:z_{mix}

Decreasing the photoperiod from 12 to 6 h d^{-1} under constant light had the well-known effect of decreasing maximum growth rates, as observed in all species, without affecting light-limited growth, as indicated by constant α_{LE} (Paasche, 1968, Thompson, 1999). Furthermore, the photoperiod and fluctuations as temporal components of the light supply seem to be related in their effects on growth, because both factors produced the same response pattern in the species tested: the decrease in maximum growth rates due to fluctuations or a shorter photoperiod was greatest in *N. acicularis*, closely followed by *L. redekei*, while *S. minutulus* was considerably less affected (Figure 14, p. 48). It also demonstrates the species-specific nature of the photoperiod and fluctuating light (Nicklisch, 1998, Litchman, 2000) and indicates that *S. minutulus* is better adapted to mixed conditions than *N. acicularis* or *L. redekei*, which tend to appear late in spring when the water column is more stable.

Despite the species-specific effects of fluctuating light, there is a tendency for cyanobacteria to be more strongly affected than diatoms or green algae (Nicklisch, 1998, Mitrovic et al., 2003). In this study *S. minutulus* and *L. redekei* followed this pattern, but *N. acicularis* was more strongly affected by fluctuating light than the range of diatoms investigated by Nicklisch (1998). Nevertheless, *N. acicularis* has a high maximum growth rate (cf. Table 6, p. 44) and so can still maintain relatively high growth rates despite stronger decreases in growth due to fluctuating light as demonstrated by growth curves nearly identical to *S. minutulus* under the FL_{12} regime at 15°C (for a description of the light regime abbreviations, see Table 3, p. 21).

The experimental results showed that, compared to constant light of the same (saturating) daily light exposure, fluctuating light decreased growth rates by a fixed percentage at z_{eu}:z_{mix} = 1, regardless of the photoperiod. Moreover, this decrease in growth due to fluctuating light was the same at z_{eu}:z_{mix} < 1 if compared with the growth rate under constant light at the same effective photoperiod (Eq. 4, p. 18, Eq. 33, p. 49). This has the implication that light fluctuation effects (as defined by Eq. 33, p. 49) and photoperiod effects (defined analogously) are simply multiplicative, so that growth rates under fluctuating light are easily predictable if these individual effects are known. Using published data, I calculated the expected growth rates of several species under fluctuating light at z_{eu}:z_{mix} = 0.67 (Nicklisch, 1998) and at z_{eu}:z_{mix} = 0.5 (Nicklisch and Fietz, 2001) as the combined decrease at z_{eu}:z_{mix} = 1 and the decrease due to a shorter photoperiod under constant light. I then compared the calculations with the actual published growth rates (Figure 30). In fact, these predictions were

very accurate (in all but 2 cases within 2%) and the predictions were within the published confidence limits in all cases except one (*Limnothrix redekei*).

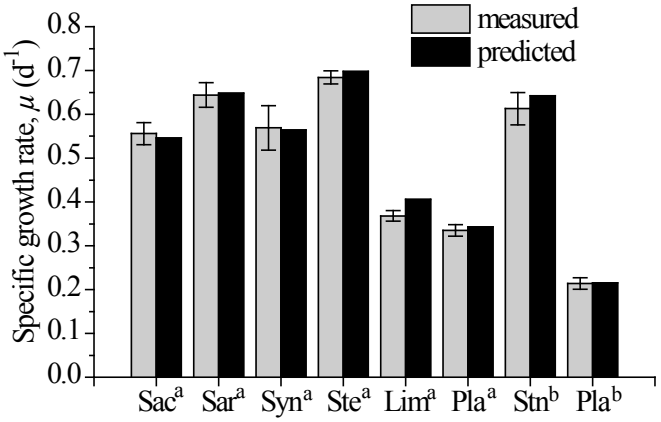

Figure 30: Published growth rates measured at 20°C under fluctuating light (grey bars) from ([a]): Nicklisch (1998) and ([b]): Nicklisch and Fietz (2001) compared to predicted growth rates (black bars). Here the published decreases in growth rates due to fluctuating light at LP_{eff} = 12 h d^{-1} were used to predict the growth rates at LP_{eff} = 8 h d^{-1} (LP = 12 h d^{-1} and z_{eu}:z_{mix} = 0.67) in ([a]) and LP_{eff} = 6 h d^{-1} (LP = 12 h d^{-1} and z_{eu}:z_{mix} = 0.5) in ([b]) by assuming that LF in Eq. 33 (p. 49) is constant. Sac: *Scenedesmus acuminatus*, Sar: *Scenedesmus armatus*, Syn: *Synedra acus*, Ste: *Stephanodiscus minutulus*, Lim: *Limnothrix redekei*, Pla: *Planktothrix agardhii*, Stn: *Stephanodiscus neoastraea.*

Thus the cumulative nature of the photoperiod and within-day light fluctuations applied at 15°C (this study) and 20°C (Figure 30). The late-spring species *N. acicularis*, and *L. redekei*, as well as the summer species *Planktothrix agardhii* showed simple multiplicative interactions between temperature and photoperiod under constant light (Nicklisch et al., 2008). *S. minutulus* showed a slightly different interaction, where the relative influence of the photoperiod decreased at lower temperatures, indicating that this early spring species is adapted to short daylengths in combination with low temperature. In the present study, fluctuating light also had a smaller effect at lower temperatures for *S. minutulus,* but not the other species, suggesting *S. minutulus* is adapted to strong mixing in combination with low temperatures as occurs in early spring or autumn. Since the physiological response to within-day fluctuations and photoperiod was similar in all tested species, and indeed the effects are cumulative as described above, it seems plausible that the temperature - photoperiod interactions described by Nicklisch et al. (2008) also apply under fluctuating light.

Of course, an important question is at what light level does growth effectively stop? The euphotic depth was defined as the depth where irradiance reaches 1% of surface irradiance

(I_o). The higher growth rates of *S. minutulus* under the $FL_{12}D$ regime than under the FL_6 regime could be explained if the compensation irradiance of photosynthesis for this species was lower than 1% of I_o. However this seems unlikely since the assumption about the euphotic depth was a good approximation for all other species in this study and also for several diatoms, green algae and cyanobacteria as shown in Figure 30, where the euphotic depth was also assumed to be at 1% of I_o (Nicklisch, 1998, Nicklisch and Fietz, 2001). *S. minutulus* had a higher chlorophyll content under the $FL_{12}D$ regime than under the FL_6 regime and thus higher light absorption at the same daily light exposure, which could explain the higher growth rates. The discrepancy between the $FL_{12}D$ and FL_6 regime for *S. minutulus* could also be related to the storage capacity for photosynthates, which can play a role under short photoperiods (Gibson and Foy, 1983). In the FL_6 regime there were 18 consecutive hours of darkness whereas light and effective dark periods were interspersed in the $FL_{12}D$ regime. Carbohydrate accumulated during light peaks could have been consumed during the subsequent dark periods in the $FL_{12}D$ regime as was demonstrated for *Microcystis aeruginosa* and *Scenedesmus protuberans* at $z_{eu}:z_{mix} = 0.5$ (Ibelings et al., 1994), so that carbohydrate storage capacity is less important in the $FL_{12}D$ regime. However, more detailed measurements would be required to confirm this.

4.2.4 Photosynthesis and growth

The experimental results agree with previous findings that cyanobacteria tend to increase chlorophyll *a* content in response to fluctuating light, whereas diatoms and green algae do not (Ibelings et al., 1994, Nicklisch and Woitke, 1999, Fietz and Nicklisch, 2002). Furthermore, the results presented here showed that the chlorophyll content of the diatoms acclimated to the mean irradiance within the photoperiod, as was found for other diatoms (Cosper, 1982, van de Poll et al., 2007). However, I also showed that the chlorophyll *a* content of the two diatoms depended on the mean irradiance over the solar daylength and not over the effective photoperiod, because the chlorophyll *a* content under the $FL_{12}D$ regime was the same as under the FL_{12} regime but different to the FL_6 regime. The same applied to the protective pigments of the diatoms (diadinoxanthin : chlorophyll ratio), supporting and supplementing the conclusions of Brunet and Lavaud (2010) concerning the pool size of xanthophyll cycle pigments. The chlorophyll content of *L. redekei* increased with decreasing irradiance, but it was unclear whether this acclimation was specifically controlled by mean or maximum irradiance or the daily light exposure. In the diatoms, the higher ratio of chlorophyll *c* and fucoxanthin to chlorophyll *a* under constant light compared to fluctuating light showed that

the photosynthetic antenna was smaller under fluctuating light, which supports findings that algae decrease antenna size and increase PSU number in response to fluctuating light (Kromkamp and Limbeek, 1993, Flameling and Kromkamp, 1997).

Overall, all three species enhanced their photosynthesis-irradiance (P-I) curves in response to fluctuating light. *L. redekei* did this mainly by increasing light absorption through increased chlorophyll, whereas the diatoms mainly enhanced their chlorophyll-specific maximum photosynthesis rate, which is in accordance with the response of other cyanobacteria and diatoms (Fietz and Nicklisch, 2002). Notably the increase in the light saturation parameter I_k in all species in response to fluctuating light indicates an acclimation of the chlorophyll-specific photosynthesis to better use the high light peaks in the fluctuating light regimes. Since the chlorophyll-specific rates of photosynthesis are not constant (which was observed in all species), the same P-I curves cannot be used under both constant and fluctuating light (Kroon et al., 1992, MacKenzie and Campbell, 2005). On the other hand, photo-acclimation seeks to maximise growth rates (Dimier et al., 2009) so that the effects of fluctuating light on growth rates in the experiments were stable and easily predictable as demonstrated above. In my opinion a growth function that explicitly considers the species-specific effects of the photoperiod with a simple empirical adjustment to account for the effects of fluctuating light is more accurate than a derivation of growth rates from photosynthesis, and thus better suited to predicting interactions between phytoplankton species.

The effects of fluctuating light can easily be modelled by modifying the base model (Eq. 5, p. 28) as follows:

$$\mu_{NR} = \left(\mathrm{LF} \times \mu_{\mathrm{mc}}\right)\left(1 - \exp\left(\frac{-\left(\mathrm{LF}_{\alpha} \times \alpha_{\mathrm{LE}}\right)\left(\mathrm{LE} - \mathrm{LE}_{\min}\right)}{\left(\mathrm{LF} \times \mu_{\mathrm{mc}}\right)}\right)\right) \tag{41}$$

Here the light saturated growth rate under constant light (μ_{mc}) has been decreased by a factor LF for light fluctuations (cf. Eq. 33, p. 49), which takes on the value of 0.82, 0.67 and 0.71 corresponding to the measured decreases of 18%, 33%, and 29% for *S. minutulus*, *N. acicularis*, and *L. redekei*, respectively. Similarly, the initial slope for constant light (α_{LE}) has been decreased by the factor LF_{α}, which takes on the value of 0.54 for *L. redekei* (Table 6, p. 44) and 1 for the two diatoms. Since fluctuation and photoperiod effects were cumulative as described above, LF is independent of z_{eu}:z_{mix}, at least in the range 0.5 – 1 and different fluctuation intensities (z_{eu}:z_{mix}) are implicitly accounted for if the effective photoperiod (LP_{eff},

Eq. 4, p. 18) is used in the estimation of μ_{mc}. Therefore, Eq. 41 can easily be generalised to account for temperature and photoperiod using the base model (Nicklisch et al., 2008), which describes the interactions between these factors under constant light. Here μ_{mc} in Eq. 41 above can simply be calculated using the base model (Eq. 6, p. 29), which applies for constant light. These relations should apply over the range of z_{eu}:z_{mix} encountered in most temperate eutrophic lakes, although the effects far outside the tested range of 0.5 – 1 are unclear. In general, when z_{eu}:z_{mix} tends to ∞ then LF tends to 1 (constant light) and when z_{eu}:z_{mix} tends to 0 then LP_{eff} and therefore μ_{mc} and growth also tend to 0.

4.2.5 Light limitation and ecological considerations

As described above, strongly light-limited growth is independent of temperature and the photoperiod and I found that it was also independent of light fluctuations at z_{eu}:z_{mix} = 1 for the two diatoms. On the other hand, light saturated growth is dependent on these factors. Therefore, the low temperatures, short daylengths and fluctuating light encountered during spring would decrease maximum growth rates without affecting growth efficiency at low light, so that growth is light-saturated even at low light levels. In this case light energy during spring, expressed as daily light exposure, is likely to limit growth only on some overcast days, as demonstrated for a shallow eutrophic lake (Figure 31) (Nicklisch et al., 2008).

Nicklisch et al. (2008) estimated that fluctuating light should decrease maximum growth rates of *S. minutulus, N. acicularis* and *L. redekei* by roughly 20%, 25% and 40% respectively, and that fluctuating light should contribute to growth control during spring. These predictions were somewhat speculative, but can now be verified by the results of this thesis (Figure 31).

The fact that limitation by light exposure only occurs on certain overcast days has consequences for the notion of light limitation: a shorter photoperiod, for example when the vegetation period begins earlier after mild winters, would decrease algal growth rates, whereas a longer effective photoperiod, for example due to increased water clarity and euphotic depth (Shatwell et al., 2008), would increase growth rates, provided nutrient limitation has not commenced. Thus the temporal components of the light supply such as photoperiod and light fluctuations may be more important than the daily amount of light energy.

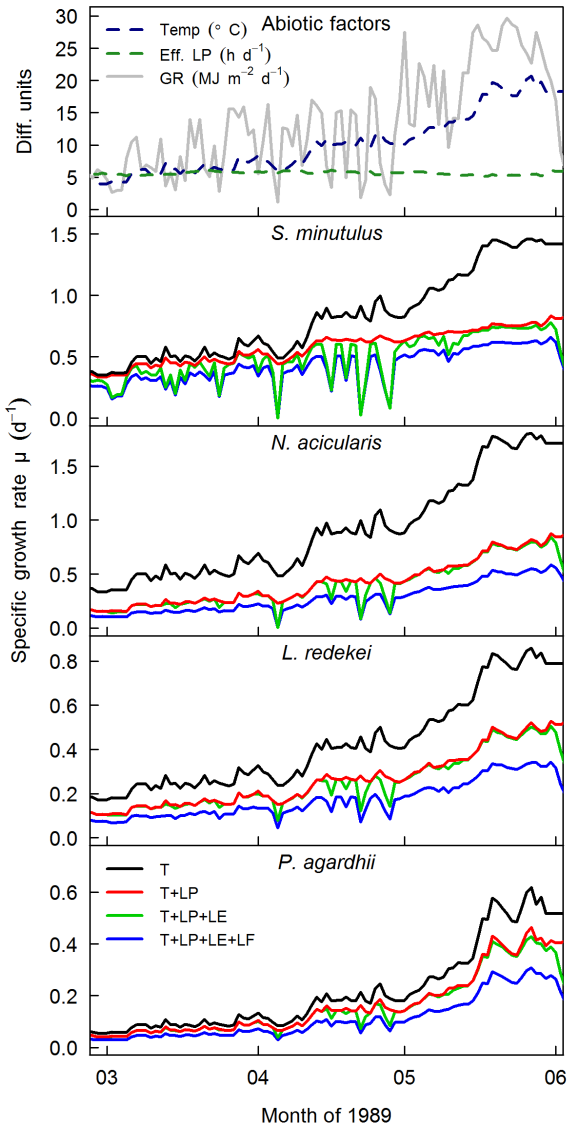

Figure 31: Abiotic growth factors during spring in Lake Müggelsee (top panel) and the corresponding growth rates predicted by the model for *S. minutulus, N. acicularis, L. redekei* and *Planktothrix agardhii*. The data is reproduced from Figs. 7 and 8 in Nicklisch et al. (2008) where the effect of light fluctuations was estimated for these species. T: temperature, (eff.) LP: (effective) photoperiod, LE: light exposure, LF: light fluctuations, GR: global radiation. The different lines show growth rates limited by T only, T + LP, T + LP + LE, and T + LP + LE + LF. The downward spikes in the green lines show light limitation only on certain overcast days. Results for P. agardhii are based on measurements of Nicklisch and Fietz (2001).

Furthermore, photosynthesis becomes saturated at much higher irradiances than growth (Gibson and Foy, 1983). In this study, photosynthetic electron transport rates saturated at irradiances up to 11 times higher than growth. Therefore light limitation cannot be deduced directly from P-I curves.

Altogether the temporal components of the light supply such as photoperiod and light fluctuations should significantly limit algal growth rates in temperate eutrophic lakes during spring and autumn as well as in summer, when the euphotic depth is low and the water column is instable. Since these effects are species-specific, they should influence the community structure of phytoplankton if the relationships between water clarity, daylength, temperature and mixing intensity shift as a result of climate or trophic change. To predict these effects models should account for the temporal effects of the light supply, and care should be taken not to draw false conclusions when inferring light limitation from photosynthesis-irradiance relationships.

4.3 Phosphorus interactions

4.3.1 The Droop relation and model comparison

In the experiments on interactions with phosphorus, the P-replete growth rates (μ_{NR}) increased non-linearly as expected with increasing temperature and photoperiod. These growth rates agreed very well with the predictions of the base model (Nicklisch et al., 2008), which shows that the decrease in μ'_m at 12 h d^{-1} compared to 9 h d^{-1} in *S. minutulus* at 15°C (Figure 19, p. 55) was related to the slightly lower light exposure and not the photoperiod, because the model took this lower light exposure into account.

Of the four different quota curves fitted to the data, the Droop equation provided the poorest fit in all cases. One reason for this is that the fixed form of the Droop equation could not adequately describe the growth rates of *N. acicularis* because the half-saturation coefficient, k_Q was greater than the minimum quota, Q_0 whereas the Droop equation implies that $k_Q = Q_0$ and that there is a linear relationship between growth rate, μ and the reciprocal of the quota, 1/Q. Other authors have implied that the Droop relation does not apply to all species, usually referring to non-linear relationships between μ and 1/Q (Brown and Button, 1979, Goldman, 1979, Healey, 1985, Ahlgren, 1987, Sterner, 1995), which typically occur when the growth-quota curve has a flatter form such that k_Q is higher than Q_0. In the experiments presented here, the Droop relation applied quite well to *S. minutulus*, but not to *N. acicularis* (Figure 32). This explains why the 3-parameter models (Eqs. 12, 14, p. 31) fitted better than the 2-parameter models (Eqs. 11, 13, p. 31) for *N. acicularis*.

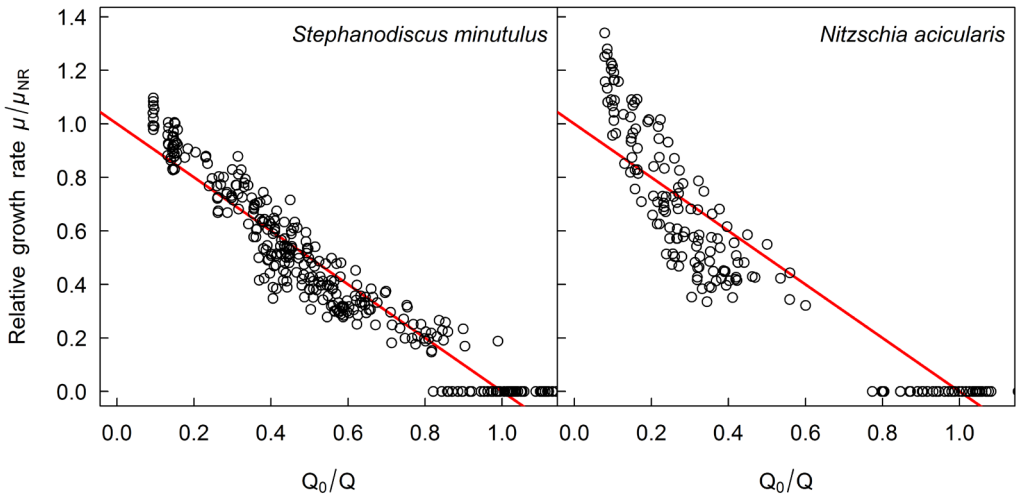

Figure 32: Relative growth rate vs. relative quota reciprocal for *Stephanodiscus minutulus* and *Nitzschia acicularis*. The data points are the experimental data from Figure 18 (p. 54), and the red lines show the Droop relation: a linear relationship between growth rate and quota reciprocal, which is equivalent to the case when $k_Q = Q_0$. Non-linear ("concave") forms indicate that $k_Q > Q_0$ as is the case with *N. acicularis*.

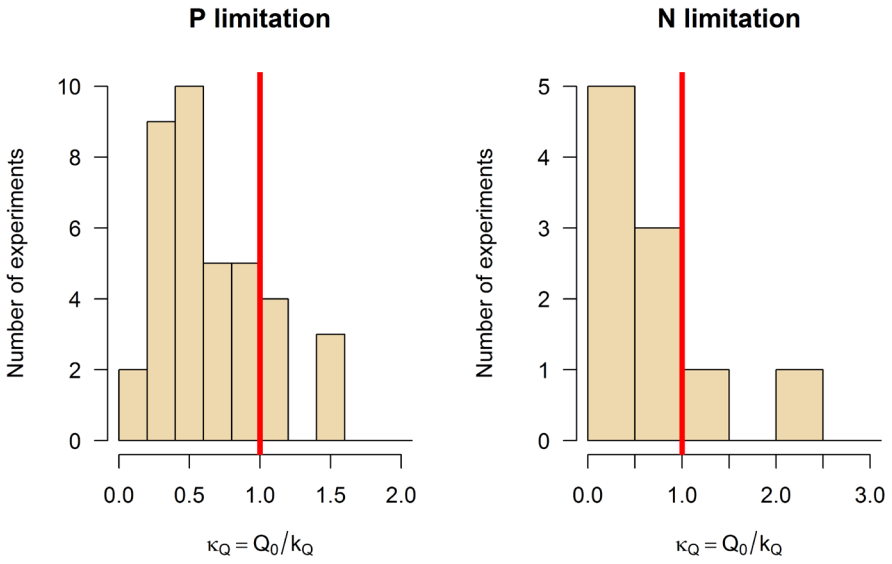

Figure 33: Histograms of the normalised half saturation coefficient κ_Q for model fits to growth data from the literature under P and N limitation. The red lines show the Droop relation, when $\kappa_Q = 1$ and $k_Q = Q_0$. Data from 50 experiments (curves) of 21 different species, $n = 1031$. Measurements from this thesis were included.

To test whether this non-linearity in *N. acicularis* is a more general phenomenon or just an exception, I collected growth rate data from 50 experiments under P and N-limitation by digitising plots from the literature and fitting the growth models (Eqs. 11 – 14, p. 31) to the data (see Appendix 1, p. 120).

Out of 39 curves under P-limitation, the normalised half saturation constant $\kappa_Q = Q_0/k_Q$, was smaller than 1 in 31 cases and was larger than 1 in 8 cases. The median value was 0.57. Of the 11 curves fitted under N limitation, κ_Q was less than 1 in 8 cases and greater than 1 in 3 cases, with a median value of 0.58. This indicates that the half saturation coefficient k_Q is closer to $2Q_0$ than Q_0, which is a clear non-linearity in the μ vs. 1/Q relationship. Species like *Nitzschia acicularis*, which did not conform to the Droop relation, may therefore be more the rule rather than the exception.

The importance of Droop's quota concept (Droop, 1968, Droop, 1973) is unquestionable and it forms the basis not only for calculating phytoplankton growth rates, but also for understanding phytoplankton stoichiometry in general (Sterner and Elser, 2002, Klausmeier et al., 2008). However a different mathematical formulation than Droop's equation might be better. The best equation of the ones that I tested was the 3-parameter exponential curve (Eq. 14, p. 31) followed by the Fuhs (1969) equation (Eq. 13). Flynn (2002) suggested using a normalised quota curve based on Caperon and Meyer's (1972) model with a normalised half saturation coefficient, which he termed KQ. Flynn used a different formulation to normalise the half-saturation coefficient than I did, by making it relative to Q within the range Q_m-Q_0. Using a normalised half-saturation coefficient allows a flexible shape of the quota curve (Flynn, 2008a), which is particularly useful for describing N-limited growth because the curve form is much flatter (less hyperbolic) than it is for P (Flynn, 2008c).

4.3.2 Temperature

The experimental results showed that the P-quota increased with decreasing temperature as evident from a temperature-dependent initial slope, α_Q and maximum quota, Q_m, which is in accordance with other studies (Rhee and Gotham, 1981b, Wernicke and Nicklisch, 1986). The half saturation coefficient k_Q clearly increased with decreasing temperature in *N. acicularis*, which indicates that the shape of the quota curve changes with temperature, and consequently, that P-limited growth has a different temperature dependence than P-replete growth, as observed previously (Goldman, 1979). The increase in k_Q with decreasing temperature was only small (but nevertheless significant) for *S. minutulus*. An increase in k_Q corresponds to a decrease in growth rate at a certain P-quota, which suggests that the much smaller temperature effect on k_Q may reflect an adaptive strategy of *S. minutulus* because it is a cold-adapted, early spring species, whereas *N. acicularis* is adapted to warmer temperatures and longer photoperiods and typically grows in late spring (Nicklisch et al., 2008, Shatwell et al., 2012).

The absence of a temperature dependency of the minimum quota Q_0 in this study is not consistent with other findings that Q_0 increases with decreasing temperature (Goldman, 1979, Rhee and Gotham, 1981b, Ahlgren, 1987), although there are some examples where Q_0 did not increase with decreasing temperature (Fuhs, 1969, Wernicke and Nicklisch, 1986, van Donk and Kilham, 1990). A decrease in cell size with increasing temperature (Rhee and Gotham, 1981b), which was also observed in this study (Table 8), might partially explain this discrepancy if nutrient quotas are given on a cell basis, but there does not seem to be a consistent pattern in the literature to provide a clear answer to this. Another explanation could be that the discrepancy is due to methodological differences or curve fitting, since the choice of model substantially affects the parameter values. Furthermore, if the Droop equation is fitted, then a change in Q_0 with temperature will also reflect a change in k_Q due to the fixed form of the quota curve ($k_Q = Q_0$). Even the model fits that used k_Q indicated an apparent temperature dependence of Q_0, which in reality did not exist according to actual measured values at stationarity ($\mu = 0$), suggesting that the temperature dependence of Q_0 found by model fitting was just an artefact.

It is therefore interesting to note that studies that found a temperature dependence of Q_0 estimated this as the axis intercept extrapolated from a fitted curve (Goldman, 1979, Rhee and Gotham, 1981b, Ahlgren, 1987). On the other hand, the studies that found no temperature dependence measured Q_0 directly from the maximum yield of cultures grown to stationary phase (Wernicke and Nicklisch, 1986, van Donk and Kilham, 1990; this study). One exception was the study of Fuhs (1969), who estimated Q_0 by extrapolation, but nevertheless did not find a temperature dependence. Ahlgren (1988) also questioned the significance of the temperature dependence of Q_0 for phosphorus in some studies. I checked the possibility that the temperature dependence of Q_0 could be an artefact of model fitting by removing the data points measured at stationarity ($\mu = 0$) and refitting the Droop equation to the data. This resulted in a highly significant temperature dependence of Q_0 for *N. acicularis* but no temperature dependence for *S. minutulus*, analogous to the respective results for k_Q for these species. Therefore, what appears to be a temperature dependence of Q_0 is probably really a temperature dependence of k_Q, which authors do not detect when using the Droop equation. A temperature dependence of k_Q is consistent with the need for additional P-rich ribosomes (Sterner and Elser, 2002) to compensate for a decrease in temperature and still maintain the same protein synthesis and growth rate (Tempest and Hunter, 1965, Rhee and Gotham, 1981b, Nicklisch and Steinberg, 2009). However, it seems plausible that this does not apply when the growth rate is zero at Q_0. It appears that further research is necessary to clarify whether Q_0 is

temperature dependent since Q_0 determines optimum nutrient ratios and is relevant for overall phytoplankton stoichiometry (Klausmeier et al., 2004).

The majority of published results and the results obtained here for *N. acicularis* indicate that the form of the quota curve changes with temperature, making a fixed-form curve such as the Droop model inappropriate in most cases to account for temperature interactions with phosphorus (Goldman, 1979). The fact that temperature interactions with phosphorus-limited growth of *S. minutulus* could be relatively well described by a multiplicative model with a fixed curve is presumably due to specific adaptation of this cold-water species and serves to highlight the species-specific nature of the effect of temperature on P-limited growth.

4.3.3 Photoperiod

The lack of a significant effect of the photoperiod on Q_0 or k_Q indicates that the photoperiod does not alter the shape of the quota curve for *S. minutulus* or *N. acicularis*. Further, it suggests that the effects of photoperiod and P-limitation are multiplicative and that a decrease in the photoperiod would require an increase in P-quota to maintain the same growth rate, as was evident from the interaction diagrams (Figure 20, p. 60). This is consistent with the results of Litchman et al. (2003), who found that the response of several phytoplankton species to daylength depended on the P-status and vice versa. A similar result was also found for *Limnothrix* (formerly *Oscillatoria*) *redekei* since k_Q and Q_0 were the same under both continuous light and a photoperiod of 12 h d^{-1} (Wernicke and Nicklisch, 1986). On the other hand, Riegman and Mur (1985) found only a narrow range of interaction between internal phosphorus and the photoperiod for *Planktothrix* (formerly *Oscillatoria*) *agardhii*. These authors suggested that Liebig's Minimum Law applies to *O. agardhii* since it is a shade adapted species, and they hypothesised that high light adapted species might have a broader interaction range. The model of factor interactions developed here, which contains a multiplicative interaction between P-quota and photoperiod, was used to examine the interactions of *S. minutulus* and *N. acicularis* (which are slightly less shade-adapted than *O. agardhii*) under the same conditions as used by Riegman and Mur (Figure 34).

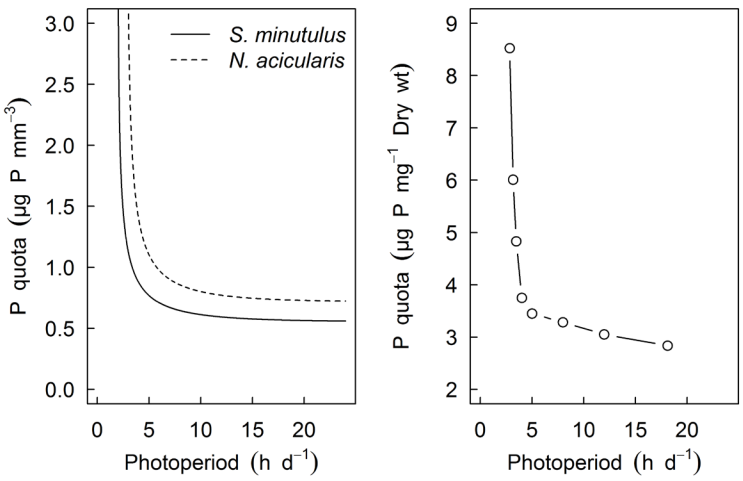

Figure 34: Comparison of interaction diagrams drawn for *S. minutulus* and *N. acicularis* based on the coupled model of factor interactions (left panel) and measured data for *Planktothrix* (formerly *Oscillatoria*) *agardhii* digitised from Fig. 1 in Riegman and Mur (1985) (right panel). Conditions 20°C, irradiance = 30 W m^{-2}, μ = 0.01 h^{-1}.

The interaction range was somewhat broader, supporting Riegman and Mur's hypothesis, but also demonstrating that a multiplicative interaction can produce visually similar results at the low growth rates these authors used (0.01 h^{-1}).

A decrease in irradiance generally requires an increase in P-quota to maintain the same growth rate, suggesting an interaction between light and P-limitation (Healey, 1985, Ahlgren, 1988). Furthermore, Healey's (1985) results demonstrated that Q_0 and Q_m for phosphorus were independent of irradiance, indicating that the interaction between irradiance and phosphorus is multiplicative. This might help to explain the similar interaction with the photoperiod in this study, where k_Q was independent of the photoperiod and, according to Healey's results, also the irradiance. Further evidence is provided by the fact that Q_m in *S. minutulus* and *N. acicularis* is unaffected by either irradiance or photoperiod (Giersdorf, 1988). These results also show that the slightly lower irradiance in some of the experiments did not affect the conclusions because Q_0, Q_m and k_Q for P-limitation appear to be independent of irradiance over a wide range. Although the photoperiod may not have a strong influence on P-limited growth, the role of photosynthesis in dark assimilation of nitrate would suggest that the photoperiod does have an influence on N-limited growth (Flynn, 2001, Flynn et al., 2002, Clark et al., 2002, Flynn and Fasham, 2003).

4.3.4 Competition and P-uptake

To estimate relative P uptake rates, a new approach was employed, which uses the relationship between growth and P-quota and the outcome of competition experiments. Using this approach, it was possible to quantify the contribution of P-uptake and P-usage efficiency

to competitive ability, but the calculations could not produce absolute values of uptake rates. The assumption of a simple linear relationship between uptake rate and external concentration can provide reliable results (Olsen, 1989, Andersen, 1997) and applies if the external P concentration is lower than the half-saturation coefficient of uptake (k_m). The P-concentration in the fresh medium (1.2 μM P) was lower than measured k_m values for most species provided by Gotham and Rhee (1981b) (mean 1.5 μM P, n = 6) and the external concentrations in experimental cultures can therefore generally be expected to be much lower than k_m. The linear relationship used also ignores the feedback of the quota, which causes the maximum uptake rate V_m to decrease as the quota increases. However, the P-quota was always lower than Q_m in model simulations for both species, except very occasionally after cultures were strongly diluted. Furthermore, this feedback depends on nutritional history rather than the instantaneous P-status (Perry, 1976, Olsen, 1989) allowing phytoplankton to exceed their maximal quotas in the short term (Riegman et al., 2000). Therefore, ignoring the feedback from the quota did not appear to affect the results to any great degree.

The outcome of the experiments showed that *N. acicularis* was a strong competitor under P-limitation, which is consistent with other studies (Grover, 1989, Nicklisch, 1999). Interestingly *S. minutulus*, which was the weaker competitor under all experimental conditions, could use internal P more efficiently than *N. acicularis* under most conditions, due to its lower Q_0 and k_Q. The competitive advantage of *N. acicularis* was due to a higher uptake affinity and storage capacity (Q_m). Other studies found similar results, where the stronger of two species competing under nutrient limitation had higher uptake rates and a higher storage capacity whereas the weaker competitor produced a higher yield from a given amount of nutrient (Olsen, 1989, Ducobu et al., 1998). A high maximum quota in combination with a high uptake rate enables a species to maintain a relatively high quota so that efficient use of internal P for growth is less important. This may suggest a trade-off between resource gathering and resource usage in biomass assembly (Klausmeier et al., 2008) and stresses the importance of linking uptake and the quota curve (Flynn, 2008b). It thus seems that the parameters of the quota curve alone provide little information on the competitive ability of a species without knowledge of the uptake kinetics.

The influence of temperature on relative P-uptake rates was clear in the competition experiments. It was not possible to estimate the absolute temperature dependencies of uptake for each species, but it was possible to deduce how P was distributed between the species and how temperature and photoperiod influenced this distribution. *S. minutulus* increased its share

of absorbed P from around 10% at 20°C to 25-30% at 10°C, indicating that the uptake kinetics of *S. minutulus* are more cold-adapted than those of *N. acicularis*, which parallels the interaction between temperature and the growth-quota curve described above.

The photoperiod appeared to have no influence on the relative uptake rates of the two test species. It cannot be ruled out that the photoperiod did affect the absolute uptake rates of each species but that these effects cancelled each other out; however, this appears unlikely since there was no evidence that the photoperiod influenced other P-limited growth parameters such as k_Q or Q_0. Sommer (1994) found that the total daily light exposure rather than photoperiod or irradiance alone influenced the outcome of competition between marine phytoplankton under Si or N limitation. In the competition experiments shown here, the daily light exposure was held approximately constant, but the photoperiod still influenced the outcome. However, this was obviously due to the effect of the photoperiod on maximum growth rates because relative P-uptake rates were unaffected.

Altogether the phosphorus limitation experiments showed that temperature interactions with P-limited growth are complex and reflect species-specific niche adaptation. The influence of the photoperiod seems to be restricted to nutrient replete rather than P-limited growth rates, although the same need not apply to N-limitation. The nature of the temperature interactions with P-quota suggests that warming should counteract reoligotrophication and benefit warm-adapted species more than cold-adapted species under P-limitation.

4.4 Silicon interactions

Stephanodiscus is recognised as being probably the most competitive genus under silicon limitation among the freshwater diatoms (Kilham, 1971, Mechling and Kilham, 1982, Sommer, 1985, Kilham et al., 1986, van Donk and Kilham, 1990). Accordingly, the k_S values for *Stephanodiscus minutulus* measured in chemostat cultures were very low, and similar to those measured by Mechling and Kilham (1982) for *Stephanodiscus minutus* (0.31-1.03 μmol L^{-1} in batch culture) and slightly higher than those found by van Donk and Kilham (1990) for *Stephanodiscus hantzschii* (0.19-0.47 μmol L^{-1}). The k_S value measured for *S. minutulus* at a photoperiod of 9 h d^{-1} (1.47 μmol L^{-1}) thus seems unusually high and should be treated with caution. *Nitzschia acicularis* on the other hand is adapted to higher Si:P ratios (Sommer, 1985, Kilham et al., 1986), supporting my result of higher k_S values for this

species, which are at the lower end of typical k_S values measured for other pennate diatoms (Tilman et al., 1982 and references therein, Kilham, 1984, van Donk and Kilham, 1990).

4.4.1 Temperature and photoperiod effects

The experimental results indicated that there was a tendency for k_S to increase with temperature for *S. minutulus* roughly in parallel with μ_{NR}, so that a constant initial slope $\alpha_S = \mu_{NR}/k_S$ described the temperature interactions significantly better than a constant k_S when the model was fitted to the whole data set (Shatwell et al., 2013). The k_S values measured by Tilman et al. (1981) for *Asterionella formosa* seemed to increase with temperature, but these authors concluded that a temperature dependence was unlikely at temperatures below optimal. Overall increases in k_S with temperature were also observed by Mechling and Kilham (1982) and van Donk and Kilham (1990). A constant initial slope was also observed in a cold-adapted (psychrophyllic) marine diatom (Stapleford and Smith, 1996). Kilham (1984) found that temperature did not affect k_S for *Stephanodiscus minutus* or *Synedra acus*, which, on the other hand, agrees with my observation that temperature (and also photoperiod) did not influence k_S for *N. acicularis*, granted that I only measured two different temperatures and photoperiods for this species.

There is not much literature available on the influence of the photoperiod on silicon limited growth. In a study on marine species, daylength influenced the outcome of competition between diatoms along a Si:N gradient (Sommer, 1994), which seems to indicate some sort of interactive effect of the photoperiod. Silicon metabolism is independent of photosynthesis and tightly coupled to the cell cycle in many species (Brzezinski, 1992, Martin-Jézéquel et al., 2000). Thus the photoperiod may have an effect on silicon limited growth under phased growth (Chisholm et al., 1978), however it has been suggested that this effect is pronounced on daily time-scales but tends to be less important over longer periods (Brzezinski, 1985). The results of a cell-cycle-based model of Si metabolism suggested that growth rates at low Si concentrations should be similar under both continuous irradiance and a light:dark cycle (when growth is less than 1 division per day) (Flynn and Martin-Jézéquel, 2000), which might imply that the initial slope of the Monod curve should be independent of the photoperiod as I suggested for *S. minutulus*. The laboratory results in this study for the effect of the photoperiod on silicon limited growth were not as reliable as for temperature. However, without placing too much emphasis on the result, it seems that the species-specific effect of the photoperiod on silicon limited growth kinetics is similar to the effect of temperature.

4.4.2 Competition and Monod vs. cell-cycle model

The competition experiments showed that *Stephanodiscus minutulus* was more competitive under silicon limitation than *Nitzschia acicularis*, as expected from the Monod kinetics measured in the chemostat and batch culture experiments. However, when coupled to the base model of nutrient replete growth, the Monod model could only poorly represent the dynamics of the competition experiments (rate of competitive exclusion) in model simulations. The reason was that the two species were hardly competing with each other in the simulations, but for the most part were growing maximally between dilutions. In the simulations, limitation, and therefore competition, only began when the silicon concentrations in the culture approached the half-saturation constant of the species ($k_S < 2\ \mu mol\ Si\ L^{-1}$). Silicate then quickly became completely depleted, stopping growth abruptly, so that the duration of limitation between dilutions was short. Decreasing the concentration of silicon in the fresh medium from 60 to 15 μmol Si L^{-1} in Monod simulations greatly improved the fit because the ambient Si concentrations in the medium were much closer to the half-saturation coefficients (k_S) of the species. On the other hand simulating growth with a cell-cycle model at the true input concentration of 60 μmol Si L^{-1} also greatly improved the fit because the half-saturation coefficient of uptake k_m in the cell-cycle model was much higher than k_S in the Monod simulations. In both cases the effect is the same: decreasing the ambient concentration relative to k_S or increasing k_m relative to the ambient concentration both act to increase the degree of competition between the two species. It is unlikely that the base model of nutrient replete growth is inaccurate because it described the growth rates of these species in the fluctuating light and phosphorus limitation experiments, and also published growth rates, very accurately (Nicklisch et al., 2008, Shatwell et al., 2012).

Because diatoms cannot store substantial amounts of silicon, they accumulate most of what they require directly before cell division during certain parts of the cell cycle (Azam, 1974, Brzezinski, 1992, Martin-Jézéquel et al., 2000, Hildebrand et al., 2007, Thamatrakoln and Hildebrand, 2007, Thamatrakoln and Hildebrand, 2008, Leynaert et al., 2009), predominantly the G2+M cell phase (Brzezinski et al., 1990, Claquin et al., 2002). Accordingly silicate uptake rates can be much higher than predicted by the Monod model and the half-saturation coefficients for uptake (k_m) may be much higher than k_S for growth (Flynn and Martin-Jézéquel, 2000, Martin-Jézéquel et al., 2000, Leynaert et al., 2009). Consequently, the Monod model has only a limited validity for non-steady dynamics and prediction of competition under varying silicate supply.

The cell cycle model I used to simulate the competition experiments does not attempt to explicitly model the cell cycle as other models have done in the past (Brzezinski, 1992, Flynn and Martin-Jézéquel, 2000), but simply reflect a distinct period of Si uptake that occupies a discrete portion of the cell cycle. I did not measure silicon uptake rates or the length of phases in the cell cycle. Instead, I derived the kinetics directly from the measured Monod model, incorporating non-continuous uptake in such a way that the cell-cycle model and the Monod model are equivalent at steady state with the same mean growth rates at all silicate concentrations. Therefore the cell-cycle model describes the measured growth kinetics of *S. minutulus* and *N. acicularis*. The model is based on a number of assumptions, which have been experimentally validated: that silicate uptake occurs predominantly at the end of the cell cycle in the G2 phase, that biomass growth is uncoupled from silicate uptake, and that the length of the G2 phase increases under silicon limitation, thus slowing the division rate (Brzezinski et al., 1990, Brzezinski, 1992, Flynn and Martin-Jézéquel, 2000, Martin-Jézéquel et al., 2000, Claquin et al., 2002).

In simulations, I assumed a value of $\tau_0 = 0.2$, or in other words, that the uptake (G2) phase occupied 20% of the total cell cycle under nutrient replete conditions for both *Stephanodiscus minutulus* and *Nitzschia acicularis*. Brzezinski (1990) measured the duration of cell phases in seven species of marine diatoms and found that, under exponential growth, the G2 phase occupied on average 19% of the cell cycle duration. He also observed that silicon-dependent cell-cycle phases increased in duration dramatically under silicon limitation. In my simulations with $\tau_0 = 0.2$, k_m is about 6-7 times higher than k_S according to Eq. 29 (p. 41) and the maximum cell-specific uptake rate V_m is about 9 times higher than the nutrient replete growth rate (μ_{NR}), according to Eqs. 27 and 31 (p. 39-41). This is remarkably close to observations where instantaneous Si-uptake rates were up to 8-fold higher than required for immediate growth needs (Brzezinski, 1992). Brzezinski (1992) derived a more mechanistic model of cell-cycle dependent uptake, and stated that the instantaneous uptake rate in the G2 phase and the half saturation coefficient of this uptake are higher than their corresponding continuous uptake model parameters by $1/\tau_0$ (after translating Brzezinski's model terminology into my model terminology), which is equal to 5. The simple cell-cycle model derived from steady-state Monod kinetics therefore seems to be in good agreement with other studies.

Because the cell-cycle model and the Monod model are equivalent at steady state, the difference in performance of the two models in reproducing the dynamics of the competition experiments must be due to the non-steady dynamics. Altogether these results show that the

non-steady uptake of silicon in diatoms has the potential to influence nutrient competition and that the Monod model is unable to adequately describe non-steady dynamics. Furthermore, Monod parameters of Si-limited growth may considerably underestimate the degree of Si-limitation in lakes. For example, several laboratory experiments showed that k_S (Monod) for *Asterionella formosa* is around 1.5-4 μmol Si L^{-1} (Kilham, 1975, Tilman and Kilham, 1976, Holm and Armstrong, 1981, Tilman, 1981, Tilman et al., 1981). Field data on the other hand show that *Asterionella formosa* becomes Si-limited at much higher concentrations because in Windermere, the biomass peak of this species almost always coincides with a silica concentration of around 18 μmol Si L^{-1} (Reynolds, 2006, Thackeray et al., 2008), which is interestingly around 5-12 times higher than the measured k_S (Monod) values.

4.5 Other factor interactions

So far I have addressed the interactions between physical factors and nutrients. But what about the light exposure and its interactions with these nutrients? What about the interactions between the nutrients themselves? In this section, I will briefly characterise the remaining interactions required to assemble the overall model of factor interactions using the published literature.

4.5.1 Interactions between nutrients

Tilman (1980) stated that plant macro-nutrients can be considered as non-interactive essential resources. This means that the interaction between nutrients is a threshold type described by Liebig's Minimum Law, where only one nutrient can limit growth at one time, and limitation switches to another nutrient at the optimum nutrient ratio. This is supported by experimental evidence, for example for N and P (Rhee, 1978) and for vitamin B12 and P (Droop, 1974). More recent evidence based on a review of published factorial nutrient addition experiments or modelling considerations suggests that this may not always be the case for N and P, putting into question the applicability of Liebig's Minimum Law for these nutrients (Elser et al., 2007, North et al., 2007, Pahlow and Oschlies, 2009, Harpole et al., 2011). Co-limitation by C and P has also been demonstrated (Spijkerman, 2010). In this case C and P independently limited growth, which indicates that the type of interaction was multiplicative (Spijkerman et al., 2011). Nevertheless it seems likely that Liebig's Law does apply to interactions between silicon and other nutrients because silicon metabolism is uncoupled from C, N, and P metabolism (Claquin et al., 2002).

4.5.2 Interactions between light and nutrients

On the other hand, there appears to be an interaction between light and nutrients because P and N quotas increase with decreasing irradiance at constant, moderately limited growth rates (Zevenboom et al., 1980, Rhee and Gotham, 1981a, Healey, 1985, Ahlgren, 1988). The type of interaction between nutrients and light depends on the nutrient (Flynn, 2003). Riegman and Mur (1985) suggested a threshold type of interaction between light and P, but these authors used very low growth rates, and the interaction type could be interpreted differently as described in section 4.3.3 for the photoperiod. Thus a threshold type of interaction (minimum function) seems unlikely. Giersdorf (1988) found no effect of irradiance or photoperiod on the maximum P quota for *S. minutulus* and *N. acicularis* and Healey (1985) found that irradiance had no effect on the minimum or maximum P quota for *Synechococcus linearis*. Since the Droop relation, which is fixed by the ratio of minimum to maximum quota, applied in Healey's experiments, the interaction between light and P is multiplicative. This type of interaction implies that both light and phosphorus can simultaneously co-limit growth and that the degree of limitation of one resource (in terms of relative growth rate) is unaffected by the degree of limitation of the other resource.

Similarly to phosphorus, the N-quota generally decreases with increasing light at the same growth rate, but the interaction appears not to be simply multiplicative for N (Ahlgren, 1988). Experimental studies found that the minimum N-quota decreases with increasing irradiance (Rhee and Gotham, 1981a, Healey, 1985). Flynn (2003) and Geider et al. (1998) argue for a model formulation where N-limitation only affects the light-saturated growth rate and has no effect on strongly light limited growth. On the other hand, Chalup and Laws (1990) showed that the relative growth rate under N-limitation is the same at different irradiances, which would suggest that the interaction between light and N is multiplicative. The majority of evidence indicates that the interaction between light and N is more complex than for P, probably due to the link between N assimilation and the cell's energy budget (Ahlgren, 1988).

The interaction of light with silicon in terms of diatom growth seems to be less well characterised. Silicon metabolism is closely related to the cell cycle including the growth rate, but is weakly related to other aspects of cellular metabolism, and the degree of silicification is inversely related to the growth rate (Martin-Jézéquel et al., 2000). This also applied to light-limited growth (Taylor, 1985), which might reflect a threshold type of interaction, but silica was unlikely to be limiting at the concentrations used in Taylor's experiments, and so the

results may not be applicable here. The energy required for silicification seems to be derived from respiration rather than photosynthesis because silica uptake also occurs in the dark (Azam and Chisholm, 1976). Flynn proposed a model in which silicon metabolism was independent of light (Flynn and Martin-Jézéquel, 2000), and thus used a threshold type of interaction between light and silicon (Flynn, 2001). However, if the silicon uptake is influenced by light and temperature (Martin-Jézéquel et al., 2000), and if silicon limited growth depends on the uptake rate as suggested by the cell-cycle model presented here, then the interaction between light and silicon may be more multiplicative.

For modelling purposes, it seems reasonable to assume a threshold (Liebig) interaction type between Si and P, as is usually applied in phytoplankton models (Andersen, 1997, Flynn, 2003), and a multiplicative interaction between light and P. In the absence of more accurate information, a multiplicative relationship between light and silicon was also assumed for reasons of simplicity and convenience. These interactions are shown in Eq. 42.

$$\mu = \mu_{NR} \times \min\begin{cases} f(Q) \\ f(S) \end{cases} \tag{42}$$

Here μ is the specific growth rate, μ_{NR} is the light limited (nutrient replete) growth rate and f(Q) and f(S) are functions to describe limitation by P quota and Si concentration respectively.

4.6 Ecological implications of factor interactions

4.6.1 Niche differentiation

Van Donk and Kilham (1990) postulated that the Monod half-saturation constant k_S shows little variation with temperature for the nutrient for which a particular species is a good competitor, but the results presented here tend to contradict this. Lower values of the half-saturation constant usually indicate a higher affinity and higher competitive ability. In *N. acicularis*, a poorer competitor for silicon but a good competitor for phosphorus, k_S for Si-limited growth did not change with temperature but the half saturation coefficient of P-limited growth (k_Q) decreased significantly according to the experiments on phosphorus interactions performed here. In contrast, for *S. minutulus*, a good competitor for Si but a poor competitor for P, I observed that k_S for Si-limited growth increased with temperature, but the half saturation coefficient for P-limited growth was relatively constant. I propose that the type of

interaction between nutrients and physical factors reflects more the environmental niche of a species such that its competitive ability under nutrient limitation is relatively increased at the ambient conditions for growth. Thus, according to the measured kinetics, cold-adapted *S. minutulus* is less influenced by Si or P limitation at low temperatures, but *N. acicularis*, which appears at the end of spring, is less influenced at higher temperatures. This is supported by the results of the competition experiments under Si-limitation and P-limitation, because the competitive ability of *N. acicularis* always increased relative to *S. minutulus* with increasing temperature and photoperiod regardless of whether it was the weaker or stronger competitor. Similarly, a decrease in temperature and photoperiod combined with silicon limitation favoured centric diatoms in Lake Müggelsee according to the statistical analysis of field data, whereas an increase in light and photoperiod combined with P limitation favoured pennate diatoms (Shatwell et al., 2008). Accordingly the R* (minimum equilibrium resource requirement after Tilman (1982)) calculated here for *S. minutulus* under silicon limitation was low and invariant with temperature, whereas it decreased with increasing temperature in *N. acicularis*, thus increasing its competitive ability relative to *S. minutulus* at higher temperatures. The response of the test species to fluctuating light and photoperiod point to the same conclusion: *Stephanodiscus minutulus*, with a lower optimum temperature than the other species (Giersdorf, 1988, Kohl and Giersdorf, 1991) and more competitive under short daylengths (Nicklisch et al., 2008), was less inhibited by fluctuating light, with a marginal tendency to become even less inhibited at low temperatures. Altogether, the tested species seem to be highly adapted to their environment and the type of interaction between physical factors and nutrients reflects this adaptation.

4.6.2 Spring phytoplankton composition

One question that remains is whether factor interactions play a role in phytoplankton dynamics *in situ*. The regression analysis of data from Lake Müggelsee showed that centric diatoms, which are early spring species (Sommer et al., 1986, Sommer et al., 2012) and thus adapted to low temperatures and short daylengths, were strongly favoured by low Si:P, low temperature and short photoperiods (Eq. 38, p. 73). Since temperature, photoperiod, silicon and phosphorus were the best predictors of centric diatom biovolume, it seems clear that the interactions between these parameters play a role. The results of silicon limitation experiments indicated that if the initial slope of the Monod curve is high and independent of temperature and photoperiod, as found for *S. minutulus*, then the interaction between silicon and temperature or photoperiod effectively represents Liebig's Minimum Law under typical

spring conditions. For centric diatoms, in particular the dominant *Stephanodiscus neoastraea* in Müggelsee, this would increase their competitive ability at combined low temperature and low DSi, as was clearly supported by the field data. Lower silicon levels can also arrest spring diatom growth earlier (Thackeray et al., 2008, Meis et al., 2009, Feuchtmayr et al., 2012) when temperatures and daylengths are also lower, which probably contributed to these observations in Lake Müggelsee. However, the results showed that the timing of the diatom peak was not an important predictor of the biovolume of centric diatoms.

Other studies have shown evidence of interactions between phosphorus and the physical factors. For example, warming combined with high phosphorus concentrations caused the spring peak to come earlier whereas there was no change in the peak timing when warming and oligotrophication counteracted each other (Köhler et al., 2005), which is consistent with the observation that phytoplankton require less phosphorus at higher temperatures (Rhee and Gotham, 1981b, Wernicke and Nicklisch, 1986). The results showed that *Nitzschia acicularis* is adapted to low phosphorus levels, as is typical for pennate diatoms (Kilham, 1971, Kilham et al., 1986, Sommer, 1989) and longer photoperiods. Accordingly, an increase in photoperiod and decrease in phosphorus in Lake Müggelsee favoured pennate diatoms in spring (Shatwell et al., 2008). This does not seem surprising because phosphorus limitation generally occurs towards the end of spring when daylengths are longer, and the effective photoperiod is generally longer in eutrophic systems when phosphorus is limiting due to increased euphotic depth and water clarity (Jeppesen et al., 2005). The statistical relation for the biomass of pennate diatoms in this study suggested that, in addition to the physical factors, other factors were important for the dynamics of this group, notably the start population size and grazing. The positive relationship between grazers and pennate diatoms might indicate bottom up control of this group rather than top down control by grazers. The relationship with grazers was stronger for pennate diatoms than for centric diatoms, probably because pennate diatoms and cladocerans are adapted to higher temperatures (Sommer et al., 1986). Studies show that diatoms peak earlier at lower temperatures when silicon is limiting, whereas the peak is delayed when phosphorus is limiting (Shatwell et al., 2008, Thackeray et al., 2008, Feuchtmayr et al., 2012). This also agrees with results that show that grazing is stronger in warm springs with high Si:P ratios because the time between the diatom peak and main grazers is shorter (Shatwell et al., 2008, Huber et al., 2008).

Altogether, the interactive effects of physical factors like temperature and photoperiod with silicon and phosphorus seem to play a role in shaping the spring diatom community, as

demonstrated by laboratory kinetic data, competition experiments and field data. The experiments suggested that the main mechanism for this is a high phosphorus- or silicon-limited growth efficiency that is independent of temperature or photoperiod in cold adapted species. This interaction type did not exist in species adapted to warmer temperatures like *Nitzschia acicularis* and *Limnothrix redekei*, which seem to invest more into strategies of velocity or grazing resistance than dealing with adverse physical conditions (Nicklisch, 1999). Moreover, cold-adapted species appear to be more adapted to fluctuating light in mixed environments (Nicklisch, 1998, Nicklisch and Fietz, 2001). A warmer climate may lead to warmer water, decreased inflows and longer residence times with accompanying eutrophication effects (Nixdorf et al., 2009, Schindler, 2009). Since phytoplankton require less phosphorus at higher temperatures, as demonstrated in P-limitation experiments, climate warming may counteract reoligotrophication. At the same time silicate inputs may decrease due to the lower inflows and decreased weathering in the catchment (Schindler et al., 1996, Schindler, 2006), which should increase the importance of silicon as a nutrient and possibly decrease Si:P and Si:N ratios. Understanding the species-specific interactions between growth factors will help increase our understanding of phytoplankton diversity and improve prediction of dynamics, including the complex combined effects of climate and trophic change.

5. Conclusions

- Temperature and photoperiod have the same influence on growth under fluctuating light as they do under constant light.
- The photoperiod and short term light fluctuations caused by mixing have additive effects on growth. They are thus inherently related as different aspects of temporal variation of the light supply. Their combined effects can be accounted for with a simple empirical equation.
- Phosphorus and silicon interact strongly with temperature with respect to growth, but less with the photoperiod.
- The Droop relation fits well to some, but probably not the majority of species under N and P limitation. Quota curves with normalised half-saturation coefficients are a good alternative.
- The previously accepted temperature dependence of the minimum P-quota (Q_0) may be an artefact of the methods used to measure it. The apparent temperature dependence may actually reflect a temperature dependence of the half-saturation coefficient of the quota curve (k_Q).
- The Monod equation cannot sufficiently account for non-steady dynamics of diatom growth under silicon limitation. The Monod model underestimates silicon uptake rates and overestimates uptake affinity due to non-steady uptake, dependent on the cell cycle. Estimates based on the Monod model may therefore considerably underestimate the degree of silicon limitation.
- The types of factor interactions (notably with light, temperature, photoperiod, phosphorus, silicon, light fluctuations) are generally species-specific, reflect niche adaptation and enhance niche differentiation.
- Interactions between nutrients and physical factors are relevant to growth during spring and contribute to the phytoplankton composition. Knowledge of the interactions should improve our understanding of the complex effects of climate and trophic change.

6. References

Ahlgren, G. (1985) Growth of *Oscillatoria agardhii* in chemostat culture. 3. Simultaneous limitation of nitrogen and phosphorus. *British Phycological Journal,* **20,** 249-261.

Ahlgren, G. (1987) Temperature functions in biology and their application to algal growth constants. *Oikos,* **49,** 177-190.

Ahlgren, G. (1988) Phosphorus as growth-regulating factor relative to other environmental factors in cultured algae. *Hydrobiologia,* **170,** 191-210.

Andersen, T. (1997) *Pelagic Nutrient Cycles: Herbivores as Sources and Sinks.* Springer-Verlag, Berlin.

Azam, F. (1974) Silicic acid uptake in diatoms studied with Ge-68 Germanic acid as tracer. *Planta,* **121,** 205-212.

Azam, F. & Chisholm, S. W. (1976) Silicic acid uptake and incorporation by natural marine phytoplankton populations. *Limnology and Oceanography,* **21,** 427-435.

Bates, D. M. & Watts, D. G. (1988) *Nonlinear Regression Analysis and Its Applications.* Wiley, New York.

Berger, S. A., Diehl, S., Stibor, H., Trommer, G. & Ruhenstroth, M. (2010) Water temperature and stratification depth independently shift cardinal events during plankton spring succession. *Global Change Biology,* **16,** 1954-1965.

Berger, S. A., Diehl, S., Stibor, H., Trommer, G., Ruhenstroth, M., Wild, A., Weigert, A., Jager, C. G. & Striebel, M. (2007) Water temperature and mixing depth affect timing and magnitude of events during spring succession of the plankton. *Oecologia,* **150,** 643-654.

Brown, E. J. & Button, D. K. (1979) Phosphate-limited growth kinetics of *Selenastrum capricornutum*. *Journal of Phycology,* **15,** 305-311.

Brunet, C. & Lavaud, J. (2010) Can the xanthophyll cycle help extract the essence of the microalgal functional response to a variable light environment? *Journal of Plankton Research,* **32,** 1609-1617.

Brzezinski, M. A. (1985) The Si:C:N ratio of marine diatoms: Interspecific variability and the effect of some environmental variables. *Journal of Phycology,* **21,** 347-357.

Brzezinski, M. A. (1992) Cell-cycle effects on the kinetics of silicic acid uptake and resource competition among diatoms. *Journal of Plankton Research,* **14,** 1511-1539.

Brzezinski, M. A., Olson, R. J. & Chisholm, S. W. (1990) Silicon availability and cell-cycle progression in marine diatoms. *Marine Ecology-Progress Series,* **67,** 83-96.

Button, D. K. (1978) On the theory of control of microbial growth kinetics by limiting nutrient concentrations. *Deep-Sea Research,* **25,** 1163-1177.

Caperon, J. & Meyer, J. (1972) Nitrogen-limited growth of marine phytoplankton. 1. Changes in population characteristics with steady-state growth rate. *Deep-Sea Research,* **19,** 601-618.

Castenholz, R. W. (1964) The effect of daylength and light intensity on the growth of littoral marine diatoms in culture. *Physiologia Plantarum,* **17,** 951-963.

Cembella, A. D., Antia, N. J. & Harrison, P. J. (1984a) The Utilization of Inorganic and Organic Phosphorus-Compounds as Nutrients by Eukaryotic Microalgae - a Multidisciplinary Perspective .1. *Crc Critical Reviews in Microbiology,* **10,** 317-391.

Cembella, A. D., Antia, N. J. & Harrison, P. J. (1984b) The Utilization of Inorganic and Organic Phosphorus-Compounds as Nutrients by Eukaryotic Microalgae - a Multidisciplinary Perspective .2. *Crc Critical Reviews in Microbiology,* **11,** 13-81.

Chalup, M. S. & Laws, E. A. (1990) A test of the assumptions and predictions of recent microalgal growth models with the marine phytoplankter *Pavlova lutheri*. *Limnology and Oceanography,* **35,** 583-596.

Chisholm, S. W., Azam, F. & Eppley, R. W. (1978) Silicic acid incorporation in marine diatoms on light:dark cycles: Use as an assay for phased cell division. *Limnology and Oceanography,* **23,** 518-529.

Claquin, P., Martin-Jézéquel, V., Kromkamp, J. C., Veldhuis, M. J. W. & Kraay, G. W. (2002) Uncoupling of silicon compared with carbon and nitrogen metabolisms and the role of the cell cycle in continuous cultures of *Thalassiosira pseudonana* (Bacillariophyceae) under light, nitrogen, and phosphorus control. *Journal of Phycology,* **38,** 922-930.

Clark, D. R., Flynn, K. J. & Owens, N. J. P. (2002) The large capacity for dark nitrate-assimilation in diatoms may overcome nitrate limitation of growth. *New Phytologist,* **155,** 101-108.

Cosper, E. (1982) Influence of light-intensity on diel variations in rates of growth, respiration and organic-release of a marine diatom - comparison of diurnally constant and fluctuating light. *Journal of Plankton Research,* **4,** 705-724.

Crawley, M. (2007) *The R Book.* Wiley, Chichester.

Davison, I. R. (1991) Environmental effects on algal photosynthesis: temperature. *Journal of Phycology,* **27,** 2-8.

DEV (2007) Deutsche Einheitsverfahren (DEV) zur Wasser-, Abwasser- und Schlammuntersuchung. *Analytical standard DIN 38405, part 21*. VCH Verlagsges. mbH, Beuth Verlag GmbH, Weinheim.

Dickman, E. M., Vanni, M. J. & Horgan, M. J. (2006) Interactive effects of light and nutrients on phytoplankton stoichiometry. *Oecologia,* **149,** 676-689.

Dimier, C., Brunet, C., Geider, R. & Raven, J. (2009) Growth and photoregulation dynamics of the picoeukaryote *Pelagomonas calceolata* in fluctuating light. *Limnology and Oceanography,* **54,** 823-836.

Droop, M. R. (1968) Vitamin B12 and marine ecology. 4. Kinetics of uptake, growth and inhibition in *Monochrysis lutheri*. *Journal of the Marine Biological Association of the United Kingdom,* **48,** 689-733.

Droop, M. R. (1973) Some thoughts on nutrient limitation in algae. *Journal of Phycology,* **9,** 264-272.

Droop, M. R. (1974) Nutrient status of algal cells in continuous culture. *Journal of the Marine Biological Association of the United Kingdom,* **54,** 825-855.

Ducobu, H., Huisman, J., Jonker, R. R. & Mur, L. R. (1998) Competition between a prochlorophyte and a cyanobacterium under various phosphorus regimes: Comparison with the Droop model. *Journal of Phycology,* **34,** 467-476.

Eilers, P. H. C. & Peeters, J. C. H. (1988) A model for the relationship between light intensity and the rate of photosynthesis in phytoplankton. *Ecological Modelling,* **42,** 199-215.

Elrifi, I. R. & Turpin, D. H. (1985) Steady-state luxury consumption and the concept of optimum nutrient ratios: A study with phosphate and nitrate limited *Selenastrum minutum* (Chlorophyta). *Journal of Phycology,* **21,** 592-602.

Elser, J. J., Bracken, M. E. S., Cleland, E. E., Gruner, D. S., Harpole, W. S., Hillebrand, H., Ngai, J. T., Seabloom, E. W., Shurin, J. B. & Smith, J. E. (2007) Global analysis of nitrogen and phosphorus limitation of primary producers in freshwater, marine and terrestrial ecosystems. *Ecology Letters,* **10,** 1135-1142.

Falkner, G., Wagner, F., Small, J. V. & Falkner, R. (1995) Influence of fluctuating phosphate supply on the regulation of phosphate uptake by the blue-green alga *Anacystis nidulans*. *Journal of Phycology,* **31,** 745-753.

Feuchtmayr, H., Thackeray, S. J., Jones, I. D., De Ville, M., Fletcher, J., James, B. E. N. & Kelly, J. (2012) Spring phytoplankton phenology – are patterns and drivers of change consistent among lakes in the same climatological region? *Freshwater Biology,* **57,** 331-344.

Fietz, S. & Nicklisch, A. (2002) Acclimation of the diatom *Stephanodiscus neoastraea* and the cyanobacterium *Planktothrix agardhii* to simulated natural light fluctuations. *Photosynthesis Research,* **72,** 95-106.

Flameling, I. A. & Kromkamp, J. (1997) Photoacclimation of *Scenedesmus protuberans* (Chlorophyceae) to fluctuating irradiances simulating vertical mixing. *Journal of Plankton Research,* **19,** 1011-1024.

Flynn, K. J. (2001) A mechanistic model for describing dynamic multi-nutrient, light, temperature interactions in phytoplankton. *Journal of Plankton Research,* **23,** 977-997.

Flynn, K. J. (2002) How critical is the critical N : P ratio? *Journal of Phycology,* **38,** 961-970.

Flynn, K. J. (2003) Modelling multi-nutrient interactions in phytoplankton; balancing simplicity and realism. *Progress In Oceanography,* **56,** 249-279.

Flynn, K. J. (2008a) The importance of the form of the quota curve and control of non-limiting nutrient transport in phytoplankton models. *Journal of Plankton Research,* **30,** 423-438.

Flynn, K. J. (2008b) Use, abuse, misconceptions and insights from quota models - The Droop cell quota model 40 years on. *Oceanography and Marine Biology: An Annual Review, Vol 46* (eds R. N. Gibson, R. J. A. Atkinson & J. D. M. Gordon), pp. 1-23.

Flynn, K. J. (2008c) Use, abuse, misconceptions and insights from quota models - The Droop cell quota model 40 years on. *Oceanography and Marine Biology: An Annual Review, Vol 46,* **46,** 1-23.

Flynn, K. J., Clark, D. R. & Owens, N. J. P. (2002) Modelling suggests that optimization of dark nitrogen-assimilation need not be a critical selective feature in phytoplankton. *New Phytologist,* **155,** 109-119.

Flynn, K. J. & Fasham, M. J. R. (2003) Operation of light-dark cycles within simple ecosystem models of primary production and the consequences of using phytoplankton models with different abilities to assimilate N in darkness. *Journal of Plankton Research,* **25,** 83-92.

Flynn, K. J. & Martin-Jézéquel, V. (2000) Modelling Si-N-limited growth of diatoms. *Journal of Plankton Research,* **22,** 447-472.

Foy, R. H. (1983) Interaction of temperature and light on the growth rates of two planktonic *Oscillatoria* species under a short photoperiod regime. *British Phycological Journal,* **18,** 267-273.

Foy, R. H. & Gibson, C. E. (1993) The influence of irradiance, photoperiod and temperature on the growth kinetics of three planktonic diatoms. *European Journal of Phycology,* **28,** 203-212.

Foy, R. H., Gibson, C. E. & Smith, R. V. (1976) The influence of daylength, light intensity and temperature on the growth rates of planktonic blue-green algae. *British Phycological Journal,* **15,** 151-163.

Fuhs, G. W. (1969) Phosphorus content and rate of growth in the diatoms *Cyclotella nana* and *Thalassiosira fluviatilis*. *Journal of Phycology,* **5,** 312-321.

Geider, R. J., MacIntyre, H. L. & Kana, T. M. (1998) A dynamic regulatory model of phytoplanktonic acclimation to light, nutrients, and temperature. *Limnology and Oceanography,* **43,** 679-694.

Gibson, C. E. (1985) Growth rate, maintenance energy and pigmentation of planktonic cyanophyta during one-hour light : dark cycles. *British Phycological Journal,* **20,** 155-161.

Gibson, C. E. & Foy, R. H. (1983) The photosynthesis and growth efficiency of a planktonic blue-green alga, *Oscillatoria redekei*. *British Phycological Journal,* **18,** 39-45.

Giersdorf, K. (1988) *Der Einfluß von Licht und Temperatur auf das Wachstum der planktischen Diatomeen Stephanodiscus minutulus (Kütz.) Cleve & Möller und Nitzschia acicularis W. Smith*. Doctor rerum naturalium Doctoral Thesis, Humboldt-Universität zu Berlin, Berlin.

Goldman, J. C. (1977) Temperature effects on phytoplankton growth in continuous culture. *Limnology and Oceanography,* **22,** 932-936.

Goldman, J. C. (1979) Temperature effects on steady-state growth, phosphorus uptake, and the chemical composition of a marine phytoplankter. *Microbial Ecology,* **5,** 153-166.

Goldman, J. C., McCarthy, J. J. & Peavey, D. G. (1979) Growth rate influence on the chemical composition of phytoplankton in oceanic waters. *Nature,* **279,** 210-215.

Gotham, I. J. & Rhee, G. Y. (1981a) Comparative kinetic studies of nitrate-limited growth and nitrate uptake in phytoplankton in continuous culture. *Journal of Phycology,* **17,** 309-314.

Gotham, I. J. & Rhee, G. Y. (1981b) Comparative kinetic studies of phosphate-limited growth and phosphate uptake in phytoplankton in continuous culture. *Journal of Phycology,* **17,** 257-265.

Grover, J. P. (1989) Phosphorus-dependent growth kinetics of 11 species of freshwater algae. *Limnology and Oceanography,* **34,** 341-348.

Guillard, R. R. L. & Lorenzen, C. J. (1972) Yellow-green algae with chlorophyllide c. *Journal of Phycology,* **8,** 10-14.

Harpole, W. S., Ngai, J. T., Cleland, E. E., Seabloom, E. W., Borer, E. T., Bracken, M. E. S., Elser, J. J., Gruner, D. S., Hillebrand, H., Shurin, J. B. & Smith, J. E. (2011) Nutrient co-limitation of primary producer communities. *Ecology Letters,* **14,** 852-862.

Havelkova-Dousova, H., Prasil, O. & Behrenfeld, M. J. (2004) Photoacclimation of *Dunaliella tertiolecta* (Chlorophyceae) under fluctuating irradiance. *Photosynthetica,* **42,** 273-281.

Healey, F. P. (1980) Slope of the Monod equation as an indicator of advantage in nutrient competition. *Microbial Ecology,* **5,** 281-286.

Healey, F. P. (1985) Interacting effects of light and nutrient limitation on the growth rate of *Synechococcus linearis* (Cyanophyceae). *Journal of Phycology,* **21,** 134-146.

Hildebrand, M., Frigeri, L. G. & Davis, A. K. (2007) Synchronized growth of Thalassiosira pseudonana (Bacillariophyceae) provides novel insights into cell-wall synthesis processes in relation to the cell cycle. *Journal of Phycology,* **43,** 730-740.

Holm, N. P. & Armstrong, D. E. (1981) Role of nutrient limitation and competition in controlling the populations of *Asterionella formosa* and *Microcystis aeruginosa* in semicontinuous culture. *Limnology and Oceanography,* **26,** 622-634.

Huber, V., Adrian, R. & Gerten, D. (2008) Phytoplankton response to climate warming modified by trophic state. *Limnology and Oceanography,* **53,** 1-13.

Hutchinson, G. E. (1961) The paradox of the plankton. *American Naturalist,* **95,** 137-145.

Huwaldt, J. A. & Steinhorst, S. (2012) Plot Digitizer.

Ibelings, B. W., Kroon, B. M. A. & Mur, L. R. (1994) Acclimation of photosystem II in a cyanobacterium and a eukaryotic green alga to high and fluctuating photosynthetic photon flux densities, simulating light regimes induced by mixing in lakes. *New Phytologist,* **128,** 407-424.

Jeppesen, E., Moss, B., Bennion, H., Carvalho, L., DeMeester, L., Feuchtmayr, H., Friberg, N., Gessner, M. O., Hefting, M., Lauridsen, T. L., Liboriussen, L., Malmquist, H. J., May, L., Meerhoff, M., Olafsson, J. S., Soons, M. B. & Verhoeven, J. T. A. (2010) Interaction of climate change and eutrophication. *Climate Change Impacts on Freshwater Ecosystems* (eds M. Kernan, R. Battarbee & B. Moss), pp. 119-151. Wiley-Blackwell, Oxford, UK.

Jeppesen, E., Sondergaard, M., Jensen, J. P., Havens, K. E., Anneville, O., Carvalho, L., Coveney, M. F., Deneke, R., Dokulil, M. T., Foy, B., Gerdeaux, D., Hampton, S. E., Hilt, S., Kangur, K., Köhler, J., Lammens, E., Lauridsen, T. L., Manca, M., Miracle, M. R., Moss, B., Noges, P., Persson, G., Phillips, G., Portielje, R., Schelske, C. L., Straile, D., Tatrai, I., Willen, E. & Winder, M. (2005) Lake responses to reduced nutrient loading - an analysis of contemporary long-term data from 35 case studies. *Freshwater Biology,* **50,** 1747-1771.

Kilham, P. (1971) A hypothesis concerning silica and the freshwater planktonic diatoms. *Limnology and Oceanography,* **16,** 10-18.

Kilham, P., Kilham, S. S. & Hecky, R. E. (1986) Hypothesized resource relationships among African planktonic diatoms. *Limnology and Oceanography,* **31,** 1169-1181.

Kilham, S. S. (1975) Kinetics of silicon-limited growth in the freshwater diatom *Asterionella formosa*. *Journal of Phycology,* **11,** 396-399.

Kilham, S. S. (1984) Silicon and phosphorus growth kinetics and competitive interactions between *Stephanodiscus minutus* and *Synedra* sp. *Verhandlungen Internationale Vereinigung für Theoretische und Angewandte Limnologie,* **22,** 435-439.

Kirillin, G. (2010) Modeling the impact of global warming on water temperature and seasonal mixing regimes in small temperate lakes. *Boreal Environment Research,* **15,** 279-293.

Klausmeier, C. A., Litchman, E., Daufresne, T. & Levin, S. A. (2008) Phytoplankton stoichiometry. *Ecological Research,* **23,** 479-485.

Klausmeier, C. A., Litchman, E. & Levin, S. A. (2004) Phytoplankton growth and stoichiometry under multiple nutrient limitation. *Limnology and Oceanography,* **49,** 1463-1470.

Kohl, J. G. & Giersdorf, K. (1991) Competition ability of two planktic diatoms under different vertical light gradients, mixing-depth and -frequencies: An experimental approach. *Verhandlungen des Internationalen Verein Limnologie,* **24,** 2652-2656.

Kohl, J. G. & Nicklisch, A. (1988) *Ökophysiologie der Algen: Wachstum und Ressourcennutzung.* Akademie Verlag, Berlin.

Köhler, J., Hilt, S., Adrian, R., Nicklisch, A., Kozerski, H. P. & Walz, N. (2005) Long-term response of a shallow, moderately flushed lake to reduced external phosphorus and nitrogen loading. *Freshwater Biology,* **50,** 1639-1650.

Kromkamp, J. & Limbeek, M. (1993) Effect of short-term variation in irradiance on light harvesting and photosynthesis of the marine diatom *Skeletonema costatum*: a laboratory study simulating vertical mixing. *Journal of General Microbiology,* **139,** 2277-2284.

Kroon, B. M. A., Burgerwiersma, T., Visser, P. M. & Mur, L. R. (1992) The effect of dynamic light regimes on *Chlorella*. 2. Minumum quantum requirement and photosynthesis-irradiance parameter. *Hydrobiologia,* **238,** 79-88.

Laws, E. A. & Bannister, T. T. (1980) Nutrient- and light-limited growth of *Thalassiosira fluviatilis* in continuous culture, with implications for phytoplankton growth in the ocean. *Limnology and Oceanography,* **25,** 457-473.

Lehman, J. T., Botkin, D. B. & Likens, G. E. (1975) The assumptions and rationales of a computer model of phytoplankton population dynamics. *Limnology and Oceanography,* **20,** 343-364.

Leynaert, A., Longphuirt, S. N., Claquin, P., Chauvaud, L. & Ragueneau, O. (2009) No limit? The multiphasic uptake of silicic acid by benthic diatoms. *Limnology and Oceanography,* **54,** 571-576.

Litchman, E. (2000) Growth rates of phytoplankton under fluctuating light. *Freshwater Biology,* **44,** 223-235.

Litchman, E. & Klausmeier, C. A. (2001) Competition of phytoplankton under fluctuating light. *American Naturalist,* **157,** 170-187.

Litchman, E., Klausmeier, C. A. & Bossard, P. (2004) Phytoplankton nutrient competition under dynamic light regimes. *Limnology and Oceanography,* **49,** 1457-1462.

Litchman, E., Steiner, D. & Bossard, P. (2003) Photosynthetic and growth responses of three freshwater algae to phosphorus limitation and daylength. *Freshwater Biology,* **48,** 2141-2148.

MacKenzie, T. D. B. & Campbell, D. A. (2005) Cyanobacterial acclimation to rapidly fluctuating light is constrained by inorganic carbon status. *Journal of Phycology,* **41,** 801-811.

Marra, J. (1978) Effect of short-term variations in light-intensity on photosynthesis of a marine phytoplankter - laboratory simulation study. *Marine Biology,* **46,** 191-202.

Martin-Jézéquel, V., Hildebrand, M. & Brzezinski, M. A. (2000) Silicon metabolism in diatoms: implications for growth. *Journal of Phycology,* **36,** 821-840.

Mechling, J. A. & Kilham, S. S. (1982) Temperature effects on silicon limited growth of the Lake Michigan diatom *Stephanodiscus minutus* (Bacillariophyceae). *Journal of Phycology,* **18,** 199-205.

Mehnert, G., Rücker, J., Nicklisch, A., Leunert, F. & Wiedner, C. (2012) Effects of thermal acclimation and photoacclimation on lipophilic pigments in an invasive and a native cyanobacterium of temperate regions. *European Journal of Phycology,* **47,** 182-192.

Meis, S., Thackeray, S. J. & Jones, I. D. (2009) Effects of recent climate change on phytoplankton phenology in a temperate lake. *Freshwater Biology,* **54,** 1888-1898.

Mitrovic, S. M., Howden, C. G., Bowling, L. C. & Buckney, R. T. (2003) Unusual allometry between in situ growth of freshwater phytoplankton under static and fluctuating light environments: possible implications for dominance. *Journal of Plankton Research,* **25,** 517-526.

Nicklisch, A. (1992) The interaction of irradiance and temperature on the growth rate of *Limnothrix redekei* and its mathematical description. *Archiv fur Hydrobiologie***,** 1-18.

Nicklisch, A. (1998) Growth and light absorption of some planktonic cyanobacteria, diatoms and Chlorophyceae under simulated natural light fluctuations. *Journal of Plankton Research,* **20,** 105-119.

Nicklisch, A. (1999) Competition between the cyanobacterium *Limnothrix redekei* and some spring species of diatoms under P-limitation. *International Review of Hydrobiology,* **84,** 233-241.

Nicklisch, A. & Fietz, S. (2001) The influence of light fluctuations on growth and photosynthesis of *Stephanodiscus neoastraea* (diatom) and *Planktothrix agardhii* (cyanobacterium). *Archiv fur Hydrobiologie,* **151,** 141-156.

Nicklisch, A. & Kohl, J. G. (1989) The influence of light on the primary production of two planktic blue-green algae. *Archiv fuer Hydrobiologie - Beiheft Ergebnisse der Limnologie,* **33,** 451-455.

Nicklisch, A. & Köhler, J. (2001) Estimation of primary production with Phyto-PAM fluorometry. *Berichte des IGB,* **13,** 47-60.

Nicklisch, A., Shatwell, T. & Köhler, J. (2008) Analysis and modelling of the interactive effects of temperature and light on phytoplankton growth and relevance for the spring bloom. *Journal of Plankton Research,* **30,** 75-91.

Nicklisch, A. & Steinberg, C. E. W. (2009) RNA/protein and RNA/DNA ratios determined by flow cytometry and their relationship to growth limitation of selected planktonic algae in culture. *European Journal of Phycology,* **44,** 297-308.

Nicklisch, A. & Woitke, P. (1999) Pigment content of selected planktonic algae in response to simulated natural light fluctuations and a short photoperiod. *International Review of Hydrobiology,* **84,** 479-495.

Nixdorf, B., Mischke, U. & Rucker, J. (2003) Phytoplankton assemblages and steady state in deep and shallow eutrophic lakes - an approach to differentiate the habitat properties of Oscillatoriales. *Hydrobiologia,* **502,** 111-121.

Nixdorf, B., Rücker, J., Deneke, R. & Grüneberg, B. (2009) Gewässer im Klimastress? Eutrophierungsgefahr in Seen am Beispiel der Scharmützelseeregion. *Forum der Forschung,* **22,** 99-106.

North, R. L., Guildford, S. J., Smith, R. E. H., Havens, S. M. & Twiss, M. R. (2007) Evidence for phosphorus, nitrogen, and iron colimitation of phytoplankton communities in Lake Erie. *Limnology and Oceanography,* **52,** 315-328.

Olsen, Y. (1989) Evaluation of competitive ability of *Staurastrum leutkemuellerii* (Chlorophyceae) and *Microcystis aeruginosa* (Cyanophyceae) under P limitation. *Journal of Phycology,* **25,** 486-499.

Paasche, E. (1967) Marine plankton algae grown with light-dark cycles. I. *Coccolithus huxleyi*. *Physiologia Plantarum,* **20,** 946-&.

Paasche, E. (1968) Marine plankton algae grown with light-dark cycles. 2. *Ditylum brightwellii* and *Nitzschia turgidula*. *Physiologia Plantarum,* **21,** 66-77.

Paasche, E. (1973) Silicon and the ecology of marine plankton diatoms. 2. Silicate uptake kinetics in five diatom species. *Marine Biology,* **19,** 262-269.

Paasche, E. (1975) Growth of the plankton diatom *Thalassiosira nordenskioeldii* Cleve at low silicate concentrations. *Journal of Experimental Marine Biology and Ecology,* **18,** 173-183.

Pahlow, M. & Oschlies, A. (2009) Chain model of phytoplankton P, N and light colimitation. *Marine Ecology Progress Series,* **376,** 69-83.

Perry, M. J. (1976) Phosphate utilization by an oceanic diatom in phosphorus-limited chemostat culture and in oligotrophic waters of the central North Pacific. *Limnology and Oceanography,* **21,** 88-107.

Pickett-Heaps, J., Schmid, A. M. M. & Edgar, L. A. (1990) The cell biology of diatom valve formation. *Progress in phycological research* (eds D. B. Round & D. J. Chapman), pp. 1-168. Biopress Ltd., Bristol, U.K.

R Core Team (2013) R: A language and environment for statistical computing. R Foundation for Statistical Computing, Vienna.

R Development Core Team (2009) R: A language and environment for statistical computing. R Foundation for Statistical Computing, Vienna.

Reynolds, C. S. (1984) *The Ecology of Freshwater Phytoplankton.* Cambridge University Press, Cambridge.

Reynolds, C. S. (2006) *The Ecology of Phytoplankton.* Cambridge University Press, Cambridge.

Rhee, G. Y. (1973) Continuous culture study of phosphate uptake, growth rate and polyphosphate in *Scenedesmus* sp. *Journal of Phycology,* **9,** 495-506.

Rhee, G. Y. (1978) Effects of N:P atomic ratios and nitrate limitation on algal growth, cell composition, and nitrate uptake. *Limnology and Oceanography,* **23,** 10-25.

Rhee, G. Y. & Gotham, I. J. (1981a) The effect of environmental factors on phytoplankton growth: Light and the interactions of light with nitrate limitation. *Limnology and Oceanography,* **26,** 649-659.

Rhee, G. Y. & Gotham, I. J. (1981b) The effect of environmental factors on phytoplankton growth: Temperature and the interactions of temperature with nutrient limitation. *Limnology and Oceanography,* **26,** 635-648.

Riegman, R. & Mur, L. R. (1985) Effects of photoperiodicity and light irradiance on phosphate-limited *Oscillatoria agardhii* in chemostat cultures. 2. Phosphate uptake and growth. *Archives of Microbiology,* **142,** 72-76.

Riegman, R., Stolte, W., Noordeloos, A. A. M. & Slezak, D. (2000) Nutrient uptake and alkaline phosphatase (EC 3:1:3:1) activity of *Emiliania huxleyi* (Prymnesiophyceae) during growth under N and P limitation in continuous cultures. *Journal of Phycology,* **36,** 87-96.

Rinke, K., Yeates, P. & Rothhaupt, K. O. (2010) A simulation study of the feedback of phytoplankton on thermal structure via light extinction. *Freshwater Biology,* **55,** 1674-1693.

Roloff, B. & Nicklisch, A. (1993) Partitioning of phosphate between blue-green algae and their accompanying bacteria in phosphate-limited culture. *Archiv fur Hydrobiologie,* **126,** 405-416.

Schindler, D. W. (2006) Recent advances in the understanding and management of eutrophication. *Limnology and Oceanography,* **51,** 356-363.

Schindler, D. W. (2009) Lakes as sentinels and integrators for the effects of climate change on watersheds, airsheds, and landscapes. *Limnology and Oceanography,* **54,** 2349-2358.

Schindler, D. W., Bayley, S. E., Parker, B. R., Beaty, K. G., Cruikshank, D. R., Fee, E. J., Schindler, E. U. & Stainton, M. P. (1996) The effects of climatic warming on the properties of boreal lakes and streams at the Experimental Lakes Area, northwestern Ontario. *Limnology and Oceanography,* **41,** 1004-1017.

Schreiber, U. & Bilger, W. (1993) Progress in chlorophyll fluorescence research: Major developments during the past years in retrospect. *Progress in Botany,* **54,** 151-173.

Shatwell, T., Köhler, J. & Nicklisch, A. (2008) Warming promotes cold-adapted phytoplankton in temperate lakes and opens a loophole for Oscillatoriales in spring. *Global Change Biology,* **14,** 2194-2200.

Shatwell, T., Köhler, J. & Nicklisch, A. (2013) Temperature and photoperiod interactions with silicon-limited growth and competition of two diatoms. *Journal of Plankton Research***,** doi: 10.1093/plankt/fbt058.

Shatwell, T., Nicklisch, A. & Köhler, J. (2012) Temperature and photoperiod effects on phytoplankton growing under simulated mixed layer light fluctuations. *Limnology and Oceanography,* **57,** 541-553.

Soetaert, K. & Petzoldt, T. (2010) Inverse Modelling, Sensitivity and Monte Carlo Analysis in R Using Package FME. *Journal of Statistical Software,* **33,** 1-28.

Soetaert, K., Petzoldt, T. & Setzer, R. W. (2010) Solving Differential Equations in R: Package deSolve. *Journal of Statistical Software,* **33,** 1-25.

Sommer, U. (1985) Comparison between steady state and non-steady state competition: Experiments with natural phytoplankton. *Limnology and Oceanography,* **30,** 335-346.

Sommer, U. (1989) The Role of Competition for Resources in Phytoplankton Succession. *Plankton Ecology: succession in plankton communities* (ed U. Sommer), pp. 57-106. Springer Berlin Heidelberg.

Sommer, U. (1994) The impact of light intensity and daylength on silicate and nitrate competition among marine phytoplankton. *Limnology and Oceanography,* **39,** 1680-1688.

Sommer, U., Adrian, R., De Senerpont Domis, L., Elser, J. J., Gaedke, U., Ibelings, B., Jeppesen, E., Lürling, M., Molinero, J. C., Mooij, W. M., van Donk, E. & Winder, M. (2012) Beyond the Plankton Ecology Group (PEG) model: Mechanisms driving plankton succession. *Annual Review of Ecology, Evolution, and Systematics,* **43,** 429-448.

Sommer, U., Gliwicz, Z. M., Lampert, W. & Duncan, A. (1986) The PEG model of seasonal succession of planktonic events in fresh waters. *Archiv Fur Hydrobiologie,* **106,** 433-471.

Spijkerman, E. (2010) High photosynthetic rates under colimitation for inorganic phosphorus and carbon dioxide. *Journal of Phycology,* **46,** 658-664.

Spijkerman, E., de Castro, F. & Gaedke, U. (2011) Independent Colimitation for Carbon Dioxide and Inorganic Phosphorus. *PLoS ONE,* **6,** e28219.

Stapleford, L. S. & Smith, R. E. H. (1996) The interactive effects of temperature and silicon limitation on the psychrophilic ice diatom *Pseudonitszchia seriata*. *Polar Biology,* **16,** 589-594.

Sterner, R. W. (1993) Daphnia growth on varying quality of *Scenedesmus*: Mineral limitation of zooplankton. *Ecology,* **74,** 2351-2360.

Sterner, R. W. (1995) Elemental stoichiometry of species in ecosystems. *Linking Species and Ecosystems* (eds C. G. Jones & J. H. Lawton), pp. 240-252. Chapman & Hall, New York.

Sterner, R. W. & Elser, J. J. (2002) *Ecological Stoichiometry: The Biology of Elements from Molecules to the Biosphere.* Princeton University Press, Princeton.

Tang, E. P. Y. & Vincent, W. F. (2000) Effects of daylength and temperature on the growth and photosynthesis of an Arctic cyanobacterium, *Schizothrix calcicola* (Oscillatoriaceae). *European Journal of Phycology,* **35,** 263-272.

Taylor, N. J. (1985) Silica incorporation in the diatom *Coscinodiscus granii* as affected by light intensity. *British Phycological Journal,* **20,** 365-374.

Tempest, D. W. & Hunter, J. R. (1965) The influence of temperature and pH value on the macromolecular composition of magnesium-limited and glycerol-limited *Aerobacter aerogenes* growing in a chemostat. *Journal of General Microbiology,* **41,** 267-273.

Teubner, K. (1996) *Struktur und Dynamik des Phytoplanktons in Beziehung zur Hydrochemie und Hydrophysik der Gewässer*. PhD, Humboldt-Universität zu Berlin, Berlin.

Teubner, K. & Dokulil, M. T. (2002) Ecological stoichiometry of TN : TP : SRSi in freshwaters: nutrient ratios and seasonal shifts in phytoplankton assemblages. *Archiv fur Hydrobiologie,* **154,** 625-646.

Teubner, K., Feyerabend, R., Henning, M., Nicklisch, A., Woitke, P. & Kohl, J. G. (1999) Alternative blooming of *Aphanizomenon flos-aquae* or *Planktothrix agardhii* induced by the timing of the critical nitrogen:phosphorus ratio in hypertrophic riverine lakes. *Archiv für Hydrobiologie - Advances in Limnology,* **54,** 325-344.

Thackeray, S. J., Jones, I. D. & Maberly, S. C. (2008) Long-term change in the phenology of spring phytoplankton: species-specific responses to nutrient enrichment and climatic change. *Journal of Ecology,* **96,** 523-535.

Thamatrakoln, K. & Hildebrand, M. (2007) Analysis of Thalassiosira pseudonana silicon transporters indicates distinct regulatory levels and transport activity through the cell cycle. *Eukaryotic Cell,* **6,** 271-279.

Thamatrakoln, K. & Hildebrand, M. (2008) Silicon uptake in diatoms revisited: A model for saturable and nonsaturable uptake kinetics and the role of silicon transporters. *Plant Physiology,* **146,** 1397-1407.

Thompson, P. (1999) Response of growth and biochemical composition to variations in daylength, temperature, and irradiance in the marine diatom *Thalassiosira pseudonana* (Bacillariophyceae). *Journal of Phycology,* **35,** 1215-1223.

Tilman, D. (1980) Resources: A graphical-mechanistic approach to competition and predation. *American Naturalist,* **116,** 362-393.

Tilman, D. (1981) Tests of resource competition theory using four species of Lake Michigan algae. *Ecology,* **62,** 802-815.

Tilman, D. (1982) *Resource Competition and Community Structure.* Princeton University Press, Princeton, N.J.

Tilman, D. & Kilham, S. S. (1976) Phosphate and silicate growth and uptake kinetics of the diatoms *Asterionella formosa* and *Cyclotella meneghiniana* in batch and semicontinuous culture. *Journal of Phycology,* **12,** 375-383.

Tilman, D., Kilham, S. S. & Kilham, P. (1982) Phytoplankton community ecology: The role of limiting nutrients. *Annual Review of Ecology and Systematics,* **13,** 349-372.

Tilman, D., Mattson, M. & Langer, S. (1981) Competition and nutrient kinetics along a temperature gradient: an experimental test of a mechanistic approach to niche theory. *Limnology and Oceanography,* **26,** 1020-1033.

van de Poll, W. H., Visser, R. J. W. & Buma, A. G. J. (2007) Acclimation to a dynamic irradiance regime changes excessive irradiance sensitivity of *Emiliania huxleyi* and *Thalassiosira weissflogii*. *Limnology and Oceanography,* **52,** 1430-1438.

van Donk, E. & Kilham, S. S. (1990) Temperature effects on silicon- and phosphorus-limited growth and competitive interactions among three diatoms. *Journal of Phycology,* **26,** 40-50.

van Leeuwe, M. A., van Sikkelerus, B., Gieskes, W. W. C. & Stefels, J. (2005) Taxon-specific differences in photoacclimation to fluctuating irradiance in an Antarctic diatom and a green flagellate. *Marine Ecology-Progress Series,* **288,** 9-19.

van Leeuwe, M. A., Villerius, L. A., Roggeveld, J., Visser, R. J. W. & Stefels, J. (2006) An optimized method for automated analysis of algal pigments by HPLC. *Marine Chemistry,* **102,** 267-275.

Walz, N., Hintze, T. & Rusche, R. (1997) Algae and rotifer turbidostats: studies on stability of live feed cultures. *Hydrobiologia,* **358,** 127-132.

Wernicke, P. & Nicklisch, A. (1986) Light/dark cycle and temperature - their impact on phosphate-limited growth of *Oscillatoria redekei* VAN GOOR in semicontinuous culture. *Internationale Revue Der Gesamten Hydrobiologie,* **71,** 297-313.

Winder, M. & Schindler, D. E. (2004) Climatic effects on the phenology of lake processes. *Global Change Biology,* **10,** 1844-1856.

Woitke, P., Martin, C. D., Nicklisch, S. & Kohl, J. G. (1994) HPLC determination of lipophilic photosynthetic pigments in algal cultures and lake water samples using a non-endcapped C-18-RP column. *Fresenius Journal of Analytical Chemistry,* **348,** 762-768.

Wright, S. W. & Jeffrey, S. W. (1997) High-resolution HPLC system for chlorophylls and carotenoids of marine phytoplankton. *Pigments in oceanography* (eds S. W. Jeffrey, R. F. C. Mantoura & S. W. Wright), pp. 327-341. UNESCO, Paris.

Wright, S. W., Jeffrey, S. W. & Mantoura, R. F. C. (1997) Evaluation of methods and solvents for pigment extraction. *Pigments in oceanography* (eds S. W. Jeffrey, R. F. C. Mantoura & S. W. Wright), pp. 261-282. UNESCO, Paris.

Yoder, J. A. (1979) Effect of temperature on light-limited growth and chemical composition of *Skeletonema costatum* (Bacillariophyceae). *Journal of Phycology,* **15,** 362-370.

Zevenboom, W., Degroot, G. J. & Mur, L. R. (1980) Effects of light on nitrate-limited *Oscillatoria agardhii* in chemostat cultures. *Archives of Microbiology,* **125,** 59-65.

Acknowledgements

I thank Dr. Andreas Nicklisch for help in all aspects of laboratory work and for performing flow cytometric analyses, Marion Kaulfuß for help in algae cultivation and daily laboratory work, Antje Lüder for phosphorus measurements, assistance with silicon measurements and her general help in the laboratory, Thomas Hintze for writing the computer program to control the light fluctuations and for technical assistance with the chemostats and light measurements, Ursula Newen for technical assistance with the chemostats, Barbara Meinck for high performance liquid chromatography analyses, Marianne Graupe for assistance with filtration and carbon measurements, Helgard Täuscher for microscopic algal counts of *L. redekei* and assistance with microscopy, Reinhard Hölzel for technical assistance with the experimental setup, Dr. Kirsten Pohlmann for statistical advice, Dr. Thomas Mehner for advice on scientific writing, Dr. Thomas Petzoldt for advice on dynamic modelling in R and the IGB's Gleichstellungskommission for their financial support. I thank Prof. Norbert Walz, Prof. Rita Adrian and Dr. Michael Hupfer for a happy and productive work environment.

For funding this work I thank the Berlin NaFöG program and the IGB's Gleichstellungsfonds.

I would like to thank my family for all their support during this work. I could not have done the thesis without them – my parents Susie and Dave Shatwell for loving encouragement and much needed financial help, my mother-in-law Daglind Kirchhof for without fail being there to help and take care of the kids, my two boys Kilian and Bennet for being a steady source of inspiration and joy, and my wife Astrid Kirchhof for her loving support and encouragement without whom I probably would not have begun this undertaking nor finished it.

I thank my supervisor Dr. Jan Köhler for fruitful and thought provoking discussions and for support in all aspects of the dissertation, and for always standing behind me not just for the dissertation but also for my scientific career. I also gratefully acknowledge my supervisor Dr. Klaus Jöhnk for discussions and advice on modelling and more, and for continuing his supervision from the other side of the world.

I dedicate this work to Dr. Andreas Nicklisch, who could not have been a better supervisor, who always supported and guided me also in the minor but important practical details and daily measurements, and whose patient help and thoughtful discussions taught me more about biology than any book or university course.

Image credits

Figure 1: This is a reproduction of the upper portion of Figure 1 from the PEG review paper (Sommer et al., 2012), with kind permission of Annual Reviews Inc. publishers, Copyright Clearance Center order licence ID: 3196500663069.

Figure 5a: *Stephanodiscus minutulus,* photo author: Juan Alcober Bosch, C.H. Júcar, Ministerio de Agricultura, Alimentación y Medio Ambiente, http://eportal.magrama.gob.es/id_tax/ficha/buscador/1/30655). Used with kind permission of the author.

Figure 5b: *Nitzschia acicularis,* photo provided by Proyecto Agua **/** Water Project, http://www.flickr.com/photos/microagua/3258080731/sizes/o/in/photolist-5XUvTH/, used under the Creative Commons license (CC BY-NC-SA 2.0) http://creativecommons.org/licenses/by-nc-sa/2.0/.

Figure 5c: *Limnothrix redekei*, photo author Barbara Meyer, Max Planck Institute of Limnology, planktonnet.awi.de. Used with kind permission of planktonnet.awi.

Appendix 1: Literature data to assess the “Droop relation”

Table 13: Experimental data under P-limitation collected from the literature to assess the "Droop relation". The data are generally from chemostat experiments and were generally digitised from the published plots (for methods, see section 2.13.4, p. 32, and for a discussion, see section 4.3.1, p. 86). I: irradiance, T: temperature, LP: photoperiod, Q: nutrient quota, μ_{NR}: nutrient replete growth rate, μ'_{NR}: theoretical maximum growth rate at infinite quota for the respective model, Q_0: minimum quota, Q_m: maximum quota κ_Q: normalised half-saturation coefficient of nutrient limited growth (dimensionless, $\kappa_Q = Q_0/k_Q$), DW: dry weight. The "Droop relation" denotes the situation where $k_Q=Q_0$ or $\kappa_Q=1$. In the model-independent parameters, Q_0 was taken from direct measurements where available, or was taken as the arithmetic mean of parameter estimates of Q_0 from model fits with equations 11-14 (p. 31) otherwise. Q_m and μ_{NR} were taken from direct measurements where available or otherwise estimated from plots or taken from other experiments under nutrient replete conditions by the same authors or other authors using the same species strains. Irradiance values were converted to μmol quanta m^{-2} s^{-1} using suitable conversion factors when published in different units; specific growth rates were converted to d^{-1} analogously.

Experimental details					Model-independent parameters			Droop parameters (Eq. 11, p. 31)			Normalised-model parameters (Eq. 17, p. 33)			
I (μmol m^{-2} s^{-1})	T (°C)	LP (h d^{-1})	Q units	*n*	μ_{NR} (d^{-1})	Q_0	Q_m	μ'_{NR} (d^{-1})	Q_0	R^2	μ'_{NR} (d^{-1})	Q_0	κ_Q	R^2
Scenedesmus sp. (Rhee, 1973)														
65	20	12	10^{-12} μmol P μm^{-3}	9	1.16	25.7	200	1.35	27.6	0.99	1.17	23.3	0.84	0.99
Scenedesmus acutus (Sterner, 1993)														
200	20	14	P:C by atoms	6	1.21	0.00045	0.011	0.76	0.00059	0.78	1.02	0.00030	0.13	0.91
Scenedesmus quadricauda (Ahlgren, 1987)														
"optimum"	5	24	% of DW	6	0.19	0.106	0.37	0.28	0.108	0.88	0.21	0.102	1.43	0.87
"optimum"	10	24	% of DW	14	0.39	0.078	0.58	0.44	0.087	0.90	0.40	0.071	0.71	0.93
"optimum"	15	24	% of DW	12	0.62	0.063	0.52	0.68	0.069	0.83	0.61	0.057	0.76	0.86
"optimum"	20	24	% of DW	12	0.85	0.051	0.34	0.94	0.065	0.88	1.19	0.037	0.22	0.97
"optimum"	25	24	% of DW	12	1.03	0.059	0.38	1.04	0.070	0.86	1.37	0.048	0.29	0.96
Staurastrum lueutkemuellerii (Olsen, 1989)														
80-100	23	18	μg P mm^{-3}	15	0.94	1.44	12.3	1.06	1.68	0.88	0.98	1.15	0.53	0.90

Experimental details					Model-independent parameters			Droop parameters (Eq. 11, p. 31)			Normalised-model parameters (Eq. 17, p. 33)			
I (μmol m^{-2} s^{-1})	T (°C)	LP (h d^{-1})	Q units	*n*	μ_{NR} (d^{-1})	Q_0	Q_m	μ'_{NR} (d^{-1})	Q_0	R^2	μ'_{NR} (d^{-1})	Q_0	κ_Q	R^2
Selenastrum minutum (Elrifi and Turpin, 1985)														
100	20	24[b]	fmol P cell^{-1}	22	1.68	1.22	11.4	1.78	1.34	0.68	1.67	1.10	0.71	0.70
100	20	24[b]	P:C by atoms	22	1.68	0.0011	0.0158	1.42	0.0015	0.83	1.81	0.0007	0.16	0.95
*Limnothrix (*formerly *Oscillatoria) redekei* (Wernicke and Nicklisch, 1986)														
170	5	12	μmol P mm^{-3}	10	0.19	0.067	0.34	0.22	0.068	0.95	0.20	0.066	1.05	0.95
170	10	12	μmol P mm^{-3}	9	0.41	0.044	0.33	0.37	0.045	0.84	0.54	0.041	0.30	0.99
170	15	12	μmol P mm^{-3}	10	0.60	0.044	0.56	0.64	0.044	0.96	0.61	0.044	0.69	0.99
170	20	12	μmol P mm^{-3}	20	0.80	0.046	0.34	0.83	0.046	0.82	0.88	0.044	0.51	0.92
91	20	24	μmol P mm^{-3}	9	1.02	0.071	0.3	1.38	0.073	0.88	1.04	0.072	1.59	0.89
170	20	12	μmol P mm^{-3}	7	0.82	0.082	0.34	1.07	0.085	1.00	0.84	0.082	1.44	1.00
*Planktothrix (*formerly *Oscillatoria) agardhii* (Ahlgren, 1985)														
37	15.4	24	% of DW	11	0.50	0.131	0.98	0.54	0.143	0.97	0.44	0.123	1.00	0.97
Anabaena flos-aquae (Gotham and Rhee, 1981b)														
92	20	14	10^{-9} μmol P cell^{-1}	8	0.85	2.01	16.1	0.93	2.27	0.84	0.88	1.73	0.58	0.87
Microcystis sp. (Gotham and Rhee, 1981b)														
92	20	14	10^{-9} μmol P cell^{-1}	8	0.95	1.50	9.2	1.15	1.60	0.92	0.95	1.45	1.09	0.93
Microcystis aeruginosa (Olsen, 1989)														
80-100	23	18	μg P mg^{-1} C	22	0.81	5.8	28.4	1.03	6.1	0.92	0.83	5.48	1.15	0.92
Synechococcus linearlis (Healey, 1985)														
62	[b]	24[b]	μg P mg^{-1} C	7	1.16	1.56	26.5	1.06	1.83	0.90	1.19	1.22	0.30	0.99

Experimental details					Model-independent parameters			Droop parameters (Eq. 11, p. 31)			Normalised-model parameters (Eq. 17, p. 33)			
I (μmol m^{-2} s^{-1})	T (°C)	LP (h d^{-1})	Q units	n	μ_{NR} (d^{-1})	Q_0	Q_m	μ'_{NR} (d^{-1})	Q_0	R^2	μ'_{NR} (d^{-1})	Q_0	κ_Q	R^2
Monochrysis lutheri (Goldman, 1979)														
31	15	24	pg P cell^{-1}	22	0.79	0.032	0.31	0.88	0.036	0.90	0.80	0.026	0.57	0.93
31	18.8	24	pg P cell^{-1}	33	0.92	0.015	0.7	0.92	0.018	0.75	0.90	0.011	0.38	0.80
31	23	24	pg P cell^{-1}	23	1.16	0.019	0.52	1.16	0.021	0.82	1.14	0.014	0.42	0.85
Monochrysis lutheri (Goldman et al., 1979)														
96	18	24[b]	P:C by atoms	32	0.95	0.00052	0.024	0.92	0.00066	0.91	0.92	0.00030	0.24	0.95
Cyclotella nana (Fuhs, 1969)														
various	-	24	relative (Q/Qo)	31	1[a]	1	7.4	1.05[a]	0.89	0.75	1.01[a]	0.59	0.46	0.81
Cyclotella meneghiniana (Tilman and Kilham, 1976)														
100	20	14	10^{-9} μmol P cell-1	12	0.65	7.80	350	0.62	8.89	0.57	0.63	6.15	0.41	0.65
Asterionella formosa (Gotham and Rhee, 1981b)														
92	20	14	10^{-9} μmol P cell^{-1}	6	0.53	4.96	10	1.11	4.86	0.88	0.55	5.26	4.71	0.93
Fragilaria crotonensis (Gotham and Rhee, 1981b)														
92	20	14	10^{-9} μmol P cell^{-1}	6	0.75	2.95	26.5	0.86	3.11	0.98	0.74	2.79	0.98	0.96
Nitzschia acicularis (this study)														
95	11	12	μg P mm^{-3}	35	0.79	0.60	5.88	0.70	0.58	0.83	1.03	0.59	0.24	0.98
130	15	12	μg P mm^{-3}	33	1.09	0.50	6.09	0.84	0.51	0.84	1.18	0.50	0.31	0.99
90	20	12	μg P mm^{-3}	30	1.27	0.56	3.85	1.23	0.57	0.91	1.38	0.54	0.55	0.95
200	15	6	μg P mm^{-3}	51	0.80	0.57	7.01	0.69	0.56	0.76	0.80	0.57	0.51	0.89
130	15	9	μg P mm^{-3}	38	0.95	0.54	5.91	0.80	0.55	0.80	1.01	0.45	0.27	0.94

Experimental details					Model-independent parameters			Droop parameters (Eq. 11, p. 31)			Normalised-model parameters (Eq. 17, p. 33)			
I (μmol m^{-2} s^{-1})	T (°C)	LP (h d^{-1})	Q units	n	μ_{NR} (d^{-1})	Q_0	Q_m	μ'_{NR} (d^{-1})	Q_0	R^2	μ'_{NR} (d^{-1})	Q_0	κ_Q	R^2
Stephanodiscus minutulus (this study)														
140	16	9	μg P mm^{-3}	46	0.96	0.44	3.02	1.05	0.44	0.94	0.98	0.42	0.92	0.96
195	15	6	μg P mm^{-3}	77	0.74	0.43	3.02	0.82	0.43	0.87	0.78	0.43	0.84	0.93
68	16	12	μg P mm^{-3}	100	0.87	0.41	3.01	0.91	0.44	0.91	0.90	0.40	0.75	0.96
69	20	12	μg P mm^{-3}	55	0.94	0.51	3.09	1.07	0.51	0.93	0.97	0.48	1.00	0.94
69	10	12	μg P mm^{-3}	54	0.80	0.48	4.99	0.77	0.47	0.91	0.82	0.39	0.46	0.96

[a] relative growth rate (dimensionless)

[b] value not provided in the publication, value was assumed wherever applicable

Table 14: Experimental data under N-limitation collected from the literature to assess the "Droop relation". Abbreviations and details as for Table 13.

Experimental details					Model-independent parameters			Droop parameters Eq. 11, p. 31			Normalised-model parameters, Eq. 17, p. 33			
I (μmol m^{-2} s^{-1})	T (°C)	LP (h d^{-1})	Q units	n	μ_{NR} (d^{-1})	Q_0	Q_m	μ'_{NR} (d^{-1})	Q_0	R^2	μ'_{NR} (d^{-1})	Q_0	κ_Q	R^2
Scenedesmus sp. (Rhee and Gotham, 1981b)														
79	11	24	10^{-7} μmol N cell^{-1}	6	0.70	2.0	8.6	0.85	1.8	0.90	0.52	2.3	6.04	0.99
79	16	24	10^{-7} μmol N cell^{-1}	9	1.10	0.82	3.39	1.42	0.91	0.98	1.24	0.74	0.79	0.97
79	20	24	10^{-7} μmol N cell^{-1}	11	1.37	0.41	2.22	1.57	0.48	0.91	1.45	0.35	0.59	0.93
79	25	24	10^{-7} μmol N cell^{-1}	7	1.35	0.35	2.22	1.55	0.46	0.86	1.74	0.25	0.28	0.92
Scenedesmus sp. (Rhee and Gotham, 1981a)														
37	20	24	10^{-7} μmol N cell^{-1}	11	1.22	0.90	2.41	1.84	1.00	0.92	4.55	0.84	0.24	0.95
79	20	24	10^{-7} μmol N cell^{-1}	11	1.39	0.41	2.08	1.59	0.49	0.90	1.47	0.35	0.58	0.92
*Planktothrix (*formerly *Oscillatoria) agardhii* (Ahlgren, 1985)														
37	15.4	24	% of DW	12	0.50	2.9	13.2	0.66	3.4	0.86	0.97	2.5	0.31	0.89
Ankistrodesmus falcatus (Gotham and Rhee, 1981a)														
92.02	19	24	10^{-9} μmol N cell^{-1}	6	0.98	122.2	313	1.62	136.0	0.79	4.30	111.6	0.21	0.81
Thalassiosira fluviatilis (Laws and Bannister, 1980)														
247	[a]	12	μg N mg^{-1} C	6	1.15	51.0	182	1.62	53.8	0.92	1.33	50.2	1.16	0.93
244	[a]	12	μg N mg^{-1} C	5	1.15	53.4	182	1.70	53.4	0.96	1.20	56.4	2.29	0.99
Selenastrum minutum (Elrifi and Turpin, 1985)														
100	20	24[a]	fmol N cell^{-1}	18	1.68	23.5	188	1.81	28.6	0.87	1.88	18.8	0.40	0.93

[a] value not provided in the publication, value was assumed wherever applicable

Appendix 2: Final equations for model of factor interactions

This appendix is designed to be a quick reference for the final model and is only a summary of information already contained in the main thesis. The model equations given below are repeated from the text with the corresponding equation numbers and page references. The model parameters are given in Table 15 (p. 129) and all other model parameters and variables are given in Table 1 (p. ix). The final model calculates specific growth rate (μ, d^{-1}) based on daily light exposure (LE, mol quanta m^{-2} d^{-1}), phosphorus quota (Q, μg P mm^{-3}), silicate concentration (S, μmol Si L^{-1}), temperature (T, °C), and effective photoperiod (LP_{eff}, h d^{-1}). The species-specific interactions between these factors are also considered.

The specific growth rate is calculated based on the availability of the resources light, phosphorus and silicon (for diatoms). The nutrient replete growth rate (μ_{NR}), which is limited by light and the other physical factors (temperature, photoperiod and light fluctuations), is decreased to account for nutrient limitation by functions of P quota (Q) and silicon concentration (S). The model considers a multiplicative interaction between light limited (nutrient replete) growth and nutrient limitation, and a threshold interaction between phosphorus and silicon as follows:

$$\mu = \mu_{NR} \times \min\begin{cases} f(Q) \\ f(S) \end{cases} \qquad \text{(Eq. 42, p. 99)}$$

The dependency of μ_{NR} on light is described by an exponential light curve as a function of the daily light exposure (LE)

$$\mu_{NR} = LF \times \mu_m \left(1 - \exp\left(\frac{-LF_\alpha \times \alpha_{LE}(LE - LE_{min})}{LF \times \mu_m}\right)\right) \qquad \text{(Eq. 41, p. 83)}$$

where μ_m is the light saturated growth rate, measured under constant light and limited only by suboptimal temperature and photoperiod. α_{LE} (m^2 mol^{-1} quanta) is the initial slope of the curve, and LE_{min} (mol quanta m^{-2} d^{-1}) is the light compensation point representing the minimum amount of light required for growth. The light fluctuation factors, LF and LF_α are dimensionless and decrease the light maximum growth rate μ_m and the initial slope α_{LE}, respectively to account for the effects of fluctuating light. Under constant, non-fluctuating

light, LF and LF_{α} are equal to 1. The interactions between light and temperature or light and photoperiod are not simply multiplicative. Temperature and photoperiod do not affect α_{LE}, which is a constant model parameter, but they do affect μ_m as follows

$$\mu_m = \mu_{max} \times f(T) \times f(LP_{eff}) \qquad \text{(Eq. 6, p. 29)}$$

where $f(T)$ and $f(LP_{eff})$ are functions to account for the effects of suboptimal temperature and effective photoperiod, respectively, and μ_{max} (d^{-1}) is the absolute maximum specific growth rate under optimal conditions (light and nutrient saturation, optimum temperature and an effective photoperiod of 24 h d^{-1}). Here a temperature function after Lehman et al. (1975) is used, which increases with temperature up until the optimum temperature (T_{opt}, °C) and then decreases at temperatures above T_{opt} due to temperature inhibition:

$$f(T) = \exp\left(-2.3\left(\frac{T_{opt} - T}{T_{opt} - T_{min}}\right)^2\right) \qquad \text{(Eq. 7, p. 29)}$$

where T_{min} is the minimum temperature, at which $f(T)$ attains a value of 0.1. The growth rate increases non-linearly with the photoperiod and has saturation characteristics. Therefore the photoperiod dependence has the same form as the growth-light curve, as follows

$$f(LP_{eff}) = 1 - \exp\left(\frac{-\alpha_{LP}(LP_{eff} - LP_{min})}{\mu_{mLP}}\right) \qquad \text{(Eq. 8, p. 29)}$$

where α_{LP} (h^{-1}) is the initial slope of the curve, LP_{min} (h d^{-1}) represents the minimum photoperiod required for growth, and μ_{mLP} (d^{-1}) is the light saturated growth rate under continuous (24 h d^{-1}) light.

The type of interaction between temperature and photoperiod appears to be species-specific. Two variations are known to be possible, where the difference is essentially whether α_{LP} is temperature dependent. The interaction can be expressed as:

$$\mu_{mLP} = \begin{cases} \mu_{max} \\ \mu_{max} \times f(T) \end{cases}$$

(Eq. 9, p. 30)[a]

(Eq. 10, p. 30)[b]

[a] applies to *N. acicularis, L. redekei, P. agardhii*, probably other phytoplankton, especially cyanobacteria
[b] applies to *S. minutulus*, and probably other centric diatoms or early spring species

Different interaction types were possible for phosphorus limitation. For *S. minutulus* and *L. redekei*, the interaction was multiplicative and is well described by the Fuhs (1969) equation (Eq. 13), whereas a more complex function was required for *N. acicularis* (Eq. 14b):

$$f(Q) = \begin{cases} 1 - \exp\left[-\ln 2 \left(\frac{Q}{Q_0} - 1 \right) \right] \\ \\ 1 - \exp\left(-\alpha_Q \left(\frac{Q - Q_0}{\mu_{NR}} \right) \right) \end{cases}$$

(Eq. 13, p. 31)[c]

(Eq. 14b, p. 32)[d]

[c] applies to *S. minutulus* and *L. redekei*
[d] applies to *N. acicularis*

Q_0 (μg P mm^{-3}) is the minimum quota required for growth and α_Q (mm^3 μg^{-1} P d^{-1}) is the initial slope of the quota curve. Note that the above equations assume that μ_{NR} is equal to μ'_{NR} (theoretical maximum growth rate at infinite quota), which is acceptable for P in most cases because the difference is small, but is not acceptable for N, for example. The temperature dependence of α_Q is also described by the function of Lehman et al. (1975), which decreases the maximum initial slope at optimum temperature (α_{Qm}, mm^3 μg^{-1} P d^{-1}) as follows:

$$\alpha_Q = \alpha_{Qm} \times \exp\left(-2.3 \left(\frac{T_{opt} - T}{T_{opt} - T_{minQ}} \right)^2 \right)$$

(Eqs. 34, 35, p. 58)

However, the temperature dependence of P-limited growth was not the same as the temperature dependence of nutrient replete growth for *N. acicularis*. Here it was assumed that the optimum temperature was the same for P-limited and P-replete growth, but the minimum temperature is different under P-limitation, given by T_{minQ} (°C).

Table 15: Parameters for the final model of factor interactions

Parameter	Units	*S. minutulus*	*N. acicularis*	*L. redekei*
μ_{max}	d^{-1}	1.46	1.82	0.89
α_{LE}	$m^2\ mol^{-1}$	0.67	0.83	0.46
LE_{min}	$mol\ m^{-2}\ d^{-1}$	0.31	0.24	0
α_{LP}	h^{-1}	0.22	0.32	0.24
LP_{min}	$h\ d^{-1}$	0.4	2.0	2.0
T_{opt}	°C	20.7	21.7	23.6
T_{min}	°C	-0.6	1.0	0.4
LF†	dimensionless	0.82	0.67	0.71
LF_{α}†	dimensionless	1	1	0.54
Q_0	$\mu g\ P\ mm^{-3}$	0.452	0.532	0.91‡
k_Q	$\mu g\ P\ mm^{-3}$		-	-
α_{Qm}	$mm^3\ \mu g^{-1}\ P\ d^{-1}$	-	0.898	-
T_{minQ}	°C	-	6.6	-
k_S	$\mu mol\ Si\ L^{-1}$	-	1.87	-
S_0	$\mu mol\ Si\ L^{-1}$	0.55	0.24	-
α_S	$L\ \mu mol^{-1}\ d^{-1}$	3.14	-	-

† for growth under constant light, LF = 1 and LF_{α} = 1.

‡ Value averaged from Wernicke & Nicklisch (1986), divided by 2 (A. Nicklisch, pers. comm.) to account for presence of bacteria in the non-axenic cultures these authors used.

Silicon limited growth is described by the Monod function with a nutrient threshold S_0 (μmol Si L^{-1}), below which growth is not possible.

$$f(S) = \begin{cases} \dfrac{S - S_0}{\dfrac{\mu_{NR}}{\alpha_S} + S - S_0} & \text{(Eq. 18, p. 34)}^{e} \\ \dfrac{S - S_0}{k_S + S - S_0} & \text{(Eq. 18, p. 34)}^{f} \end{cases}$$

[e] applies to *S. minutulus*, probably other *Stephanodiscus* sp.
[f] applies to *N. acicularis*, probably other diatoms except *Stephanodiscus* sp.

Here k_s (μmol Si L^{-1}) is the half-saturation constant of silicon limited growth. For *S. minutulus*, the initial slope of the Monod curve (α_Q, L μmol^{-1} Si d^{-1}) rather than k_s was constant, so Eq. 18 was modified by substituting:

$$k_S = \frac{\mu_{NR}}{\alpha_S} \qquad \text{(Eq. 37, p. 68)}$$

Selbständigkeitserklärung (declaration)

Hiermit erkläre ich, dass ich diese Arbeit eigenständig unter Verwendung der angegebenen Hilfsmittel verfasst habe und bestätige den Wahrheitsgehalt mit meiner Unterschrift.

Ich habe mich anderwärtig nicht um einen Doktorgrad beworben und besitze einen entsprechenden Doktorgrad nicht. Die dem Verfahren zu Grunde liegende Promotionsordnung der Mathematisch-Naturwissenschaftlichen Fakultät I der Humboldt Universität zu Berlin habe ich zur Kenntnis genommen.

Berlin, den_____

Publications

(Peer reviewed):

Shatwell, T., Köhler, J. & Nicklisch, A. (2013). Temperature and photoperiod interactions with silicon limited growth and competition of two diatoms. *Journal of Plankton Research* 35, 957-971.

Shatwell, T., Köhler, J. & Nicklisch, A. (in review). Temperature and photoperiod interactions with phosphorus limited growth and competition of two diatoms.

Kirillin, G., **Shatwell, T.**, Kasprzak, P. (2013). Consequences of thermal pollution from a nuclear plant on lake temperature and mixing regime. *Journal of Hydrology* 496, 47-56.

Shatwell, T., Ackermann, G., Dokulil, M. T., Jordan, S., Rücker, J., Scharf, W., Wagner, A., Kasprzak, P. (2013). Langzeitbeobachtungen zum Einfluss von Klimawandel und Eutrophierung auf Seen und Talsperren in Deutschland. *Korrespondenz WasserWirtschaft* 12, 729-736.

Zak, D., Gelbrecht, J., Zerbe, S., **Shatwell, T.**, Barth, M., Cabezas, A., Steffenhagen, P. (2013). How helophytes influence the phosphorus cycle in degraded inundated peatlands. *Ecological Engineering*, http://dx.doi.org/10.1016/j.ecoleng.2013.10.003.

Shatwell, T., Nicklisch, A., Köhler, J. (2012) Temperature and photoperiod effects on phytoplankton growing under simulated mixed layer light fluctuations. *Limnology and Oceanography* 57:541-53.

Shatwell, T., Köhler, J., Nicklisch, A. (2008) Warming promotes cold-adapted phytoplankton in temperate lakes and opens a loophole for Oscillatoriales in spring. *Global Change Biology* 14: 2194-2200.

Nicklisch, A., **Shatwell, T.**, Köhler, J. (2008) Analysis and modelling of the interactive effects of temperature and light on phytoplankton growth and relevance for the spring bloom. *Journal of Plankton Research* 30: 75-91.

(Not peer reviewed):

Shatwell, T., Kasprzak. P., Hupfer, M. (2012) The influence of climate change on oxygen and phosphorus in deep Lake Stechlin. DGL - Erweiterte Zusammenfassungen der Jahrestagung 2011 (Weihenstephan), p. 302-306.

Kasprzak, P., **Shatwell, T.**, Kirillin, G. (2012) Warmwasser aus einem Kernkraftwerk und Klimawandel haben unterschiedlichen Einfluss auf Wassertemperaturen und thermische Schichtung des Stechlinsees. DGL - Erweiterte Zusammenfassungen der Jahrestagung 2011 (Weihenstephan), p. 287-291.

Shatwell, T. (2010) Algenentwicklung in Zeiten des Klimawandels. IGB Jahresforschungsbericht 2009: 43.

Nicklisch, A., **Shatwell, T.** (2008) Factors governing the phytoplankton spring bloom in a shallow temperate lake: a paradox of warming? SILnews 53, 19-20.

Shatwell, T., Nicklisch, A., Köhler, J. (2007) The interaction between temperature and light and the response of spring phytoplankton. Tagungsband der 8. Nachwuchswissenschaftlerkonferenz in Jena, 2007.

Schauser, I., et al. (2007) Joint Summary of the Workshop Discussions about the Current State of the Art in Modelling Aquatic Ecosystems. Ergebnisse des Workshops "Perspectives of Lake Modelling towards Predicting Reaction to Trophic Change". Schriftenreihe des Kompetenzzentrums Wasser Berlin.

Shatwell, T., Cordery, I. (1999) Nutrient Removal in Urban Wetlands, Conference Proceedings of the IUGG 99 Conference, Birmingham, 1999.

Shatwell, T., Cordery, I. (1998) A Phosphorus and Sediment Balance of an Urban Pond. Tagungsband *Hydrastorm 98*, Adelaide 1998

Presentations

Shatwell, T, N.N. (2014). IGB-Colloquium, Berlin, 3.4.2014.

Shatwell, T., Padisák, J., Kirillin, G., Hupfer, M., Kasprzak, P. (2014) Einfluss von Klimawandel und Abwärme auf den Stechlinsee. Colloquium of the Landesanstalt für Umwelt, Messungen und Naturschutz Baden-Württemberg (LUBW), Institut für Seenforschung, Langenargen, 21.2.2014.

Shatwell, T., Köhler, J., Nicklisch, A. (2013) *Colimitation by physical factors and phosphorus: species-specific response of growth and competition of two diatoms*. Annual meeting of the German Limnological Society (DGL) in Potsdam, Germany, 9.9.2013.

Shatwell, T., Hupfer, M., Padisák, J., Kasprzak, P. (2013) *Einfluss des Klimawandels auf Schichtung, Sauerstoff und Phosphor im Stechlinsee.* Presentation at the Seentherapie (Lake therapy) Workshop, Arendsee, Germany, 20.3.2013.

Shatwell, T., Padisák, J., Hupfer, M., Kasprzak, P. (2013) *Modellierung und Langzeitdatenanalyse des Stechlinsees.* Presentation at the Stechlin-Workshop: Atmosphärisch-terrestrisch-aquatische Kopplung, Neuglobsow, Germany, 12.3.2013.

Shatwell, T., Jöhnk, K., Böhrer, B. (2013) *The role of the metalimnion and other internal transition zones in lakes*. Organiser of the Special Session at the ASLO Aquatic Sciences Meeting 2013 in New Orleans, USA.

Shatwell, T., Padisák, J., Hupfer, M., Kasprzak, P. (2013) *Phytoplankton interactions with oxygen and phosphorus dynamics in an oligotrophic lake*. Presentation at the ASLO Aquatic Sciences Meeting 2013 in New Orleans, USA, 21.2.2013.

Shatwell, T., Hupfer, M., Kasprzak, P., Kirillin, G. (2012) *The influence of warming on the oxygen budget of Lake Stechlin*. Presentation at the 2nd Lake Ecosystem Modelling Workshop, Leipzig, Germany, 28.6.2012.

Shatwell, T., Hupfer, M., Kasprzak, P. (2012) *The influence of climate change and waste heat on the thermal structure and oxygen budget in deep Lake Stechlin.* Annual meeting of the Society for Freshwater Science (SFS), Louisville, USA, 21.5.2012.

Shatwell, T., Hupfer, M., Kirillin, G., Kasprzak, P. (2012) *Der Einfluss von Klimawandel und Abwärme auf die thermische Struktur und Sauerstoffhaushalt im tiefen Stechlinsee.* LTER-D annual meeting in Gelnhausen, Germany, 27.3.2012.

Shatwell, T., Kirillin, G., Kasprzak, P. (2012) *Die Auswirkungen von Sonnenschein und Atomzerfall auf die Temperatur und Schichtung im Stechlinsee.* Presentation at the Kleiner Naturschutztag, Menz, Germany, 23.2.2012.

Shatwell, T., Kasprzak, P., Hupfer, M. (2011) *The influence of climate change on oxygen and phosphorus in deep Lake Stechlin*. Annual meeting of the German Limnological Society (DGL) in Weihenstephan, Germany, 15.9.2011.

Shatwell, T., Nicklisch, A., Köhler, J. (2011). *The effects of fluctuating light on some spring phytoplankton species*. Colloquium at the Institute of Hydrobiology, Chinese Academy of Sciences, Wuhan, China.

Shatwell, T., Nicklisch, A., Köhler, J. (2011) *The effects of fluctuating light on some spring phytoplankton species.* Presentation at the Shallow Lakes Conference, Wuxi, China.

Shatwell, T. (2010) *50 Jahre Langzeitforschung am Stechlinsee: Ergebnisse, Probleme, Forschungsperspektive.* IGB Departmental colloquium in Neuglobsow, Germany.

Shatwell, T. (2009) *Modelling the effects of factor interactions on phytoplankton growth: consequences of global warming*. Final IGB colloquium, Berlin, Germany.

Shatwell, T., Nicklisch, A. (2009) *Interactions of simulated light fluctuations and temperature on the growth of some spring phytoplankton species*. Annual meeting of the German Limnological Society (DGL) in Oldenburg, Germany.

Shatwell, T., Köhler, J., Nicklisch, A. (2008) *Warming promotes cold-adapted phytoplankton and opens a loophole for Oscillatoriales in spring*. Shallow Lakes Conference in Punta del Este, Uruguay.

Shatwell, T., Nicklisch, A., Köhler, J. (2008) *The complexity of the light factor for phytoplankton*. DGL conference 2008 in Konstanz, Germany.

Shatwell, T., Nicklisch, A., Köhler, J. (2007) *Interactions between temperature, light and nutrients and the response of spring phytoplankton*. Presentation at the Lake Modelling Workshop: Perspectives of lake modelling towards predicting reaction to trophic change, Berlin, Germany.

Shatwell, T., Nicklisch, A., Köhler, J. (2007) *The interaction between temperature and light and the response of spring phytoplankton*. Presentation at the 8. Nachwuchswissenschaftlerkonferenz in Jena, Germany.

Shatwell, T., Nicklisch, A., Köhler, J. (2006) *The response of phytoplankton to the interactions between temperature, photoperiod and light exposure during warm and*

cold spring periods. Annual meeting of the Germany Limnological Society (DGL) 2006 in Dresden, Germany.

Shatwell, T. (2006) *Methoden und Erfahrungen bei der Masterarbeit*. Master Colloquium at the HS Magdeburg-Stendal, Germany (invited).

Shatwell, T. (2005) *Erfahrungen als ausländischer Studierende*. Acceptance speech of the DAAD Prize at the enrollment ceremony of the Magdeburg-Stendal University of Applied Sciences, Germany.

Shatwell, T., Cordery, I. (1998) *A phosphorus and sediment balance of an urban pond*. Presentation at the Hydrastorm 98 conference in Adelaide, Australia.